UNIVERSIDAD DE CHILE
FACULTAD DE CIENCIAS FÍSICAS Y MATEMÁTICAS
DEPARTAMENTO DE GEOLOGÍA

CRYPTIC MAGMA RECHARGE ASSOCIATED WITH 20TH CENTURY ERUPTIONS AT VILLARRICA VOLCANO

TESIS PARA OPTAR AL GRADO DE MAGÍSTER EN CIENCIAS, MENCIÓN GEOLOGÍA
MEMORIA PARA OPTAR AL TÍTULO DE GEÓLOGO

CHRISTIAN JAVIER PIZARRO ARAYA

PROFESOR GUÍA:
MIGUEL ÁNGEL PARADA REYES

MIEMBROS DE LA COMISIÓN:
ÁNGELO CASTRUCCIO ÁLVAREZ
CLAUDIA CANNATELLI

SANTIAGO DE CHILE
2018

RESUMEN DE LA MEMORIA PARA OPTAR AL TÍTULO DE: Geólogo y grado De Magíster en Ciencias, mención Geología
POR: Christian Javier Pizarro Araya
FECHA: 28/09/2018
PROFESOR GUÍA: Miguel Ángel Parada

CRYPTIC MAGMA RECHARGE ASSOCIATED WITH 20TH CENTURY ERUPTIONS AT VILLARRICA VOLCANO

El Volcán Villarrica es uno de los más activos de los Andes (ciclos de reposo de ~5.3 años), eruptando productos de composiciones basálticas a andesíticas basálticas, con estilos desde hawaiiano a estromboliano vigoroso. Estas características lo hacen un lugar destacado para determinar los parámetros pre-eruptivos y los procesos involucrados en sus erupciones. En esta tesis se compara la geoquímica de roca total y las abundancias, texturas y composiciones minerales de las lavas más relevantes del siglo XX, que fueron eruptadas en 1921, 1948 y 1971. Las lavas analizadas muestran un rango restringido en las composiciones de roca total (51.7-52.4 wt. % SiO_2), sin embargo, presentan la siguiente tendencia creciente del contenido de MgO: ~5.3 wt % MgO (1921), ~6.0 wt % MgO (1971) and ~7.0 wt. % MgO (1948). Dos grupos de composiciones de plagioclasas se observan en todas las lavas: pobres en anortita (~An_{60}) y ricas en anortita (~An_{80}). Las composiciones pobres en anortita son las más abundantes en todas las lavas y fueron comúnmente formadas en las etapas tempranas (núcleos) y en las últimas etapas (bordes externos y fenocristales pequeños y casi no zonados) de cristalización de plagioclasa, mientras que las plagioclasas ricas en anortita se formaron alrededor de núcleos pobres en anortita o como cristales aislados durante etapas intermedias. Las temperaturas de equilibrio de plagioclasa-olivino-clinopiroxeno son de aproximadamente 1090 °C y fueron obtenidas en clots de cristales de las tres lavas. Los cálculos termométricos obtenidos con simulaciones de MELTS de formación de plagioclasa indican un calentamiento (*thermal mixing*) del reservorio a ~0.5 kbar de unos 100 °C con respecto a las temperaturas de los clots cristalinos. La incorporación de pequeñas cantidades de magma máfico más rico en volátiles y más caliente, de composición similar (*cryptic mixing*), en el reservorio del Villarrica, podría también calentarlo, probablemente, de una manera más eficiente que con la sola conducción de calor. Una interacción más larga del magma máfico caliente con el reservorio podría provocar cristalización de plagioclasa rica en anortita, disolución de plagioclasa pobre en anortita (es decir, un aumento de la razón modal de rica en An/pobre en An) y una modificación composicional hacia composiciones más ricas en MgO y volátiles, que últimamente resultarían en una mayor intensidad de la erupción.

Si me preguntas por qué, te diría que es por la belleza. Pero entiéndeme bien, es la belleza en sus distintos niveles. Uno es evidente. La reacción fisiológica provocada por el objeto de estudio es inevitable. Y yo soy adicto al asombro. Otro no lo es tanto. Yace en la estética del ejercicio argumentativo. En un plano similar al del montaje cinematográfico. También hay un tercer nivel, más críptico y profundo. Más permanente y enriquecedor. Ese que, como una maldición, se impregna en la médula del sujeto y lo transforma.

AGRADECIMIENTOS

Al proyecto CONICYT-FONDAP 15090013, Centro de Excelencia en Geotermia de los Andes (CEGA) y al Departamento de Geología de la Universidad de Chile por financiar mis estudios de postgrado.

Al Departamento de Postgrado y Postítulo de la Vicerrectoría de Asuntos Académicos por su ayuda para una estadía de investigación en *School of Earth Sciences* de *University of Bristol*, en el Reino Unido.

Al profesor Miguel Ángel Parada por su inspiración, guía y apoyo. A los profesores Ángelo Castruccio y Claudia Cannatelli por su buena disposición y entusiasmo.

A las profesoras Katharine Cashman y Alison Rust por recibirme en *School of Earth Sciences* de *University of Bristol* durante una estadía, por sus consejos e interés.

A Stuart Kearns y Benjamin Buse por su ayuda con el uso de la microsonda en *University of Bristol*. A Joe Pickles por su ayuda con la microsonda en *University of Exeter*.

A Claudio Contreras y Eduardo Morgado, coautores del manuscrito producto de esta investigación, quienes me guiaron y con quienes siempre pude contar.

A mis compañeros de postgrado que directa o indirectamente colaboraron en esta tesis.

A mi amada familia, mis queridos amigos y amigas, y las valiosas personas que conocí tanto en pregrado como en postgrado.

TABLA DE CONTENIDO

ÍNDICE DE FIGURAS

ÍNDICE DE TABLAS

Capítulo 1 : Introducción

1.1. Estructura de la tesis

El presente estudio tiene por objeto tres lavas eruptadas durante el siglo XX en el Volcán Villarrica. El propósito es determinar las condiciones del reservorio magmático y los procesos involucrados en sus erupciones. Para esto, se compara la química de roca total, las abundancias, texturas y composiciones minerales, con particular énfasis en los fenocristales de plagioclasa.

En el capítulo 1 se presenta el objeto de estudio, la motivación de esta investigación, los objetivos y las metodologías utilizadas.

En el capítulo 2 se presentan los principales resultados obtenidos: la química de roca total, petrografía, las estimaciones termobarométricas y simulaciones termodinámicas.

El capítulo 3 corresponde al manuscrito de un artículo que fue sometido a la revista *Journal of Volcanology and Geothermal Research*.

Finalmente, se presentan las principales conclusiones de este estudio.

1.2. Objeto de estudio y motivación

El Volcán Villarrica está ubicado los Andes del sur de Chile (39°25’S, 71°57W) cerca de la Zona de Falla Liquiñe-Ofqui de orientación N-S intra-arco, y al extremo oeste de la cadena volcánica de orientación NW-SE formada por los volcanes Villarrica, Quetrupillán y Lanín (López-Escobar *et al.*, 1995; Cembrano *et al.* 1996; Stern *et al.*, 2007). Su altura es de 2847 m.s.n.m. y cubre un área de cerca de 400 km^2, alcanzando un volumen de 250 km^3. El volcán fue construido sobre escasas rocas metasedimentarias Paleozoicas y del Triásico Superior, abundantes rocas plutónicas Meso-Cenozoicas y rocas volcánicas y volcanoclásticas Cenozoicas.

Su actividad eruptiva comenzó hace aproximadamente 600000 años y ha producido flujos de lavas y piroclastos de composiciones basálticas y andesíticas basálticas, además de depósitos laháricos, que se dividen en tres unidades: Villarrica I (Pleistoceno Medio a Superior), Villarrica II (Holoceno, entre 13900 y 3700 años AP), Villarrica III (3700 años AP al presente) (Moreno and Clavero, 2006). La última unidad contiene el registro histórico de erupciones que incluye las erupciones de 1787, 1921, 1948, 1963, 1964, 1971 y 1984. Dos eventos mayores explosivos, de composiciones máficas a intermedias, han sido reconocidos en el desarrollo del Villarrica: la Ignimbrita Licán (13900 años AP, ~10 km3, non-DRE, Clavero y Moreno, 1994; Lohmar *et al*., 2012) y la Ignimbrita Pucón (3700 años AP, ~3 km3, non-DRE, Clavero and Moreno, 1994). El volcán Villarrica es uno de los más activos de los Andes, registrando 88 erupciones con VEI ≥ 2 entre 1523 y 1991, con un promedio de una erupción (VEI ≥ 2) cada 5.3 años (Van Daele et al., 2014). Las erupciones históricas van desde hawaiianas a estrombolianas vigorosas, con productos basálticos a andesíticos basálticos (Moreno y Clavero, 2006). Desde el final de la última erupción del siglo XX (1985), el Volcán Villarrica ha mantenido un lago de lava activo en su cumbre que se ha desgasificado continuamente (Moreno y Clavero, 2006), sin efusión de flujos de lava (Witter *et al.*, 2004), sin embargo, intermitentemente ocurre *lava spattering* y emisión de tefra de grano fino desde la cumbre. La última erupción del Villarrica ocurrió el 3 de marzo de 2015 y fue una erupción estromboliana intensa y corta (<1 hora) con 4.7 x 10^6 m^3 (DRE) de material eruptado (Bertin *et al.*, 2015).

Las condiciones pre-eruptivas de eventos particulares del volcán Villarrica han sido estimadas desde enfoques petrológicos. Witter *et al.*, 2004 estudiaron muestras del lago de lava (reticulita del año 2000) y sugirieron que toda la cristalización ocurrió a P < 0.17 kbar, T = ~1135 ºC, fO_2 = NNO, bajo condiciones saturadas de agua. Lohmar *et al.* (2012) identificaron un calentamiento y una desgasificación asociada a la Ignimbrita Licán (~13000 años) desde ~900 a ~1100°C, a P <

0.67 kbar, fO_2 ligeramente mayores a QFM, y un contenido de agua que disminuye desde ~3.2 a ~1.5 wt. % H_2O. Morgado *et al.* (2015) estudiaron la lava de 1971 del Villarrica identificando dos reservorios: uno profundo, coincidente con el rango de profundidades del límite corteza-manto, y T = ~1208 ºC; y un reservorio somero en la corteza superior con T de ~1170 °C.

En este estudio, investigamos tres lavas andesitas basálticas del Volcán Villarrica eruptadas en el siglo XX: 1921, 1948 y 1971 (Fig. 1.1). Fueron seleccionadas debido a que están entre las más voluminosas, mejor preservadas y derivadas de erupciones históricas bien documentadas. La erupción de 1921 (Fig. 1.2) comenzó el 10 de diciembre y duró aproximadamente 36 horas. Fue un evento estromboliano (VEI 1-2) con la eyección de escaso material piroclástico, la formación de una columna de gases y la emisión de 13×10^6 m^3 de lava aa y pahoehoe (Fig. 1.2 b y c) que fluyó al sur, donde se ubica el pueblo de Coñaripe (Petit-Breuilh, 1994 y las referencias que ahí se encuentran). La erupción de 1948 (Fig. 1.3) comenzó en octubre de 1948 y terminó en febrero de 1949, y es considerada la erupción más explosiva del Villarrica en el siglo XX (estromboliana vigorosa, VEI 3). Generó explosiones, emisión de piroclastos, lava, lahares y flujos piroclásticos de pequeño volumen. En varias etapas de su erupción se formaron columnas eruptivas de hasta 8 km sobre el cráter (Fig. 1.3 a) (Moreno y Clavero, 2006 y las referencias que ahí se encuentran). El principal flujo de lava, que alcanzó 15 km desde el *vent* y que llenó parcialmente el valle del Estero Molco, tiene una morfología aa (Fig. 1.3 d y e) y un volumen estimado de $\sim 16 \times 10^6$ m^3. La erupción de 1971 (Fig. 1.4) comenzó el 29 de octubre con explosiones freatomagmáticas violentas en el cráter. El 29 de noviembre ocurrió una efusión de lava y se formaron dos conos piroclásticos dentro del cráter con explosiones rítmicas cada 3 minutos. El 29 de diciembre la erupción culminó alcanzando su fase paroxismal, con una fisura eruptiva de 2 km abierta en el cono central, generando dos fuentes de lava con una altura de 400 m y una columna eruptiva de hasta 3 km (Fig. 1.4 a). Se generaron flujos de lahares hacia el sur que causaron destrucción en la

localidad de Coñaripe y en los caminos, y la pérdida de al menos 17 vidas. Dos flujos de lava aa (Fig. 1.4 c y d) de 6 y 16.5 km que fluyeron a lo largo de los valles Pedregoso (flanco NE) y Challupén (flanco SW), respectivamente, fueron emplazados en menos de 48 horas (Moreno y Clavero, 2006 y las referencias que ahí se encuentran). Se calculó un volumen total de lava de 26 $\times 10^6$ m^3.

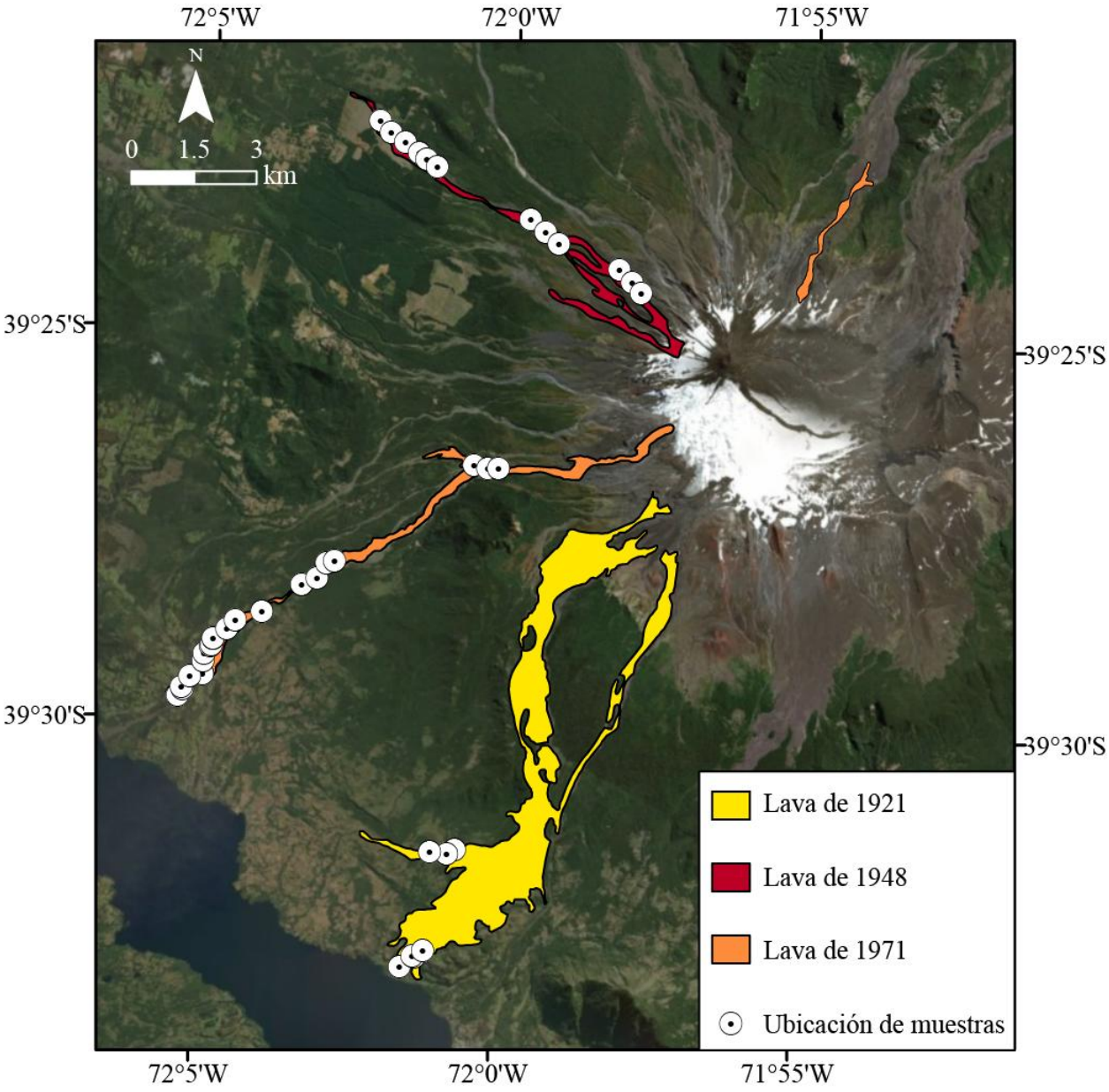

Fig. 1.1. Ubicación de las muestras de las tres lavas estudiadas del Volcán Villarrica.

(a)

(b)

(c)

Fig. 1.2. Fotografías de la lava de 1921. (a) Vista de un afloramiento del flujo de lava de 1921; (b) rocas con morfología pahoehoe; (c) rocas con morfología aa.

Fig. 1.3. Fotografías de la erupción y la lava de 1948. (a) Columna de 8000 m de altura con gases y piroclastos, durante la erupción del 18 de Octubre de 1948 (Foto Diario Austral); (b) Vista transversal del valle relleno por el flujo principal de lava; (c) Vista longitudinal del flujo de lava; (d y e) ejemplos de muestras de rocas aa recolectadas.

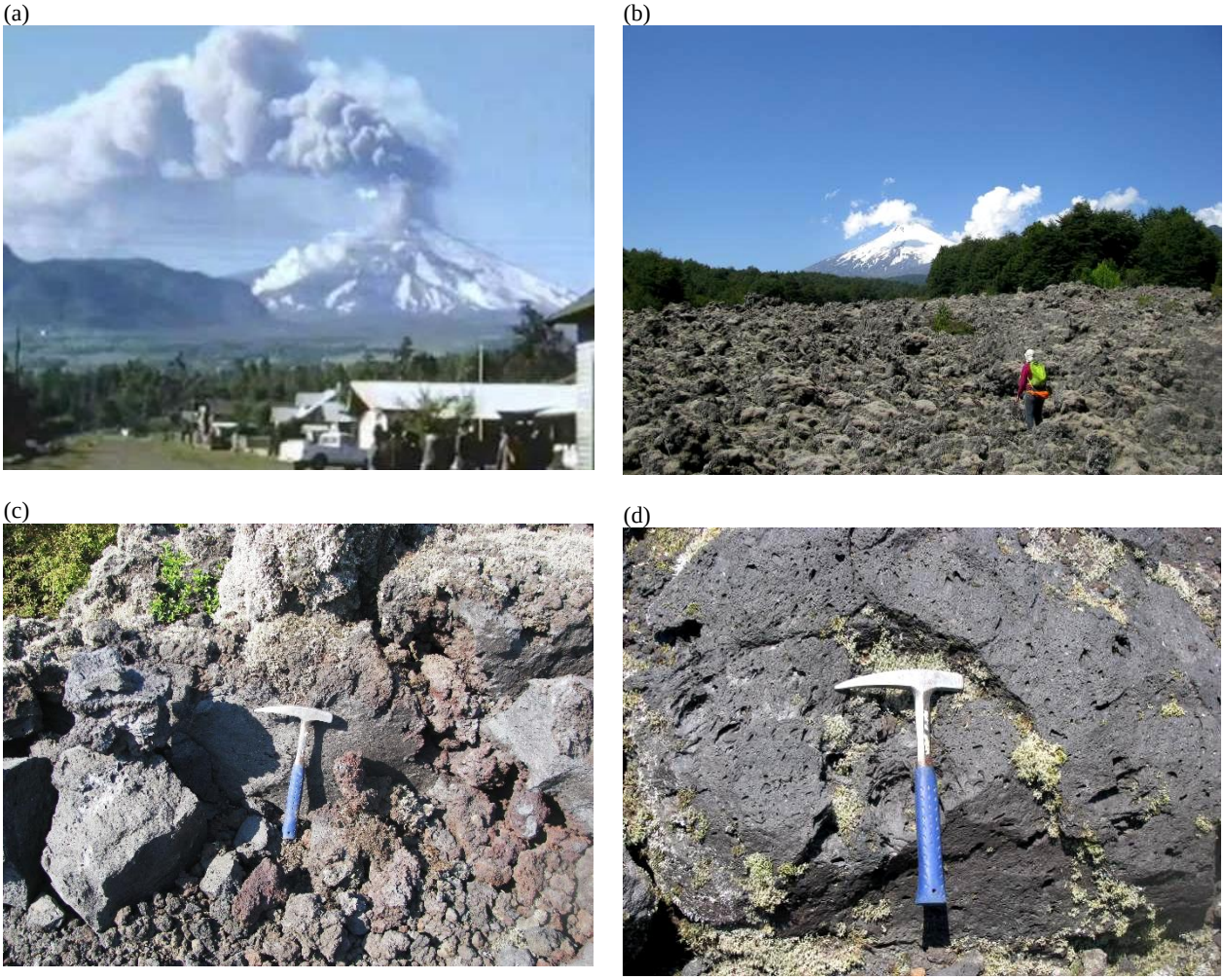

Fig. 1.4. Fotografías de la erupción y la lava de 1971. (a) Fotografía del 30 de Diciembre de 1971 desde Pucón, con la columna eruptiva de cerca de 3000 m de altura que se proyecta hacia el oriente (imagen de Franz Plötz); (b) Vista del valle Challupén (flanco SW) relleno por el flujo de lava de 1971; (c y d) ejemplos de muestras de roca aa seleccionadas.

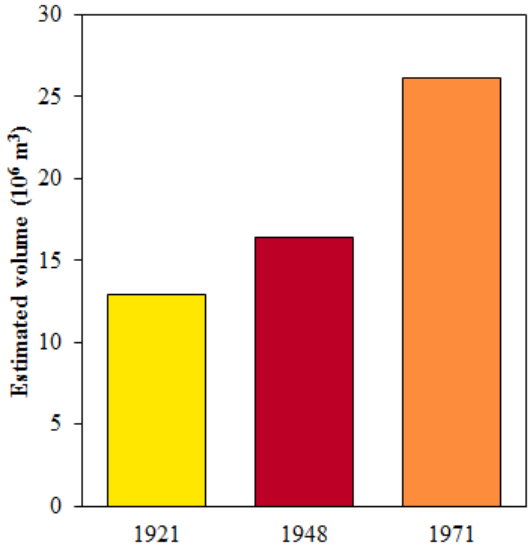

Fig. 1.5. Volúmenes estimados de los tres flujos de lava estudiados.

1.3. Objetivos

1.3.1. Objetivo general

Determinar las condiciones físicas del reservorio del Volcán Villarrica y los procesos involucrados en sus erupciones.

1.3.2. Objetivos específicos

Determinar y comparar la geoquímica de roca total y las abundancias, texturas y composiciones minerales.

Determinar las abundancias modales de plagioclasa de distinta composición.

Obtener los parámetros intensivos del sistema a través de geotermómetros y barómetros.

Simular las condiciones de formación de las composiciones de plagioclasa.

1.3.3. Hipótesis

Las condiciones físicas y los procesos magmáticos del reservorio del Volcán Villarrica han sido similares previo a las erupciones más importantes del siglo XX. Ocurrirían eventos de calentamiento (*thermal mixing*) con la incorporación de volátiles y ligeros cambios en la composición del magma (*compositional mixing*) que serían el producto de *cryptic mixing* entre el magma del reservorio y un magma de recarga más primitivo, caliente y rico en agua.

1.4. Metodología

Con el fin de determinar cuán homogéneas son las lavas estudiadas, se recolectaron 46 muestras (Tabla 1.1) de los flujos de lava de 1921 (7 muestras), 1948 (12 muestras) y 1971 (27 muestras) (Fig. 3.1). La campaña de terreno fue liderada por Eduardo Morgado y Claudio contreras, coautores del manuscrito producto de esta investigación (Capítulo 3). Las muestras de la lava de 1921 fueron recolectadas en las partes distales bien preservadas y en el frente del flujo de lava. Las muestras de las lavas de 1948 y 1971 fueron tomadas a lo largo de los, bien preservados, flujos de lava. Dependiendo del acceso y la existencia de levees, las muestras se recogieron al centro, en los levees o en los bordes del flujo.

Los volúmenes de las lavas (Fig. 1.5), ya presentados en la sección *1.2. Objeto de estudio y motivación*, fueron estimados multiplicando el área ocupada por la lava por un grosor constante representativo. El área fue obtenida con modelos de elevación digital (DEM) y la herramienta *Surface volumen* de la extensión *3D analyst* en *ArcGIS*. Los detalles de estos cálculos son presentados en la Tabla 1.2.

La composición de roca total de las 46 muestras fue analizada con XRF y ICP-MS, para los elementos mayores y trazas, respectivamente, en ACT-Labs, usando los estándares BIR-1a, DCN-1 y W-2a. La precisión fue superior al 9% (2σ) y la exactitud mayormente superior a 3%.

Los estudios petrográficos se llevaron a cabo con un microscopio electrónico de barrido (SEM) en la Universidad de Chile (FEI Quanta 250). Las composiciones de silicatos (plagioclasa, olivino y piroxeno) fueron obtenidas usando microanálisis de sonda electrónica (EPMA) en la *University of Exeter* (JEOL JXA-8200) y en la *University of Bristol* (Cameca SX100). Estas composiciones minerales fueron obtenidas para una muestra representativa de cada flujo de lava. Las condiciones analíticas para la JEOL JXA-8200 consistieron en un voltaje de aceleración de

15 kV, una corriente del haz de 15 nA y un tamaño del mismo de 2 µm. Los tiempos de conteo para cada elemento estuvieron en el rango de 20 a 40 segundos para la posición del *peak* y el mismo tiempo midiendo en el fondo. Para la Cameca SX100 las condiciones fueron un voltaje de aceleración de 20 kV, una corriente del haz de 10 nA y un tamaño del haz de 1 µm. Los tiempos de conteo fueron de 10-30 segundos en el *peak* y 5-15 segundos en el fondo. Para los análisis de piroxeno los valores de Fe^{2+} y Fe^{3+} fueron obtenidos siguiendo los procedimientos de Droop (1987).

Se obtuvieron mapas de rayos-X de calcio para los fenocristales de plagioclasa usando EPMA en la *University of Bristol* (JEOL JXA-8530F) con el propósito de obtener información de la distribución areal y las abundancias de este elemento. Las condiciones para obtener los mapas fueron un voltaje de aceleración de 20 kV, una corriente del haz de 200 nA, un *dwell time* de 2 ms, un tamaño del *spot* de 1 µm, una resolución de 2560 x 2560 pixeles con 8 µm del tamaño del *step* en los ejes X e Y. Para generar mapas de rayos-X calibrados a anortita fue necesario: (1) identificar y separar los fenocristales de plagioclasa del resto de la imagen, (2) calibrar las imágenes respecto al contenido de anortita y (3) colorear apropiadamente los mapas calibrados. El tratamiento de imágenes se realizó con los softwares ImageJ y MATLAB. Para identificar los cristales de plagioclasa se usaron mapas de Al. Debido a que la plagioclasa presenta contenidos de Al notoriamente distintos al resto de las fases (olivino, piroxenos, óxidos y vidrio), se seleccionaron los cristales de plagioclasa escogiendo los pixeles que estuvieran en un rango cercano a 129 en una escala de 1 a 256. Se aplicó está selección en los mapas de Ca, separando así las plagioclasas del resto de las fases. Para calibrar los mapas respecto al contenido de An, se utilizaron las composiciones de plagioclasa obtenidas con EPMA. Todos los mapas muestran una variación lineal entre la escala de grises y el contenido de An ($R^2 > 0.9$, Fig. 3.8) que permitió

obtener mapas de rayos-X calibrados a An. Finalmente, se aplicaron filtros de colores que resaltaran y diferenciaran visualmente las composiciones más abundantes.

Tabla 1.1. Ubicación de las muestras estudiadas. Datum WGS84.

Código	Huso	Coord. E	Coord. N	Código	Huso	Coord. E	Coord. N
1921 D04	18 H	755613	5617702	**RM 1971**	18 H	750281	5624119
R 1921 06	18 H	755961	5617945	**RMII 1971**	18 H	750281	5624119
1921 02	18 H	755916	5617961	**1971 N1**	18 H	750295	5624129
1921 03	18 H	756170	5618078	**1971 N2**	18 H	750414	5624275
1921 04	18 H	756933	5620463	**1971 02**	18 H	750387	5624340
1921 08	18 H	756733	5620383	**1971 03**	18 H	750589	5624595
1921 05	18 H	756326	5620417	**1971 04**	18 H	750911	5624952
1948 09	18 H	755158	5637722	**R 1971 04**	18 H	750941	5625123
1948 04	18 H	755415	5637440	**1971 N5**	18 H	751084	5625305
1948 05	18 H	755756	5637202	**1971 N4**	18 H	751115	5625332
1948 06	18 H	756094	5636946	**1971 05**	18 H	751156	5625479
1948 07	18 H	756267	5636800	**RM 1971 05**	18 H	751156	5625479
1948 08	18 H	756524	5636610	**1971 07**	18 H	751476	5625708
1948 10	18 H	758759	5635376	**1971 08**	18 H	751682	5625911
1948 11	18 H	759116	5635081	**1971 09**	18 H	752313	5626107
1948 12	18 H	759433	5634800	**1971 10 M1**	18 H	753273	5626752
1948 N1	18 H	760877	5634190	**1971 10 M2**	18 H	753273	5626752
1948 01	18 H	761175	5633888	**1971 11**	18 H	753635	5626907
1948 02	18 H	761393	5633634	**1971 12**	18 H	753871	5627261
1971 N6	18 H	750886	5624650	**1971 13**	18 H	754062	5627312
R 1971 DM	18 H	750897	5624634	**1971 30**	18 H	757403	5629565
R 1971 DV	18 H	750897	5624634	**1971 29**	18 H	757728	5629479
RC 1971	18 H	750281	5624119	**1971 28**	18 H	757978	5629495

Tabla 1.2. Detalle de los cálculos de volumen de lava.

Lava Flow	2D Area (m^2)		3D Area (m^2)		Espesor (m)		Estimated volume of lava (m^3)	
1921	12560686		12897120		1		13×10^6	
1948	1957068		2045146		8		16×10^6	
1971	**SW Flow**	**NE Flow**	**SW Flow**	**NE Flow**			**SW Flow**	**NE Flow**
	2465921	356118	2526923	381634	**SW Flow**	**NE Flow**	23×10^6	3.4×10^6
	Total		**Total**		9	9	**Total**	
	2822039		2908557				26×10^6	

Capítulo 2 : Resultados

2.1. Geoquímica de roca total

Las tres lavas analizadas (46 muestras) son basaltos y andesitas basálticas que se encuentran en un rango composicional restringido (51.7-52.4 wt. % SiO_2, 5.1-7.2 wt. % MgO, Fig. 2.1). Al compararlas con otros productos del Volcán Villarrica, se observa que se encuentran entre los productos más primitivos de este (Fig. 2.1). Si se utiliza el MgO como índice de diferenciación, se observa el siguiente orden creciente en el carácter primitivo: 1921 (~5.3 wt. % MgO), 1971 (~6.0 wt. % MgO) y 1948 (~7.0 wt. % MgO). El set de datos completo de composiciones de roca total se encuentra en Supplementary Data (Table A.1).

En cuanto a elementos mayores (Fig. 2.2), destaca el comportamiento de los álcalis (K_2O + Na_2O, 3.5 a 3.9 wt. %) que muestran una correlación negativa con el MgO. El Al_2O_3 muestra una correlación menos pronunciada y estricta que la anterior. Los óxidos mayoritarios Ti_2O (1.08 a 1.33 wt. %) y P_2O_5 (0.18 a 0.31 wt. %) presentan una tendencia ligeramente negativa con respecto al óxido de magnesio, con los valores de 1921 más altos que los de las otras dos lavas. El MnO (0.115 a 0.164 wt. %) presenta los valores más altos para la lava de 1921, intermedios para la de 1948 y los más bajos para la de 1971. El contenido de calcio (CaO: 9.3 a 9.7 wt %) es similar en las tres lavas, al igual que el de hierro (Fe_2O_3 y FeO).

En cuanto a elementos trazas (Fig. 2.3), destaca el comportamiento de Ni y Cr (elementos compatibles) que están correlacionados positivamente con el MgO. El Ba presenta el comportamiento inverso. Elementos como el Zr, V y La muestran una tendencia ligeramente negativa al aumentar el MgO, con los valores de la lava de 1921 mayores que los de las otras dos lavas. La razón Ba/Lu, un elemento móvil sobre uno inmóvil, podría dar cuenta de cuán alta (altas razones) o baja (bajas razones) es la adición de volátiles, y presenta una tendencia negativa

con el óxido de magnesio. Para el contenido de tierras raras (Fig. 2.4) se observa que la lava de 1948 está más empobrecida en estos elementos, seguida de la de 1971, siendo la de 1921 la más enriquecida. Las razones La_N/Yb_N fluctúan entre 1.94 y 2.67, y se observa una anomalía negativa de Eu para todas las muestras.

En síntesis, a pesar de que las muestras presentan un rango composicional acotado, hay ligeras diferencias que permiten diferenciar las tres lavas. Se destaca la correlación positiva de ciertos elementos compatibles (Ni, Cr) y la negativa de elementos incompatibles (K_2O, Na_2O y Ba) con el MgO, permitiendo establecer un gradiente en el grado de diferenciación, en orden ascendente: la lava de 1948, la de 1971 y la de 1921. No se observan variaciones significativas en la composición de roca total, ni en la petrografía (cristalinidad, mineralogía, texturas), en las muestras recolectadas en diferentes ubicaciones de las lavas.

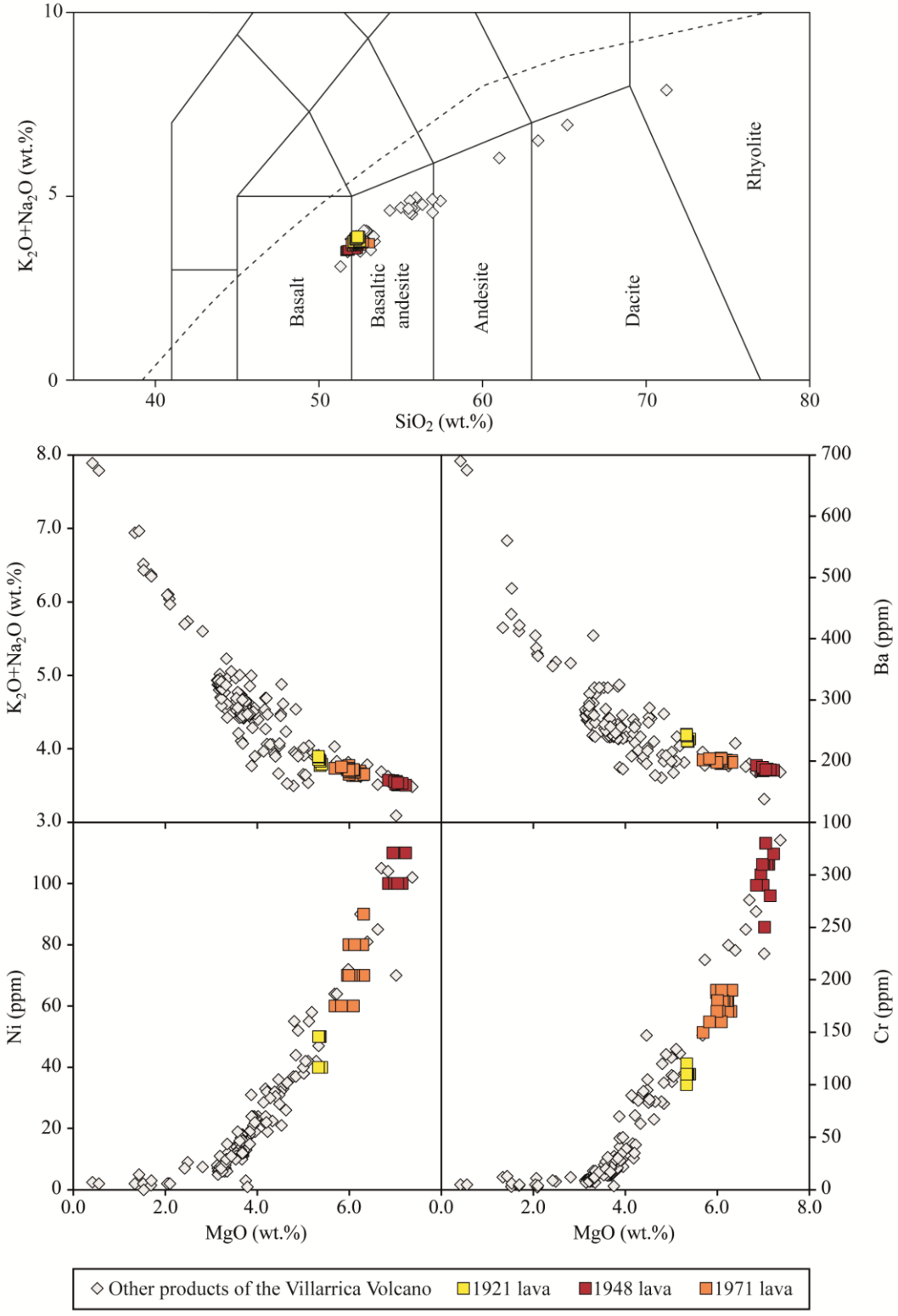

Fig. 2.1. Diagrama TAS y diagramas bivariantes de elementos seleccionados vs MgO de las muestras estudiadas y otros productos del Volcán Villarrica. Estos últimos datos fueron tomados de Hickey -Vargas *et al.*(1989) y Lohmar (2008). Cinco muestras de la lava de 1971 fueron tomadas de Morgado *et al.* (2015). Las divisiones del diagrama TAS fueron tomadas de Le Bas *et al.*, 1986.

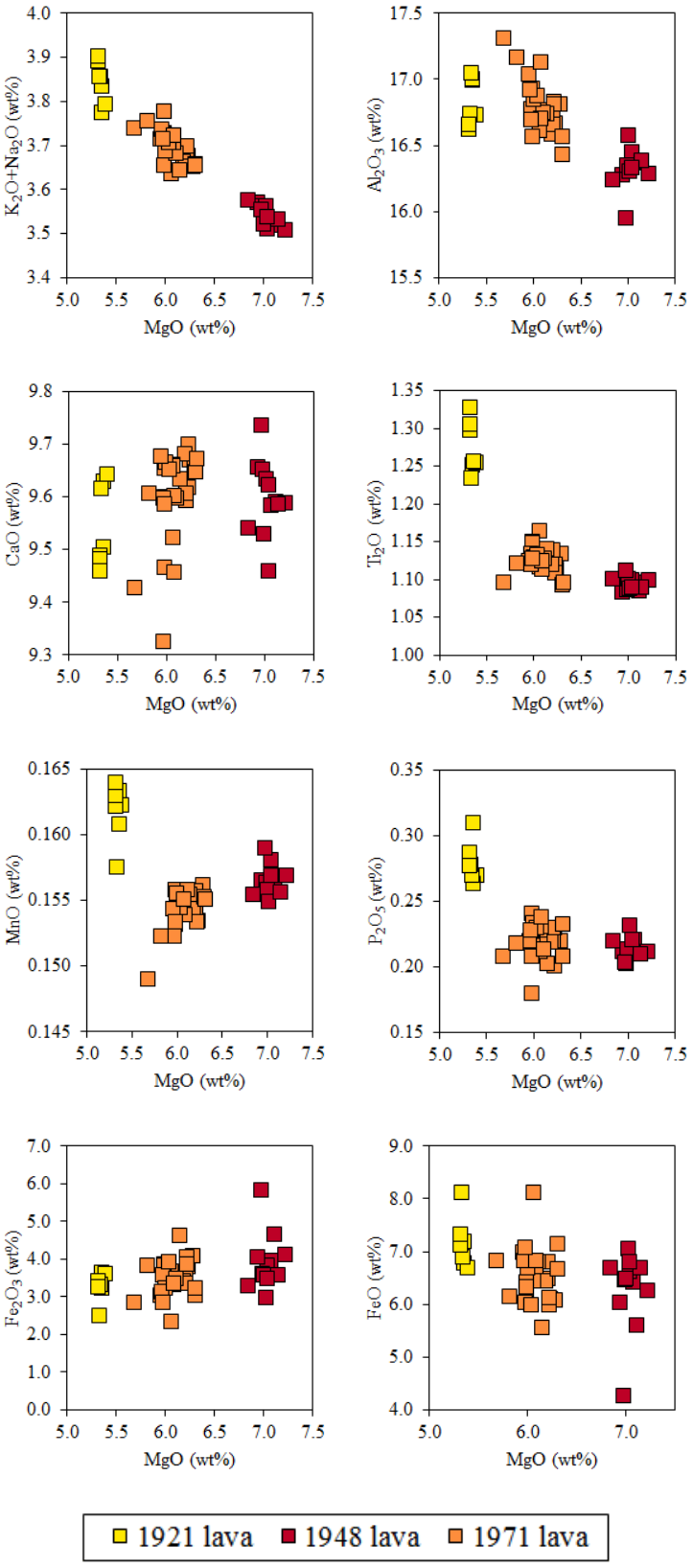

Fig. 2.2. Diagramas bivariantes de elementos mayores vs MgO.

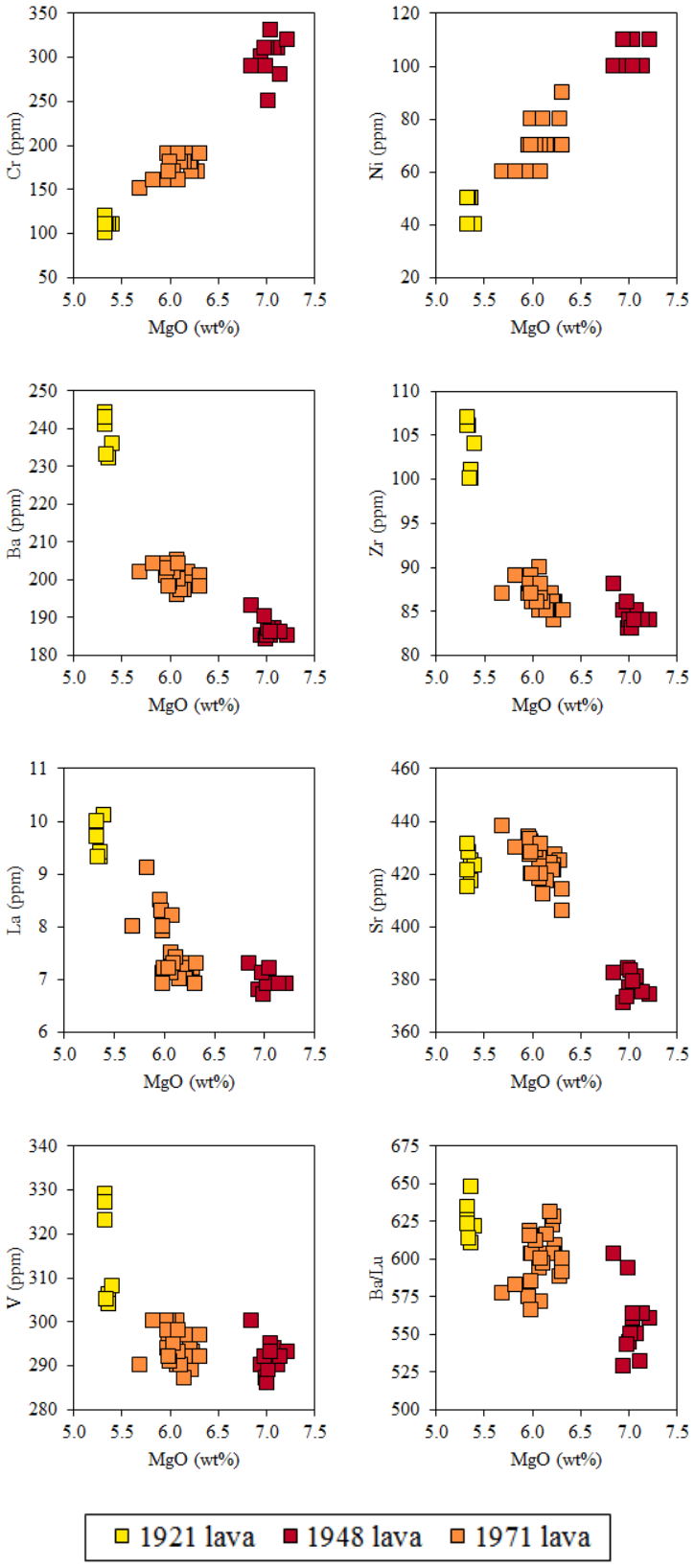

Fig. 2.3. Diagramas bivariantes de elementos trazas seleccionados vs MgO.

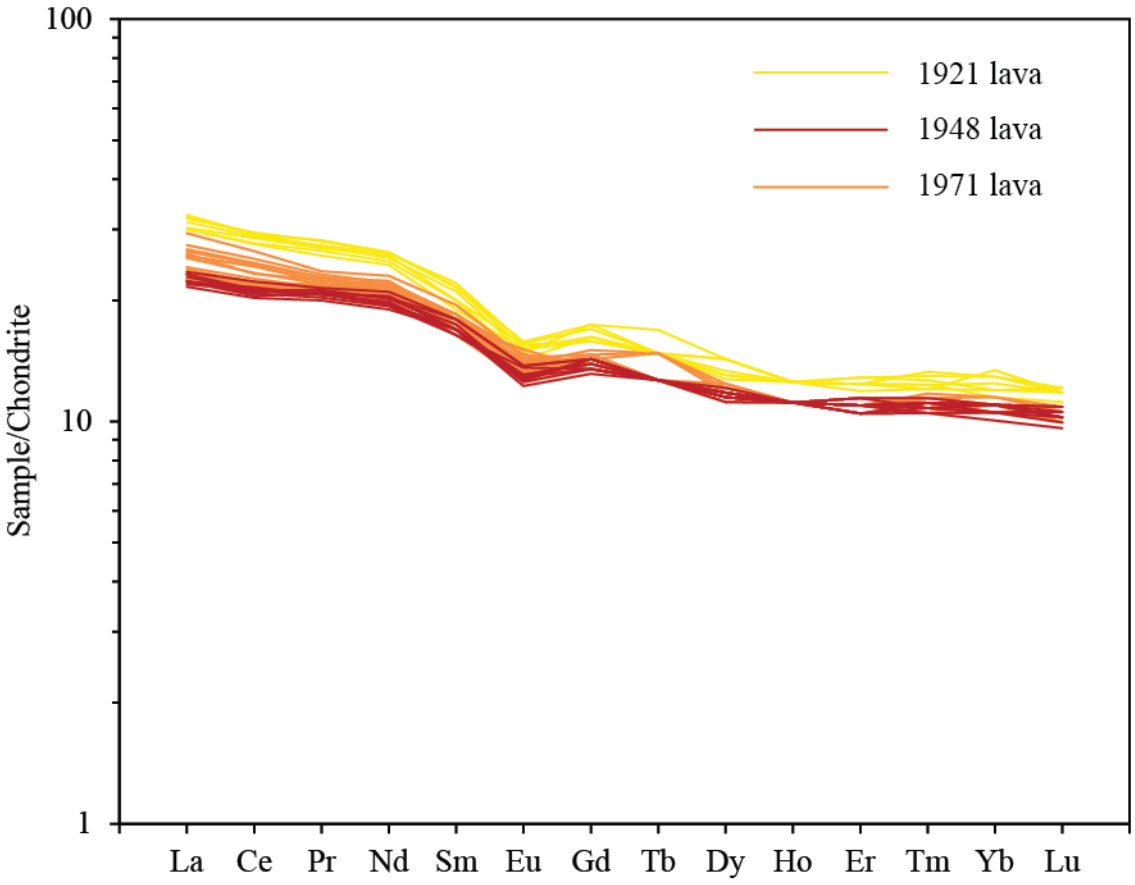

Fig. 2.4. Chondrite-normalized (Boynton, 1984) REE patterns.

2.2. Petrografía

Las lavas estudiadas (Fig. 2.5) presentan texturas porfíricas con fenocristales de plagioclasa (14-31 vol. %), olivino (3-9 vol. %), clinopiroxeno (< 4 vol. %) y un bajo contenido de cromo-espinelas. El contenido promedio de fenocristales es decreciente en el tiempo: 36 vol. % en 1921, 26 vol. % en 1948 y 20 vol. % en 1971 (Fig. 2.5). Los silicatos frecuentemente aparecen como *clots* (11-36 vol. %) y ocasionalmente como cristales aislados (3-14 vol. %). Los cristales de cromo-espinela aparecen como fenocristales aislados y como inclusiones en olivino. La razón promedio de cristales aislados/*clots* es: 0.21 en 1921, 0.58 en 1948 y 0.52 en 1971. La razón promedio máficos/plagioclasa es: 0.25 en 1921, 0.36 en 1948 y 0.23 en 1971. El detalle de las composiciones de fenocristales de silicatos se encuentra en la sección Supplementary Data (Table A.2, A.3 y A.4).

Las masas fundamentales (Fig. 2.6) de las lavas de 1948 y 1971 son similares, presentando texturas intergranulares con microlitos de plagioclasa (~60 vol. % de la masa fundamental), clinopiroxeno (~26 vol. %), titanomagnetitas (~2 vol. %), vidrio (~12 vol. %) y pequeñas cantidades de olivino (< 0.1 vol. %). La masa fundamental de la lava de 1921 tiene las mismas fases, pero presenta una textura intersertal (~35 vol. % de la masa fundamental es vidrio) con abundantes microlitos que muestran formas esqueletales y aciculares. El contenido de vesículas varía desde 1 a 22 vol. %. Las composiciones de los microlitos de plagioclasa (Fig. 2.7a) (cristales < 100 μm) son: An_{50-60} para 1921, An_{56-72} para 1948 y An_{50-61} para 1971. Los microlitos de clinopiroxeno (Fig. 2.7b) tienen composiciones: Wo_{14-39}, En_{44-65}, Fs_{16-24}. Los escasos microlitos de olivino (Fig. 2.7c) tienen composiciones de Fo_{68-79}. El detalle de estas composiciones se encuentra en los anexos A1, A2 y A3.

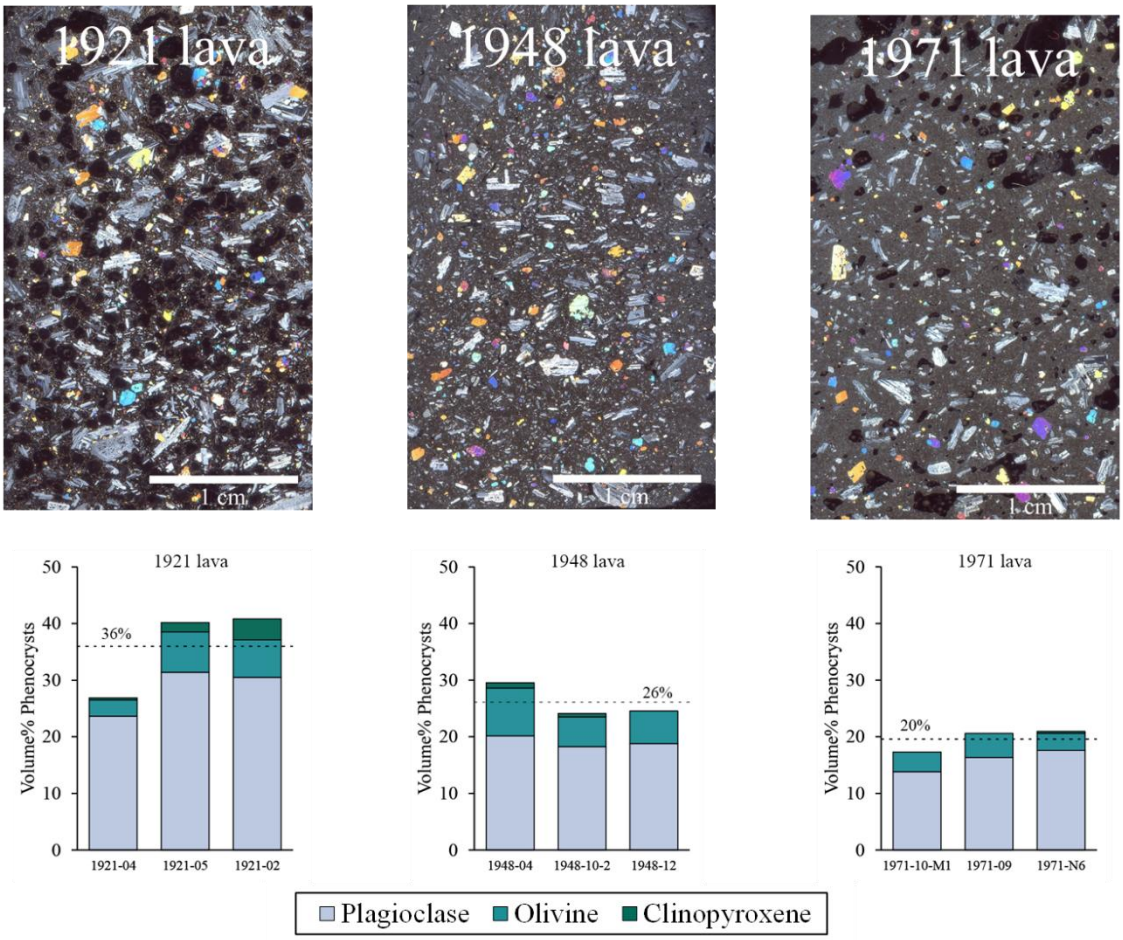

Fig. 2.5. Imágenes de las láminas delgadas representativas de las tres lavas estudiadas y el contenido modal de fenocristales, estimados por conteos de puntos usando el software JMicroVision, normalizado libre de vesículas. Las líneas punteadas corresponden al porcentaje de volumen modal promedio.

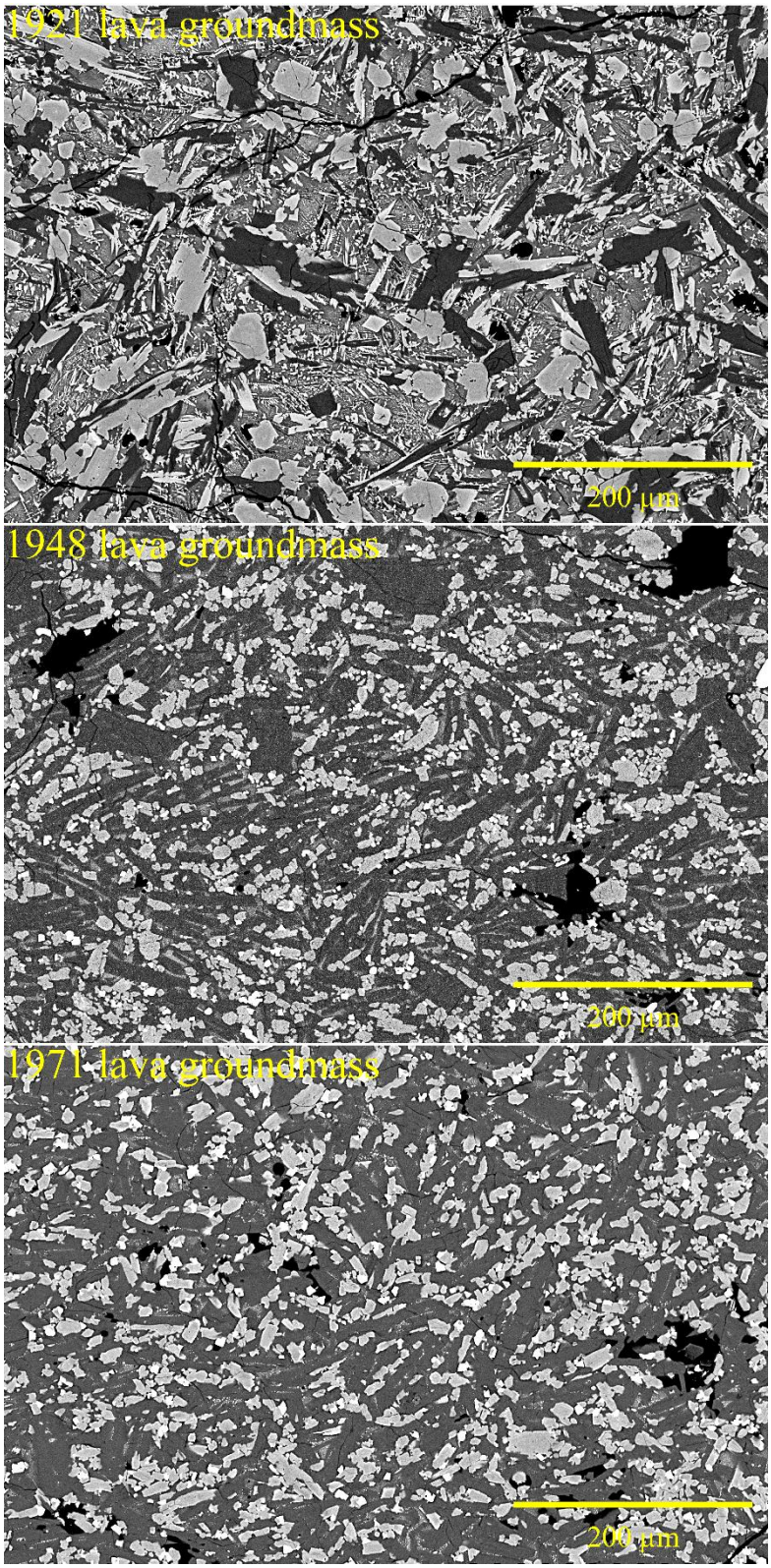

Fig. 2.6. Imágenes BSE de las masas fundamentales de las tres lavas estudiadas.

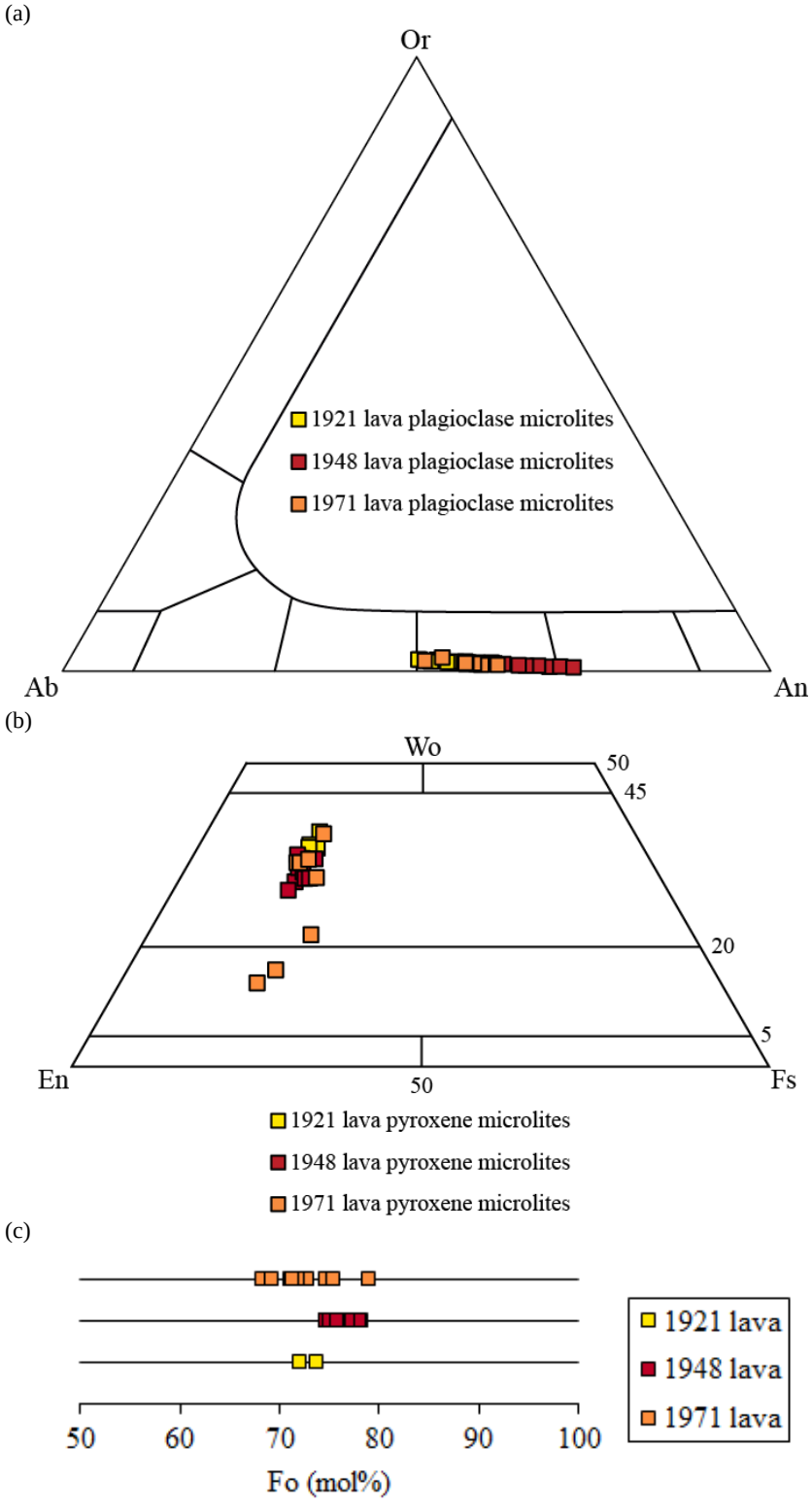

Fig. 2.7. Composiciones minerales de la masa fundamental. (a) Microlitos de plagioclasa; (b) mcrolitos de piroxeno; (c) microlitos de olivino.

2.2.1. Composiciones y texturas de plagioclasa

Se observan dos grupos de composiciones de plagioclasa en todas las lavas: pobres en An (An_{57-69}) y ricas en An (An_{76-89}). Las abundancias relativas de estas composiciones fueron obtenidas con mapas de rayos-X calibrados a An de muestras de las tres lavas (Fig. 3.6, 3.7 y 3.8) y se presentan en histogramas de frecuencia (Fig. 3.5). Las composiciones pobres en An son las más abundantes en todas las lavas, con un *peak* principal alrededor de An_{60}. También se observa en los histogramas un modesto *peak* secundario de alto contenido de An (c. An_{80}). La razón entre la frecuencia de los *peaks* rico en An/pobre en An varía de la siguiente manera: 0.06 en 1921, 0.23 en 1971 y 0.45 en 1948. Los fenocristales de plagioclasa en las tres lavas tienen similares composiciones de elementos menores y trazas (Fe, Ti y Mg) y muestran una ligera correlación negativa de Fe con An, y una fuerte correlación negativa entre Ti y Mg con An (Fig. 2.8).

Los grupos composicionales están directamente relacionados a texturas específicas de fenocristales. Las composiciones pobres en An están asociadas a cristales limpios con zonaciones oscilatorias (Fig. 2.9, 3.6a, 3.7a, 3.8a). Los fenocristales más pequeños de plagioclasa son generalmente de estas composiciones, sin embargo, las composiciones pobres en An también ocurren como nucleos limpios y/o bordes de cristales con zonaciones más complejas que muestran texturas de desequilibrio con composiciones ricas en An (Fig. 2.10, 3.6c, 3.7c, 3.8c). Las composiciones más cálcicas comúnmente forman parte de núcleos con textura sieve (Fig. 3.6c, 3.7c, 3.8c), pero también ocurren como zonas intermedias de fenocristales (Fig. 3.6b, 3.7b, 3.8b) o como cristales aislados no-zonados. En los fenocristales zonados, las zonas ricas en An muestran texturas *boxy* o *spongy cellular* (Streck, 2008), que consisten en una red de gotas de vidrio en la plagioclasa cálcica. Aparecen asociados a parches pobres en An y ocasionalmente tienen inclusiones minerales (olivino, clinopiroxeno, cromo-espinela).

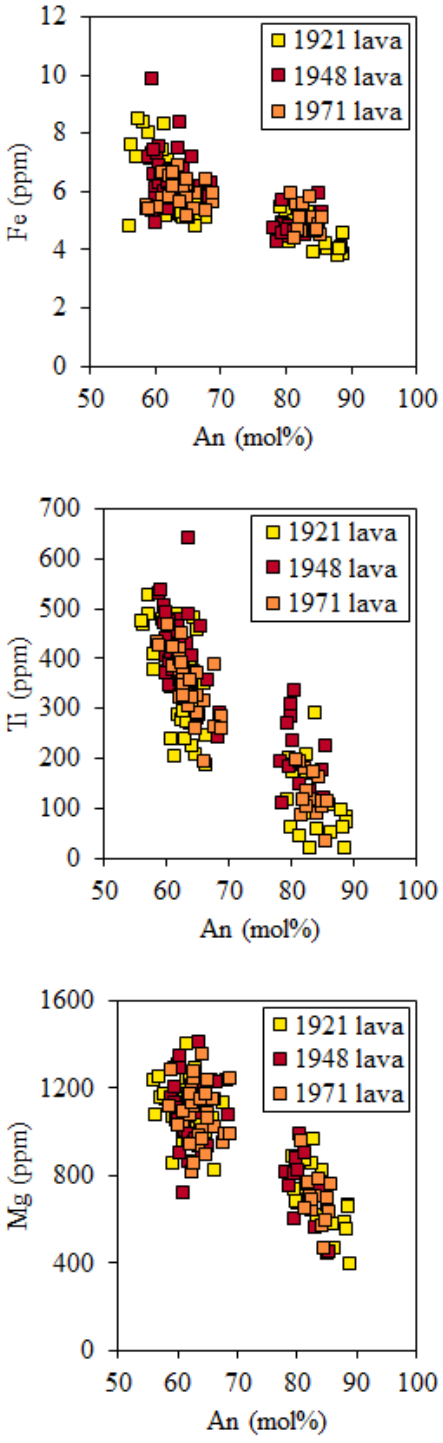

Fig. 2.8. Contenido de An vs elementos menores y traza (Fe, Ti, Mg) de los fenocristales de plagioclasa de las tres lavas.

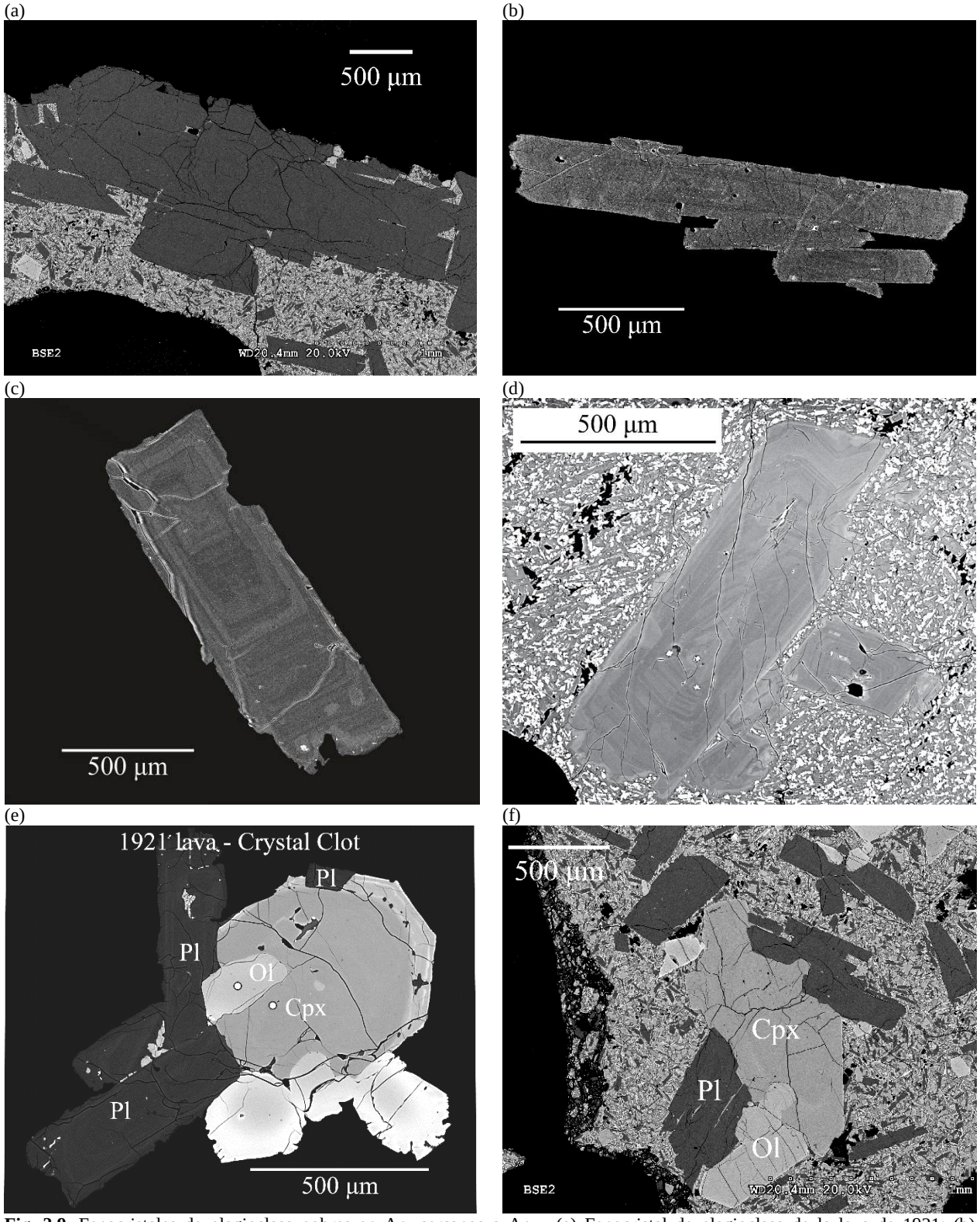

Fig. 2.9. Fenocristales de plagioclasa pobres en An, cercanos a An_{60}. (a) Fenocristal de plagioclasa de la lava de 1921; (b) fenocristal de plagioclasa de la lava de 1948; (c y d) fenocristales de plagioclasa de la lava de 1971; (e y f) fenocristales de plagioclasa formando *clots* con olivino y clinopiroxeno.

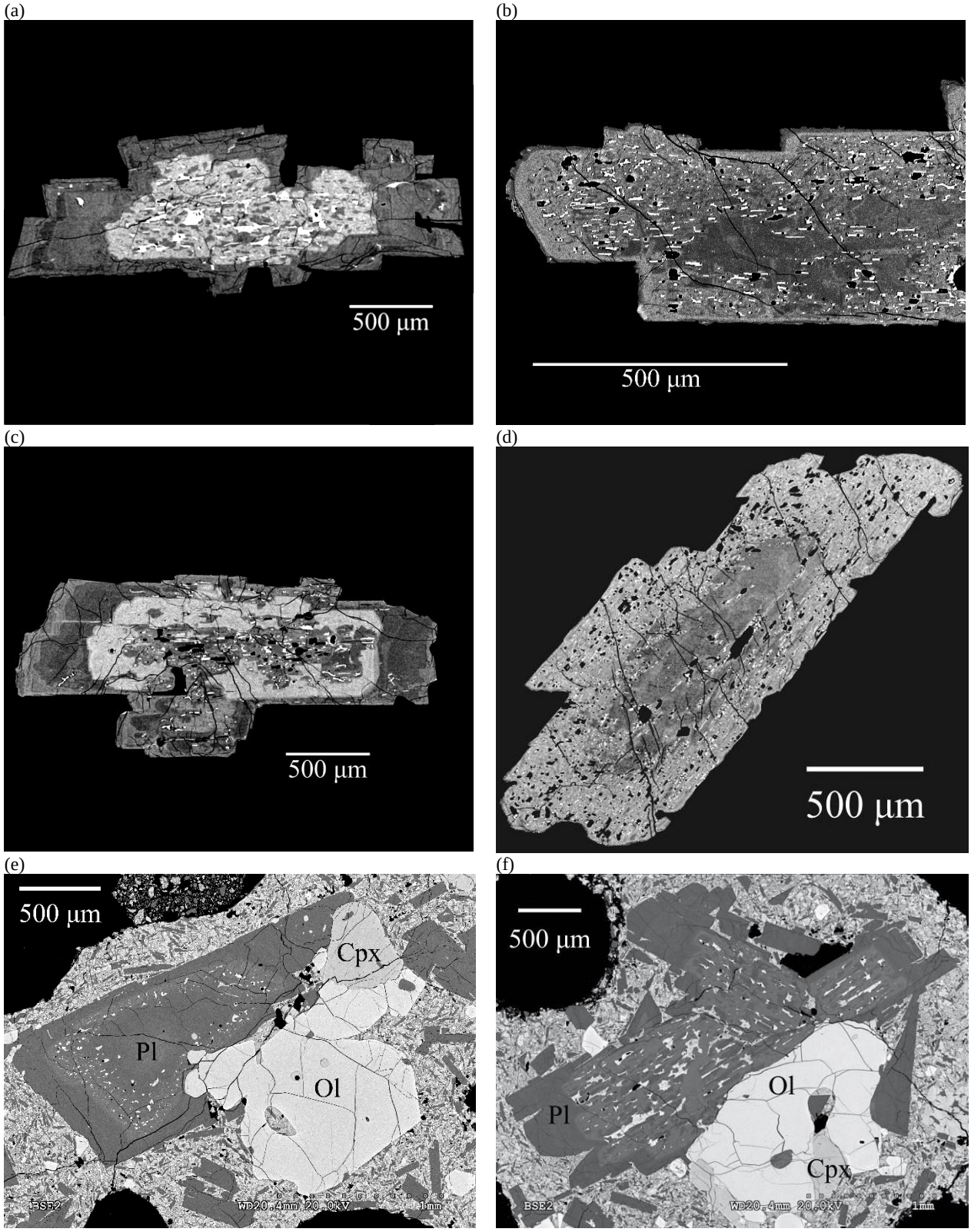

Fig. 2.10: Fenocristales de plagioclasa con zonas pobres (gris oscuro) y zonas ricas (gris claro) en An, cercanas a An_{60} y An_{80}, respectivamente. (a) Fenocristal de plagioclasa de la lava de 1921; (b) fenocristal de plagioclasa de la lava de 1948; (c y d) fenocristales de plagioclasa de la lava de 1971; (e y f) fenocristales de plagioclasa formando *clots* con olivino y clinopiroxeno.

2.2.2. Composiciones y texturas de minerales máficos

Los fenocristales de olivino son anhedrales a subhedrales (0.05-1.6 mm), usualmente con texturas de reabsorción y ligeros cambios composicionales. Aparecen como cristales aislados o formando *clots* con otros olivinos, clinopiroxenos y/o plagioclasas. El contenido de forsterita en los núcleos y las zonas intermedias de los cristales es ligeramente diferente en las tres lavas y está positivamente correlacionado con el Mg# (Mg# = molar $100\times Mg/Mg(Mg+Fe^{2+})$) de la roca hospedante: Fo_{71-78} en 1921 (Mg#: 57), Fo_{76-83} en 1948 (Mg#: 66) y Fo_{74-79} en 1971 (Mg#: 62). Las inclusiones de cromo-espinelas son abundantes en los fenocristales de olivino de 1948 (Fig. 2.11b), menos abundantes en 1971 y muy escasos o ausentes en 1921 (Fig. 2.11a). Esta variación modal se correlaciona con el contenido de Cr de la roca total. Las composiciones de cromo-espinelas disponibles en la lava de 1971 corresponden a Mt_{33-44} con #Cr = 53-62 y #Mg = 26-30 (Morgado *et al*., 2015).

Los fenocristales de clinopiroxeno son anhedrales a subhedrales (0.05-2.4 mm) y siempre están formando clots con olivino y, menos frecuentemente, con plagioclasa (Fig. 2.11c-e). Los clinopiroxenos de todas las muestras de lava tienen un rango restringido de composiciones (Wo_{33-43}, En_{47-52}, Fs_{10-15}) y Mg# (0.78-0.87 en 1921, 0.78-0.91 en 1948 y 0.79-0.86 en 1971). Los clinopiroxenos de la lava de 1948 difieren de aquellos de las otras muestras de lava debido a que tienen una reabsorción pervasiva, zonas anhedrales de ortopiroxeno (Wo_{4-5}, En_{74-77}, Fs_{18-22}) y ocurren como *clots* con olivino sin plagioclasa (Fig. 2.11e-f).

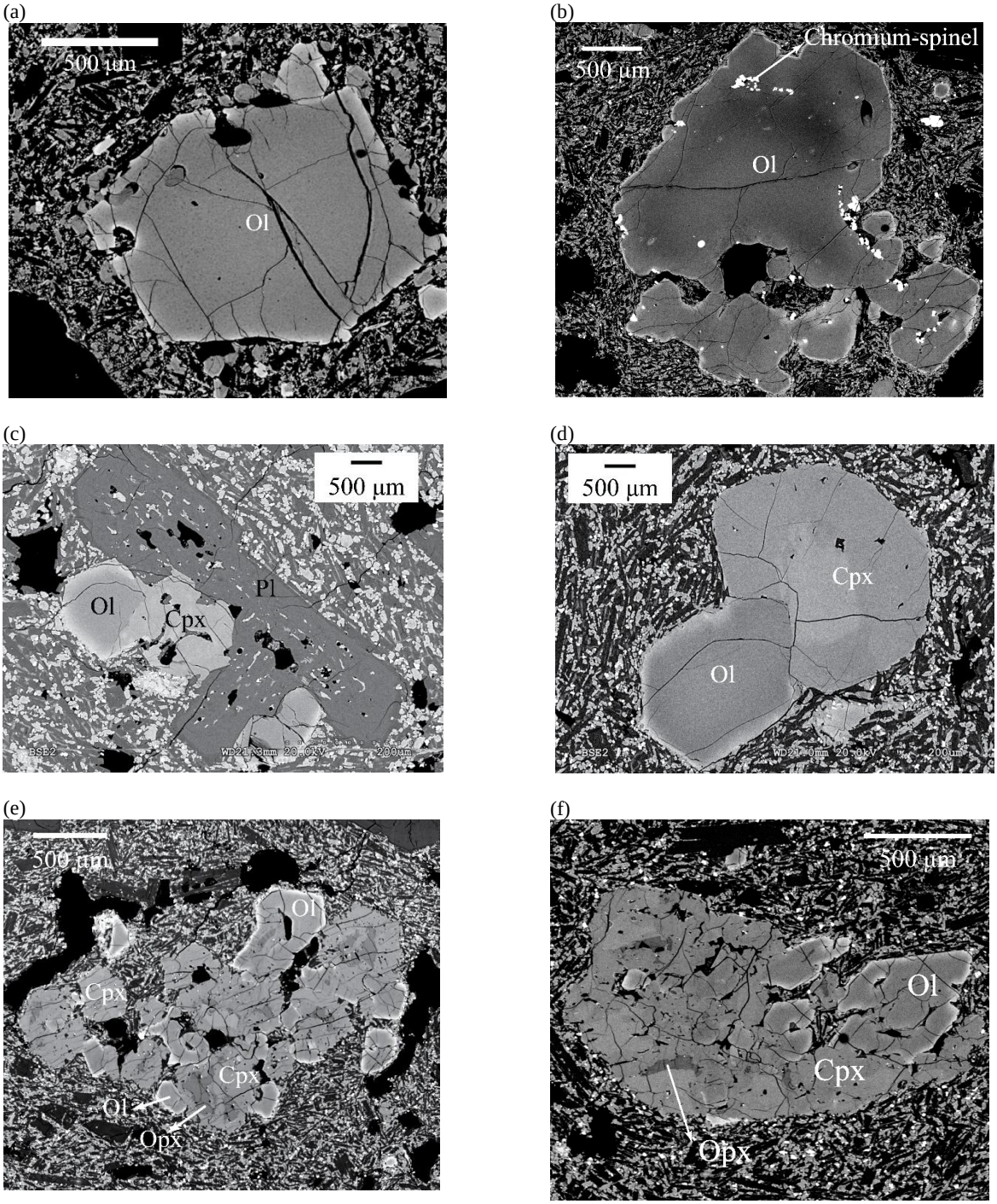

Fig. 2.11. Fenocristales máficos. (a) Fenocristal de olivino de la lava de 1921 sin inclusiones de óxidos; (b) fenocristales de olivino de la lava de 1948 con abundantes inclusiones de cromo-espinela; (c) *clot* de plagioclasa, olivino y clinopiroxeno de la lava de 1948; (d) *clot* de olivino y clinopiroxeno de la lava de 1948; (e y f) *clots* de olivino, clinopiroxeno y ortopiroxeno de la lava de 1948.

2.3. Termobarometría

El geotermómetro de intercambio de Mg-Fe en olivino-augita (Loucks, 1996) y el geobarómetro de intercambio de Ca en olivino y clinopiroxeno (Köhler & Brey, 1990) fueron usados en 30 pares de olivino y clinopiroxeno que ocurren en dos grupos de *clots* cristalinos: *clots* de olivino, clinopiroxeno y plagioclasa (presentes en todas las lavas) y *clots* de olivino y clinopiroxeno (presentes solo en la lava rica en Mg de 1948). El detalle de estos cálculos se presenta en Table 3.4. Las condiciones de equilibrio entre los pares de olivino y clinopiroxeno fueron testeadas tal como lo hicieron Morgado *et al.* (2015), es decir, usando los valores de Fe/Mg para determinar si ambos minerales están en equilibrio con la misma composición de melt, de acuerdo a las ecuaciones de Grove *et al.* (1997) (Fig. 2.12). Para el grupo de los *clots* de ol-cpx-pl (Fig. 3.9a, b) se obtuvieron temperaturas similares para todas las lavas (Fig. 3.10a), en promedio 1092 ºC (1077-1107 ºC ± 6 ºC para 1921, 1089 ºC ± 6 ºC para 1948, 1077-1099 ºC ± 6 ºC para 1971). El grupo de los *clots* de ol-cpx, presente solo en la lava de 1948, dio temperaturas superiores de ~1194 ºC (1190-1200 ºC ± 6 ºC, Fig. 3.9c) y un valor de temperatura de 1174 ºC ± 6 ºC. El geobarómetro solo dio valores positivos en el grupo de los clots de ol-cpx (Fig. 3.10b): ~3.3 ± 1.7 kbar (2.9-3.6 ± 1.7 kbar; ~12 km ± 6.17 km) y un valor de presión de 0.6 ± 1.7 kbar (2 km ± 6.17 km).

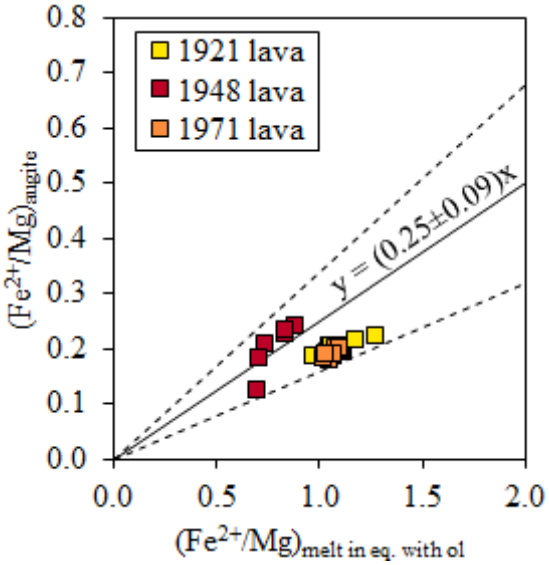

Fig. 2.12. Filtro de equilibrio de máficos en *clots*. Se evalúa el equilibrio de la augita con un *melt* que está en equilibrio con olivino, en términos de las razones Fe2+/Mg de acuerdo a las ecuaciones de Grove *et al*. (1997).

2.4. Simulación termodinámica

Con el objetivo de constreñir las condiciones termodinámicas de cristalización de plagioclasa (composiciones pobres en An y ricas en An), se usa MELTS (Asimow & Ghiorso, 1998; Ghiorso & Sack, 1995) asumiendo dos cosas: (1) un sistema cerrado (es decir, con composición química constante) y (2) las temperaturas de cristalización de la plagioclasa pobre en An corresponden a aquellas obtenidas con *clots* de plagioclasa-olivino-clinopiroxeno (~1092 °C). El primer supuesto se justifica debido al limitado rango composicional de las lavas históricas del Villarrica y los resultados de las composiciones de Fe vs An (correlación ligeramente negativa), interpretada como el resultado de *thermal mixing* en un sistema cerrado, como lo sugieren Ruprecht & Wörner (2007).

En primer lugar, se utilizó la geoquímica de una de las muestras más primitivas de las lavas históricas (1948-04) como la composición inicial del líquido en las simulaciones. Se asumieron las condiciones de buffer cuarzo-fayalita-magnetita (QFM) tal como fue sugerido por Lohmar *et al.* (2012). Se realizaron simulaciones a distintas presiones y con diferentes contenidos de agua (Fig. 2.13). Bajo ninguna condición se puede reproducir el paso de las composiciones pobres en An (~An_{60}) a las ricas en An (~An_{80}) aumentando solo la temperatura. Sí se podría, eventualmente, aumentando, además de la temperatura, el contenido de agua en condiciones subsaturadas. Por lo tanto, se realizó un segundo set de modelos usando otra composición del líquido más primitiva. Se utilizó la muestra más primitiva disponible del Villarrica (V2-8; Hickey -Vargas *et al.*, 1989) como composición del líquido inicial para las siguientes simulaciones (Fig. 2.14). Con este líquido sí es posible reproducir el paso de An_{60} a An_{80} aumentando solamente la temperatura en un amplio rango de presiones: desde cercanas a 1 atm (0.02 kbar) hasta 3.5 kbar. Siendo consistente con estimaciones previas de la presión del reservorio (Lohmar *et al.*, 2012; Morgado *et al.*, 2015), se decide utilizar una presión de 0.5 kbar como representativa del sistema.

Bajo estas condiciones, existen tres escenarios para reproducir los cambios desde ~An_{60} a ~An_{80} con la subsecuente restauración de las condiciones pobres en An. Estos resultados son analizados y discutidos en el siguiente capítulo (*3.7.1 Interpretation of plagioclase compositions and textures*).

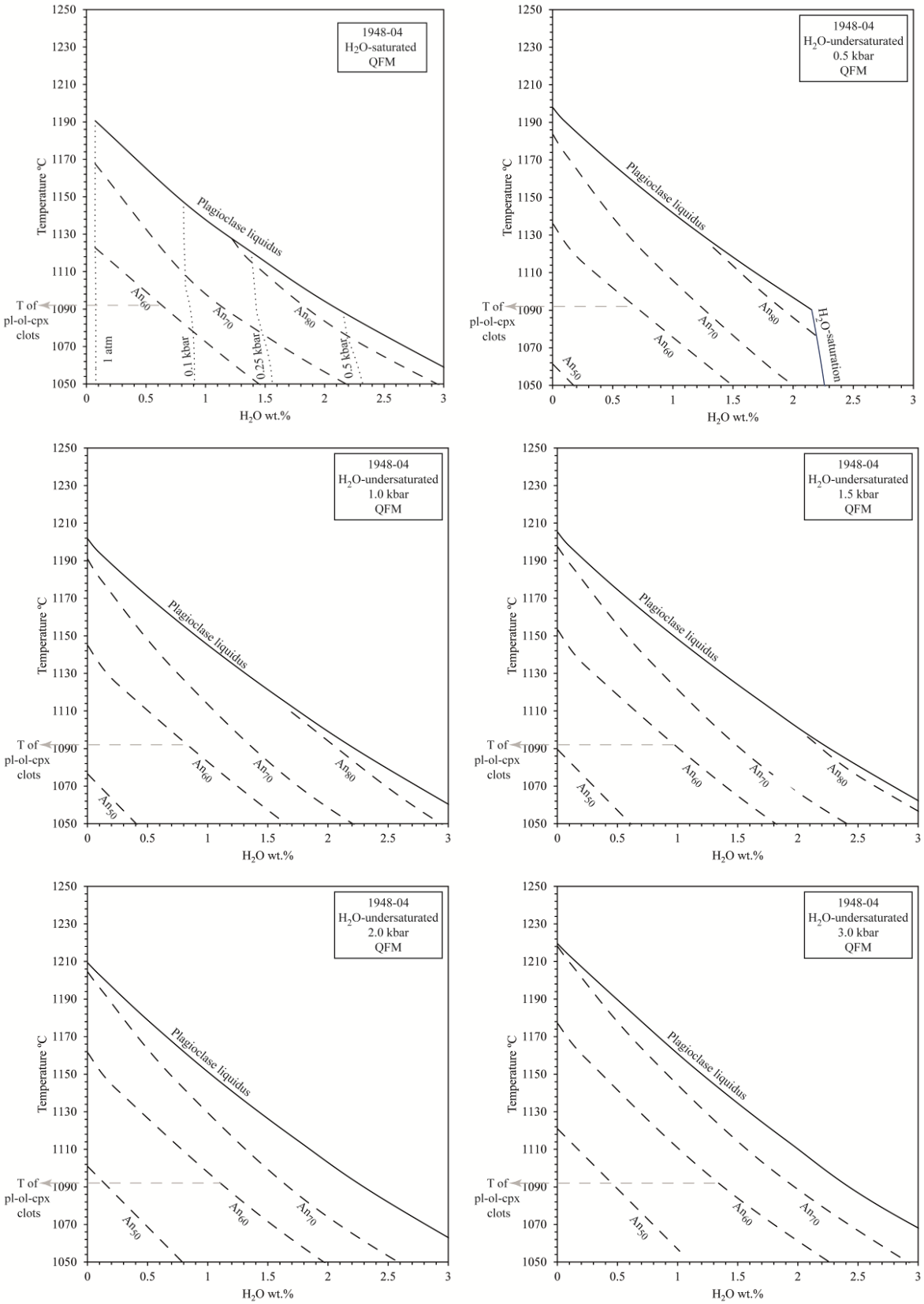

Fig. 2.13. Composiciones de equilibrio de plagioclasa para distintas presiones como función de la temperatura y el contenido de agua obtenido con MELTS. La composición inicial es la geoquímica de roca total de la muestra 1948-04 y la fO_2 corresponde al buffer QFM.

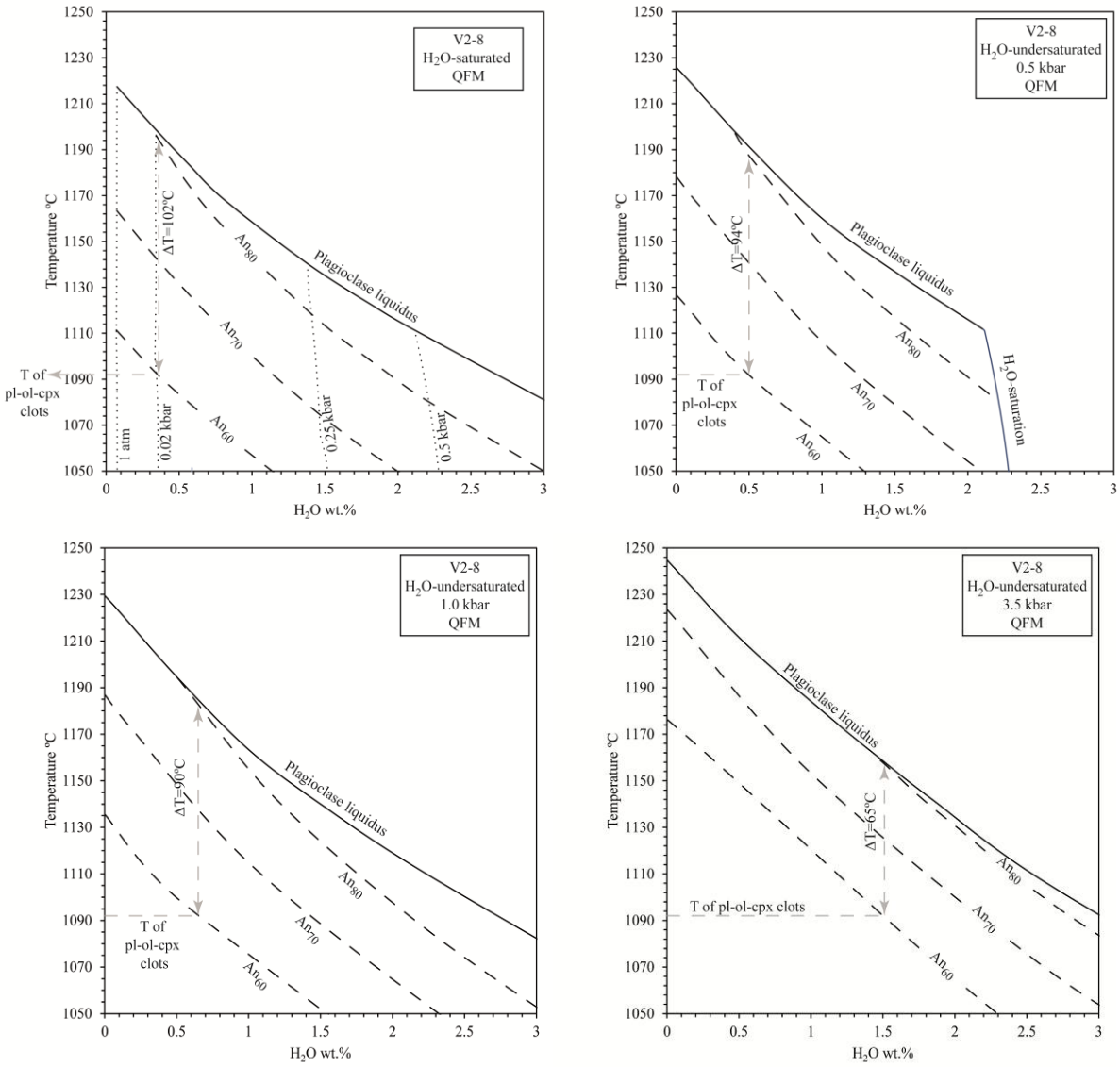

Fig. 2.14. Composiciones de equilibrio de plagioclasa para distintas presiones como función de la temperatura y el contenido de agua obtenido con MELTS. La composición inicial es la geoquímica de roca total de la muestra V2-8 (Hickey -Vargas *et al*., 1989) y la fO_2 corresponde al buffer QFM.

Capítulo 3 Cryptic magma recharge associated with 20th century eruptions at Villarrica Volcano

Christian Pizarro[1, 2, *], Miguel A. Parada[1, 2], Claudio Contreras[1, 2, 3], Eduardo Morgado[1, 2, 4]

[1]*Departamento de Geología, Facultad de Ciencias Físicas y Matemáticas, Universidad de Chile, 803 Plaza Ercilla, 8370450 Santiago, Chile.*

[2]*Centro de Excelencia en Geotermia de los Andes (CEGA), Universidad de Chile, 803 Plaza Ercilla, 8370450 Santiago, Chile.*

[3]*School of Earth Sciences, University of Bristol, Wills Memorial Building, Bristol BS8 1RJ, UK*

[4] *Institute of Geophysics and Tectonics, School of Earth and Environment, University of Leeds, Leeds LS2 9JT, UK*

*Corresponding author at: christian.pizarro@ug.uchile.cl; Centro de Excelencia en Geotermia de los Andes (CEGA), Universidad de Chile, 803 Plaza Ercilla, 8370450 Santiago, Chile.

Declarations of interest: none

Abstract

The Villarrica volcano is one of the most active volcanoes of the Andes (rest cycles of ~5.3 years) by erupting products of basaltic to basaltic-andesite compositions and styles from Hawaiian to Vigorous Strombolian. These features make it a remarkable place to determine the pre-eruptive parameters and processes involved in their eruptions. We compare whole-rock geochemistry and mineral abundances, textures and compositions of the most relevant basaltic lavas of the 20th century, which were erupted in 1921, 1948 and 1971. The analysed lavas show a restricted range in whole-rock compositions (51.7-52.4 wt. % SiO_2), but an increasing trend of MgO content is observed as follow: ~5.3 wt. % MgO (1921), ~6.0 wt. % MgO (1971) and ~7.0 wt. % MgO (1948). Two groups of plagioclase compositions are observed in all lavas: An-poor (~An_{60}) and An-rich (~An_{80}). An-poor compositions are the most abundant in all lavas and were commonly formed in both the earliest (cores) and latest stages (external rims and small and nearly unzoned phenocrysts) of plagioclase crystallization, whereas An-rich plagioclases were formed around An-poor cores during intermediate stages. Equilibrium temperatures of plagioclase-olivine-clinopyroxene of about 1090°C were obtained in crystal clots of the three lavas. Thermometry calculations obtained from MELTS simulations of plagioclase formation indicate a heating (thermal mixing) of the reservoir at ~0.5 kbar of up to 100 °C with respect to the crystal clots temperatures. Incorporation of small amounts of volatile-rich and hotter mafic magma of similar composition (cryptic mixing) into the Villarrica reservoir, could also heat it, probably in a more efficient way than heat conduction alone. A longer interaction of the hot mafic magma within the reservoir could cause crystallization of An-rich plagioclase, dissolution of An-poor plagioclase (i.e. increase in An-rich/An-poor modal content ratios) and compositional modifications toward MgO-rich and volatile-rich compositions, that ultimately result in higher intensity of eruption.

Keywords

Villarrica Volcano, Basalt, Plagioclase, Thermal mixing, Cryptic mixing

3.1. Introduction

The Villarrica volcano is located in the Chilean Southern Andes (39º25'S, 71º57'W) close to the N-S intra-arc Liquiñe-Ofqui Fault Zone, and at the western extreme of the NW-SE volcanic chain formed by Villarrica, Quetrupillán and Lanín volcanoes (López-Escobar *et al.*, 1995; Cembrano *et al.* 1996; Stern *et al.*, 2007). Its height is 2847 m a.s.l., and covers an area of ca. 400 km^2 reaching an estimated volume of 250 km^3. The volcano was built over scarce Paleozoic-Upper Triassic metasedimentary rocks, abundant Meso-Cenozoic plutonic rocks and Cenozoic volcanic and volcanoclastic rocks. Its eruptive activity started ca. 600,000 years ago and produced basalts and basaltic andesite lava flows, pyroclastic and lahar deposits that were divided into three units: Villarrica I (Middle to Upper Pleistocene), Villarrica II (Holocene, between 13900 and 3700 y BP) and Villarrica III (3700 y BP to the Present) (Moreno and Clavero, 2006). The last unit comprises a historical record of eruptions, including: 1787, 1921, 1948, 1963, 1964, 1971 and 1984 eruptive episodes. Two major explosive events, of mafic to intermediate compositions, have been recognized in the development of Villarrica: Licán (13.9 ky BP, ~10 km^3, non-DRE, Clavero and Moreno, 1994; Lohmar *et al.*, 2012) and Pucón Ignimbrites (3.7 ky BP, ~3 km^3, non-DRE, Clavero and Moreno, 1994). The Villarrica volcano is one of the most actives of the Andes, recording 88 VEI $\geq$ 2 eruptions between 1523 and 1991, with an average of one eruption (VEI $\geq$ 2) every 5.3 years (Van Daele *et al.*, 2014). Historical eruption styles range from Hawaiian to Vigorous Strombolian with basaltic to basaltic-andesite products (Moreno and Clavero, 2006). Since the end of the last eruption of the 20^{th} century (1985), Villarrica Volcano has maintained an active lava lake in its summit crater that continuously degassed (Moreno and Clavero, 2006) without effusion of lava flows (Witter *et al.*, 2004), however lava spattering and

emission of fine-grained tephra from the summit crater intermittently occur. The last eruption of Villarrica was on March 3, 2015 and it was a short (< 1 hour) and intense strombolian eruption with 4.7 x 10^6 m^3 (DRE) of erupted material (Bertin *et al.*, 2015).

Pre-eruptive conditions of particular events of the Villarrica volcano have been estimated from petrological approaches. Witter *et al.*, 2004 studied samples of the lava lake (2000 reticulite) and suggested that all crystallization occurred at P < 0.17 kbar, T = ~1135 ºC, fO_2 = NNO, under water-saturated conditions. Lohmar *et al.* (2012) identified a heating and degassing associated with the ~13 ky Licán Ignimbrite from ~900 to ~1100ºC, at P < 0.67 kbar, fO_2 slightly higher than QFM, and a water content that decrease from ~3.2 to ~1.5 wt.% H_2O. Morgado *et al.* (2015) studied the 1971 Villarrica lava identifying two reservoirs: a deep-seated reservoir coincident with a range depth equivalent to the mantle-crust boundary and T = ~1208 ºC; and a shallow reservoir at the upper crust with T of ~1170 ºC. In this paper we investigate three basaltic andesite lavas of the Villarrica volcano erupted during the 20th century, in order to determine the reservoir conditions and processes involved in their eruptions. We compare whole-rock geochemistry and mineral abundances, textures and compositions, focusing on plagioclase phenocrysts as they are useful tracers of changes of the magma from which they grew. We use anorthite calibrated X-ray maps of plagioclase to obtain their areal distribution and abundances, and thermodynamic simulations to constrain their crystallization conditions. The studied samples record pre-eruptive conditions and processes that do not significantly differ from each other. We identify a heating (thermal mixing) with subtle incorporation of volatiles and slight changes in bulk composition (compositional mixing) that appear to result from cryptic mixing between reservoir magma and recharge by hotter, water-richer and slightly more primitive magma. We also discuss the textural and mineralogical differences observed in the studied samples as a consequence of the time spent in the within-reservoir magma interaction.

3.2. The studied lavas

This contribution focuses on three representative historical lavas of Villarrica, which were erupted in 1921, 1948 and 1971 (Fig. 3.1). They were selected because are among the most voluminous and well preserved lavas and derived from historically well-documented eruptions. A summary of characteristics of the three eruptions is presented in Table 3.1. The 1921 eruption started on December 10th, and lasted approximately 36 hours. It was a strombolian episode (VEI 1-2) with the ejection of scarce pyroclastic material, formation of a gas column and emission of 13×10^6 m^3 of aa and pahoehoe lava that flowed to the south where Coñaripe village is located (Petit-Breuilh, 1994 and the references therein). The 1948 eruptive episode started on October 1948 and ended on February 1949, and is considered the most explosive eruption of Villarrica in the 20th century (Vigorous Strombolian, VEI 3). It generated explosions, pyroclasts emission, lava, lahar and pyroclastic flows of small volumes. In various stages of the eruption, eruptive columns of up to 8 km above the crater were formed (Moreno and Clavero, 2006 and the references therein). The main lava flow, that reached 15 km from the vent and partially filled the Estero Molco valley, have an aa morphology and an estimated volume of ~16×10^6 m^3. The 1971 eruption began in October 29th with violent freatomagmatic explosion in the crater. In November 29th an effusion of lava occurred and two pyroclastic cones were formed inside the crater with rhythmic explosions every 3 minutes. In December 29th the eruption culminated reaching its paroxysmal phase, with a 2 km long eruptive fissure opened in the central cone, generating two lava fountains with a height of 400 m and an eruptive column of up to 3 km. Lahar flows toward the south were generated causing destruction of Coñaripe village, roads and loss of at least 17 lives. Two aa lava flows of 6 and 16.5 km that flowed along the Pedregoso (NE flank) and Challupén (SW flank) valleys, respectively, were emplaced in less than 48 hours (Moreno and Clavero, 2006 and the references there in). We calculated a total volume of lava of 26×10^6 m^3.

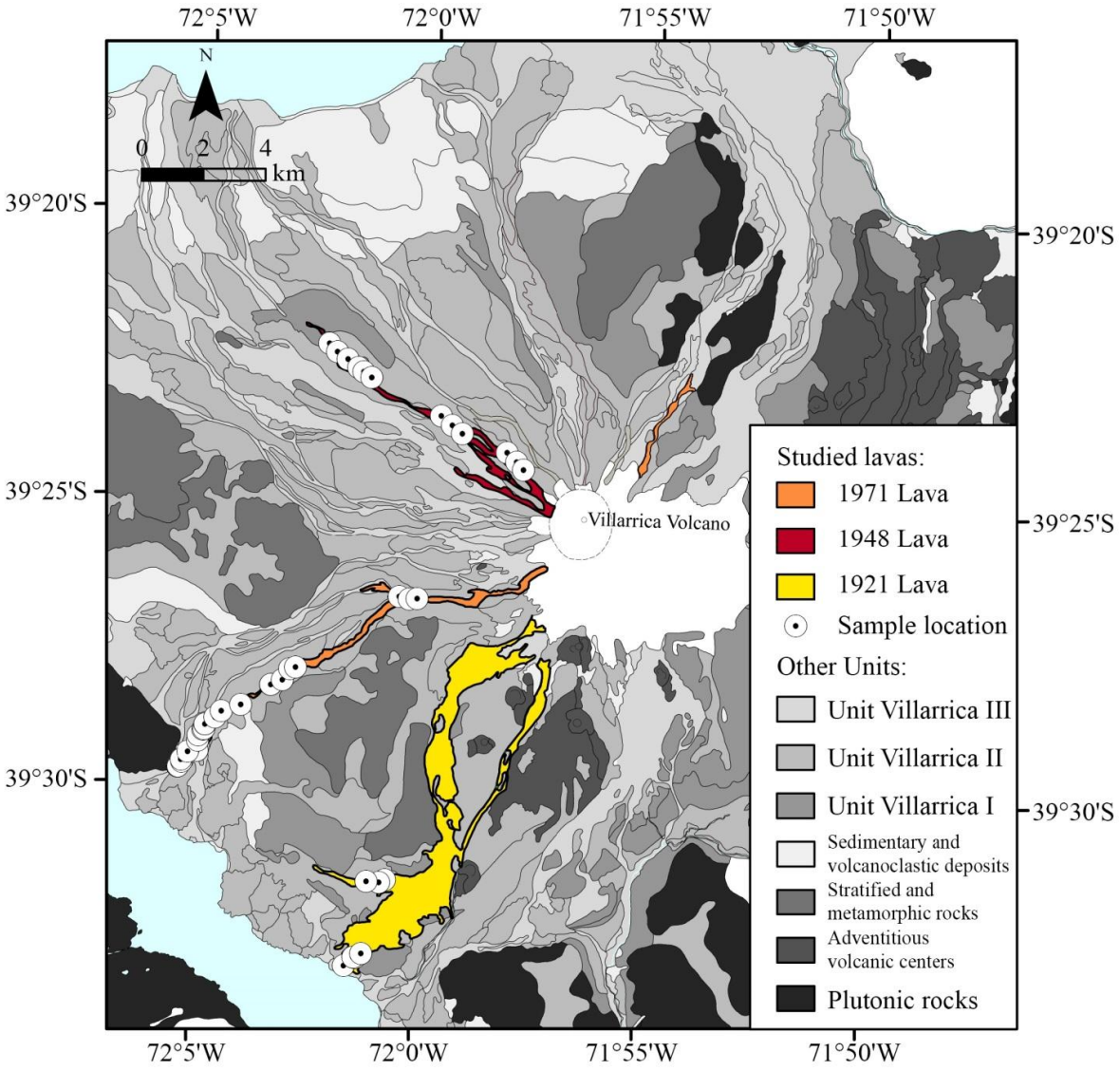

Fig. 3.1. Geologic map of Villarrica Stratovolcano highlighting the studied lavas erupted during the 1921 (yellow), 1948 (red) and 1971 (orange) eruptions (Modified after Moreno and Clavero, 2006). Sampling locations are marked with white circles.

Table 3.1. Summary of the characteristics of the 3 studied eruptions. a. Petit-Breuilh, 1994; b. Moreno and Clavero, 2006.

Eruption	1921	1948	1971
Previous eruption[a]	1920 1909-1910	1938	1964
Duration of eruption[a]	36 hours	3.5 months	2 months
Type of eruption [a]	Strombolian	Vigorous Strombolian	Strombolian
VEI[a]	1-2	3	2
Maximum height of the eruptive column[b]	-	8 km	3 km
Estimated volume of lava (m^3)	13×10^6	16×10^6	26×10^6
Morphology of lava flows	Aa - Pahoehoe	Aa[b]	Aa[b]
Duration of main lava effusion	36 hours[a]	96 hours[a]	48 hours[b]

3.3. Analytical techniques and methodology

In order to determine how homogenous are the studied lavas, 46 samples were collected from the 1921 (seven), 1948 (twelve) and 1971 (twenty seven) lava flows (Fig. 3.1). The samples of 1921 lava were only collected on the well-preserved distal parts and on the front of the lava flow. The samples of well-preserved 1948 and 1971 lavas were collected along the lava flows. Depending on the access and existence of levees, samples were collected at the center, levees or rims of the flow. Mineral compositions were obtained for one selected sample of each lava flow. Whole rock compositions of 46 samples were analyzed by XRF and ICP-MS, for major and trace elements, respectively, at ACT-Labs using BIR-1a, DNC-1, and W-2a standards. The precision was better than 9% (2σ) and accuracy was mostly better than 3%.

Petrographic studies were carried out with a Scanning Electron Microscope (SEM) at the University of Chile (FEI Quanta 250). Compositions of silicates (plagioclase, olivine and pyroxene) were obtained using an electron probe micro-analyzer (EPMA) at the University of Exeter (JEOL JXA-8200) and at the University of Bristol (Cameca SX100). The analytical conditions for the JEOL JXA-8200 consisted of an accelerating voltage of 15 kV, a beam current of 15 nA and a beam size of 2 μm. Count times for each element ranged from 20-40 seconds on the peak position and an equal time measuring the background. For the Cameca SX100 the conditions were an accelerating voltage of 20 kV, a beam current of 10 nA and a beam size of 1 μm. Count times were 10-30 seconds on the peak and 5-15 seconds at background. For pyroxene analyses the values of Fe^{2+} and Fe^{3+} were obtained following the procedure of Droop (1987).

Calcium X-ray maps were obtained for plagioclase phenocrysts using an EPMA at the University of Bristol (JEOL JXA-8530F) in order to obtain information about the areal distribution and abundances of this element. The imaging conditions for the mapping were an

accelerating voltage of 20 kV, a beam current of 200 nA, a dwell time of 2 ms, a spot size of 1 μm, a resolution of 2560x2560 pixels with 8 μm step size in X and Y axis. We used measurements of plagioclase compositions obtained with EPMA to calibrate the grayscale of the Ca X-ray maps. All show linear variations between grayscale and An content ($R^2 > 0.9$, see Fig. 3.8) that allowed us to obtain An-calibrated X-ray maps.

3.4. Whole-rock compositions

The analyzed lavas are among the most primitive products of Villarrica (Fig. 3.2). They are basalts and basaltic andesites with a restricted range in whole-rock compositions (51.7-52.4 wt. % SiO_2, 5.1-7.2 wt. % MgO, Table 3.2). However, they present slight differences as shown in Fig. 3.2. Some compatible elements (Ni, Cr) are positively correlated with MgO, whereas some incompatible elements (K_2O, Na_2O and Ba) show the opposite. REE content slightly varies in the three lavas: 1948 and 1921 lavas have lowest and highest contents, respectively. Using the MgO as an index of differentiation, a following order of increasing primitivity emerges: 1921 (~5.3 wt. % MgO), 1971 (~6.0 wt. % MgO) and 1948 (~7.0 wt. % MgO). Complete data set of whole-rock compositions are provided in Supplementary Data (Table A.1). No significant variation in whole-rock compositions and petrographic features (crystallinity, mineralogy, textures) is observed in samples collected in different sites of the lavas.

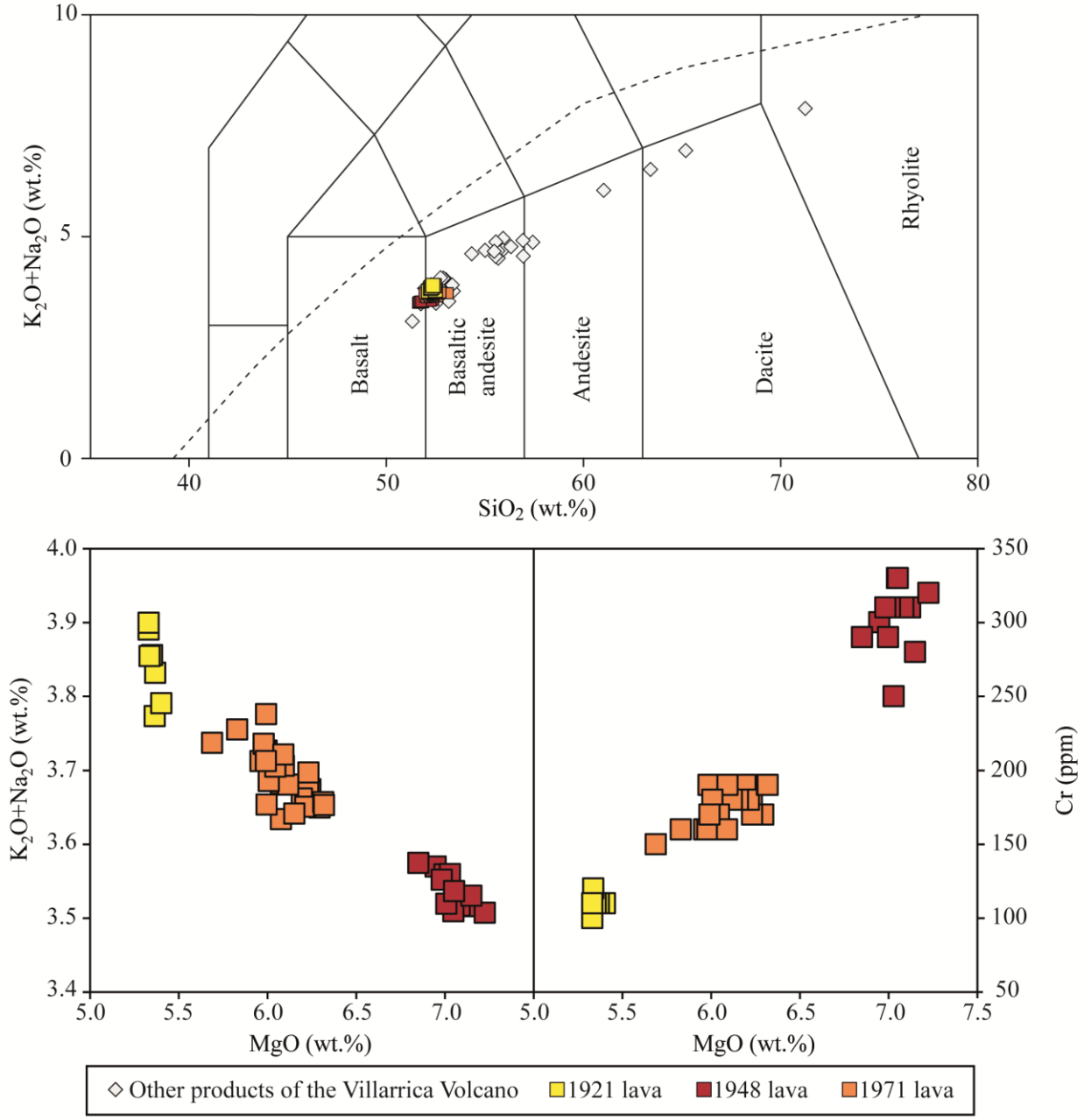

Fig. 3.2. TAS and selected variation diagrams for the studied lavas. Data of other Villarrica Volcano products were taken from Hickey -Vargas *et al*. (1989), Lohmar (2008). Five samples of the 1971 lava were taken from Morgado *et al*. (2015). Divisions in the TAS diagram were taken from Le Bas *et al*. (1986).

Table 3.2. Whole rock geochemistry of selected samples of the three Villarrica's studied lavas. Samples of 1971 lava were obtained from Morgado *et al.* (2015). Complete data set of whole-rock compositions are provided in Supplementary Data (Table A.1).

		1921 lava			1948 lava			1971 lava		
	Detection limit	1921-02	1921-04	1921-05	1948-04	1948-10	1948-12	1971-N6	1971-09	1971-10-M1
SiO_2	0.01 (%)	52.25	52.29	52.36	51.65	51.87	52.25	52.23	52.41	52.42
TiO_2	0.001 (%)	1.25	1.30	1.33	1.09	1.10	1.11	1.09	1.11	1.13
Al_2O_3	0.01 (%)	17.00	16.73	16.65	16.36	16.57	15.95	16.56	16.69	16.84
Fe_2O_3	0.01 (%)	3.19	2.46	3.23	3.94	3.57	5.81	3.01	3.31	3.20
FeO	0.1 (%)	7.18	8.10	7.31	6.39	6.47	4.25	7.12	6.69	6.66
MnO	0.001 (%)	0.16	0.16	0.16	0.16	0.16	0.16	0.16	0.15	0.16
MgO	0.01 (%)	5.37	5.34	5.33	7.08	7.01	6.98	6.32	6.09	6.01
CaO	0.01 (%)	9.50	9.49	9.46	9.58	9.53	9.73	9.65	9.60	9.66
Na_2O	0.01 (%)	3.06	3.07	3.11	2.89	2.89	2.92	3.02	3.06	3.04
K_2O	0.01 (%)	0.77	0.78	0.79	0.63	0.63	0.63	0.63	0.65	0.65
P_2O_5	0.01 (%)	0.26	0.28	0.28	0.22	0.21	0.20	0.21	0.23	0.23
LOI		-0.41	-0.45	-0.48	-0.52	-0.45	-0.38	-0.61	-0.51	-0.47
Total		98.49	100.70	100.80	99.56	98.43	98.45	100.60	99.60	98.57
V	5 (ppm)	304	323	327	294	286	292	297	293	291
Cr	20 (ppm)	110	120	110	310	310	310	190	190	180
Ni	20 (ppm)	50	50	40	100	100	100	90	70	70
Rb	2 (ppm)	18	18	18	15	15	15	14	15	14
Sr	2 (ppm)	417	421	431	381	377	373	414	420	420
Y	2 (ppm)	24	26	25	21	21	22	22	22	22
Zr	4 (ppm)	100	106	107	85	84	86	85	87	86
Ba	3 (ppm)	232	241	243	187	185	190	201	200	199
La	0.1 (ppm)	9.4	9.9	9.7	6.9	7.1	7.1	6.9	7.3	7.2
Ce	0.1 (ppm)	23.1	23.8	23.3	16.6	17.1	17.4	17.5	17.8	17.8
Pr	0.05 (ppm)	3.29	3.42	3.34	2.53	2.53	2.65	2.56	2.64	2.67
Nd	0.1 (ppm)	15.5	15.8	15.7	11.7	11.8	12.2	12	12.5	12.3
Sm	0.1 (ppm)	3.9	4.2	4.3	3.3	3.3	3.3	3.4	3.6	3.5
Eu	0.05 (ppm)	1.14	1.12	1.15	0.92	0.96	0.87	0.97	1.02	0.99
Gd	0.1 (ppm)	4.1	4.2	4.4	3.5	3.6	3.7	3.6	3.9	3.7
Tb	0.1 (ppm)	0.7	0.7	0.7	0.6	0.6	0.6	0.6	0.7	0.6
Dy	0.1 (ppm)	4.2	4.6	4.6	3.8	3.7	4	3.7	3.8	3.8
Ho	0.1 (ppm)	0.9	0.9	0.9	0.8	0.8	0.8	0.8	0.8	0.8
Er	0.1 (ppm)	2.6	2.6	2.7	2.3	2.3	2.3	2.3	2.3	2.3
Tm	0.05 (ppm)	0.4	0.43	0.41	0.36	0.35	0.35	0.37	0.35	0.36
Yb	0.1 (ppm)	2.6	2.7	2.5	2.2	2.2	2.2	2.4	2.3	2.3
Lu	0.04 (ppm)	0.38	0.38	0.39	0.34	0.34	0.35	0.34	0.35	0.33
Pb	5 (ppm)	8	8	8	7	7	7	6	7	7
Th	0.1 (ppm)	1.6	1.7	1.8	1.2	1.3	1.2	1.2	1.2	1.2

3.5. Petrography and Mineral chemistry

The studied lavas have porphyric textures with phenocrysts of plagioclase (14-31 vol. %), olivine (3-9 vol. %), clinopyroxene (< 4 vol. %) and small amounts of chromium-spinel (Table 3.3). The average phenocryst content is decreasing with time, as follow: 36 vol. % in 1921, 26 vol. % in 1948 and 20 vol. % in 1971 (Fig. 3.3). Silicate phases frequently appear as clots (11-36 vol. %) and occasionally as isolated crystals (3-14 vol. %). Chromium-spinels are found as isolated phenocrysts as well as inclusions in olivine. The average mafic/plagioclase ratio is: 0.25 in 1921, 0.36 in 1948 and 0.23 in 1971. Compositional characteristics of the phenocrysts are shown in Fig. 3.4. The groundmasses of 1948 and 1971 lavas are similar, presenting intergranular textures with microlites of plagioclase (~60 vol. % of groundmass), clinopyroxene (~26 vol. %), titanomagnetites (~2 vol. %), glass (~12 vol. %) and small amount of olivine (< 0.1 vol. %). The groundmass of 1921 lava has the same mineral phases, but it exhibits intersertal textures (~35 vol. % of groundmass corresponds to glass) with abundant microlites showing skeletal and acicular shapes. The vesicle content varies from 1 to 22 vol. %. Complete data set of silicates compositions are provided in Supplementary Data (Table A.2, A.3 and A.4).

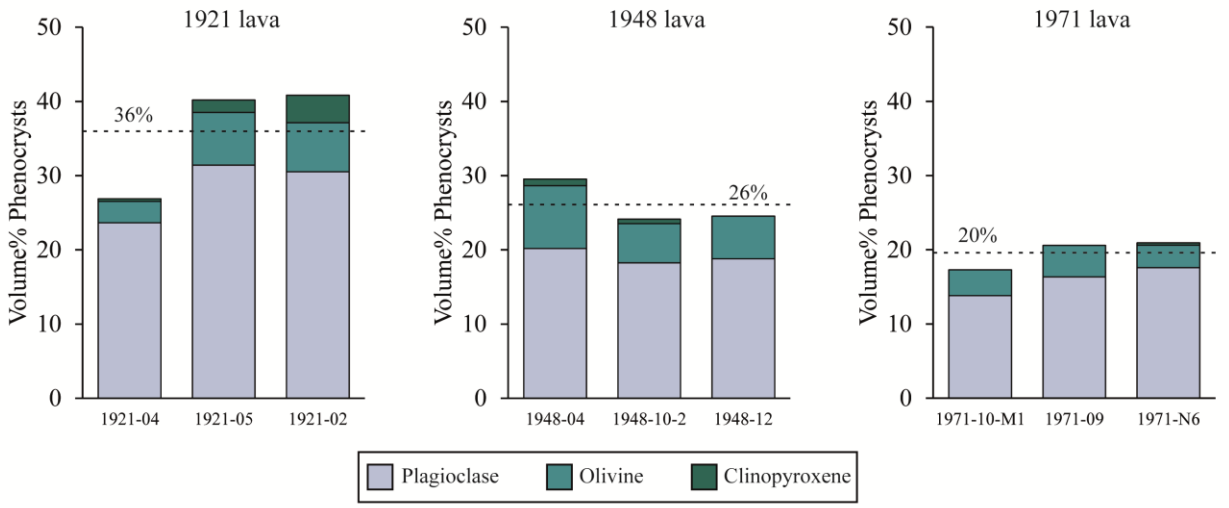

Fig. 3.3. Phenocryst content of the studied lavas estimated by point counting on a vesicle-free basis using the software JMicroVision (Roduit, 2007). Dashed lines indicate average of phenocryst modal content.

Table 3.3. Modal Mineralogy (vol. %).

	1921 lava	1948 lava	1971 lava
Phenocryst	27-41	24-30	17-21
	$\overline{X}$: 36	$\overline{X}$: 26	$\overline{X}$: 20
Plagioclase	24-31	18-20	14-18
Olivine	3-7	5-9	3-4
Clinopyroxene	0.4-4	<0.9	<0.3
Chromium-spinel	<0.1	<0.1	<0.1
Groundmass (vol. of groundmass)			
Plagioclase	28	60	59
Clinopyroxene	33	26	26
Titanomagnetite	6	2	2
Glass	34	12	11
Olivine	<0.1	<0.1	<0.1
Vesicles	15-22	2-6	1-13
Ratio isolated/clots ($\overline{X}$)	0.21	0.58	0.52
Ratio mafics/plagioclase ($\overline{X}$)	0.25	0.36	0.23

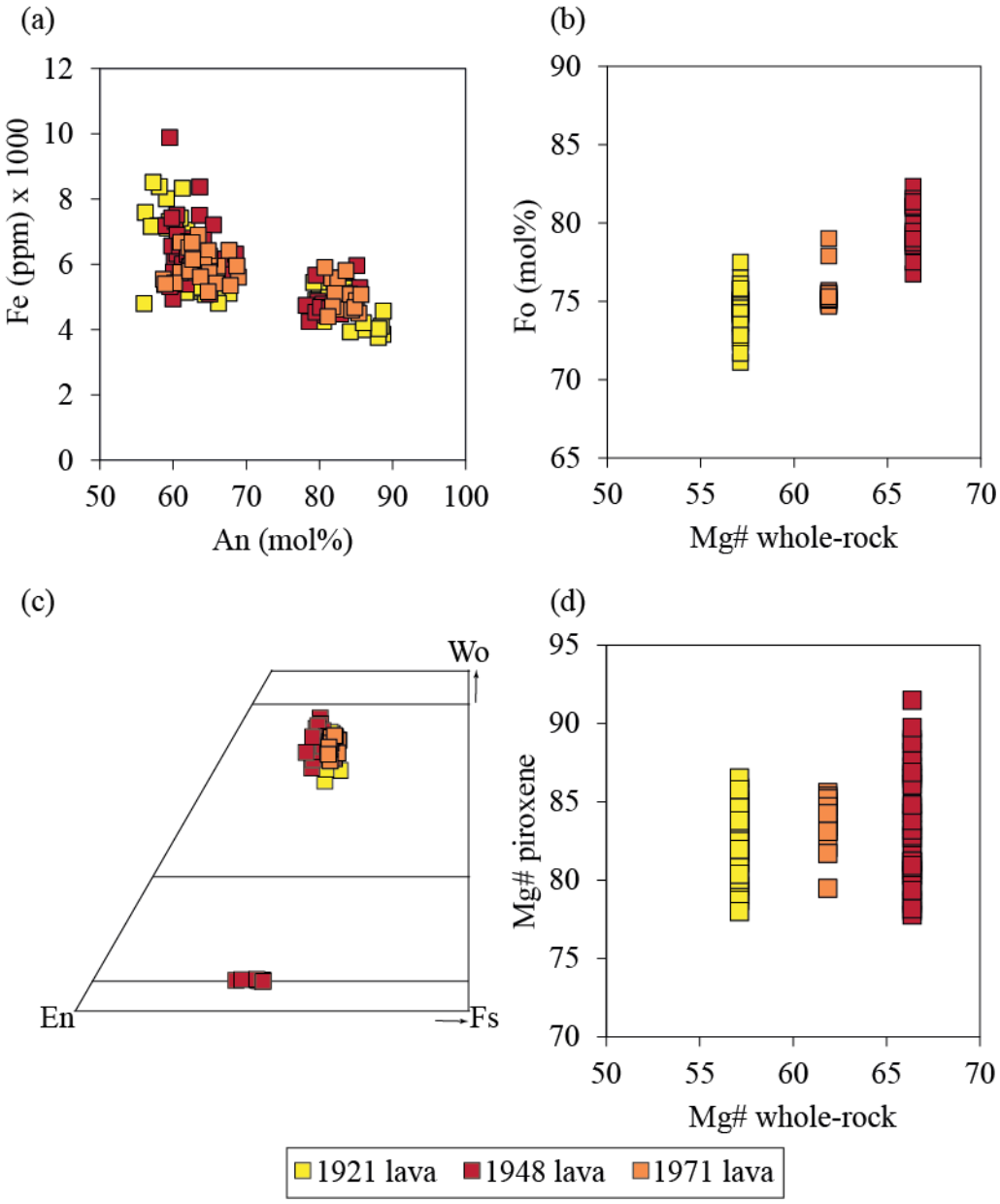

Fig. 3.4. Compositional characteristics of the phenocrysts of the studied lavas. (a) Plagioclase phenocrysts: An content vs. Fe content. (b) Olivine phenocrysts Fo content (cores and intermediate zones) vs. Mg# of the respective rock. (c) Pyroxene phenocryst compositions. (d) Mg# of pyroxene phenocrysts vs. Mg# of the respective rock.

3.5.1. Plagioclase compositions and textures

Two groups of plagioclase compositions are observed in all lavas: An-poor (An_{57-69}) and An-rich (An_{76-89}). The relative abundances of these compositions are obtained with An-calibrated X-ray maps of the three lava samples (Fig. 3.5, 3.6 and 3.7) and are presented in frequency histograms (Fig. 3.8). An-poor compositions are the most abundant in all lavas, with a main peak around An_{60}. A modest secondary peak of high-An (c. An_{80}) is observed in the histograms. The An-rich/An-poor frequency ratio varies as follow: 0.06 in 1921, 0.23 in 1971 and 0.45 in 1948. Plagioclase phenocrysts in the three lavas have similar minor and trace element (Fe, Ti and Mg) compositions and display subtle negative correlation of Fe with An content (Fig. 3.4a) and strong negative correlations of Ti and Mg values with An content (Supplementary Data, Table A.2).

The compositional groups are closely related to specific phenocryst textures. An-poor is associated with clean oscillatory zoned crystals (Fig. 3.5a, 3.6a, 3.7a). The smallest plagioclase phenocrysts are generally of these compositions, however An-poor also occurs as clean cores and/or rims of more complex zoned crystals exhibiting disequilibrium textures with An-rich plagioclases compositions (Fig. 3.5b, c; 3.6b, c; 3.7b, c). The more calcic compositions are commonly part of sieved cores (Fig. 3.5c, 3.6c, 3.7c) but also occur as intermediate zone of plagioclase phenocrysts (Fig. 3.5b, 3.6b, 3.7b). In zoned phenocrysts, the An-rich zones exhibit boxy or spongy cellular texture (Streck, 2008), consisting of a network of glass droplets into calcic plagioclase. They appear associated with An-poor patches and occasionally have mineral inclusions (olivine, clinopyroxene, chromium-spinels).

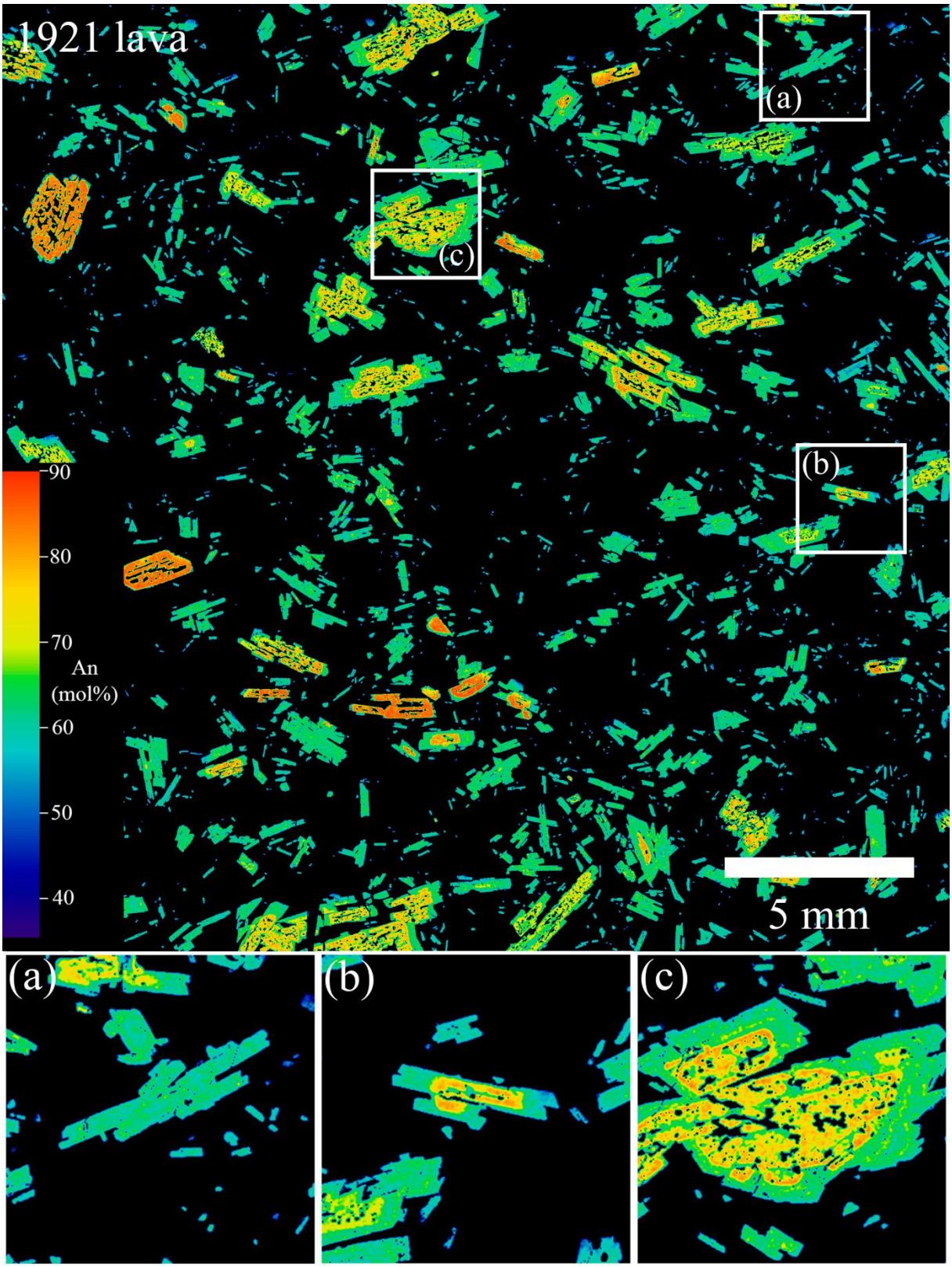

Fig. 3.5. Anorthite calibrated X-Ray map of plagioclase of 1921 lava sample. (a) Example of An-poor phenocryst. (b) Example of a phenocryst with An-poor core, intermediate sieved zone with An-rich compositions and An-poor rim. (c) Example of a phenocryst with sieved core associated with An-rich compositions and An-poor rim.

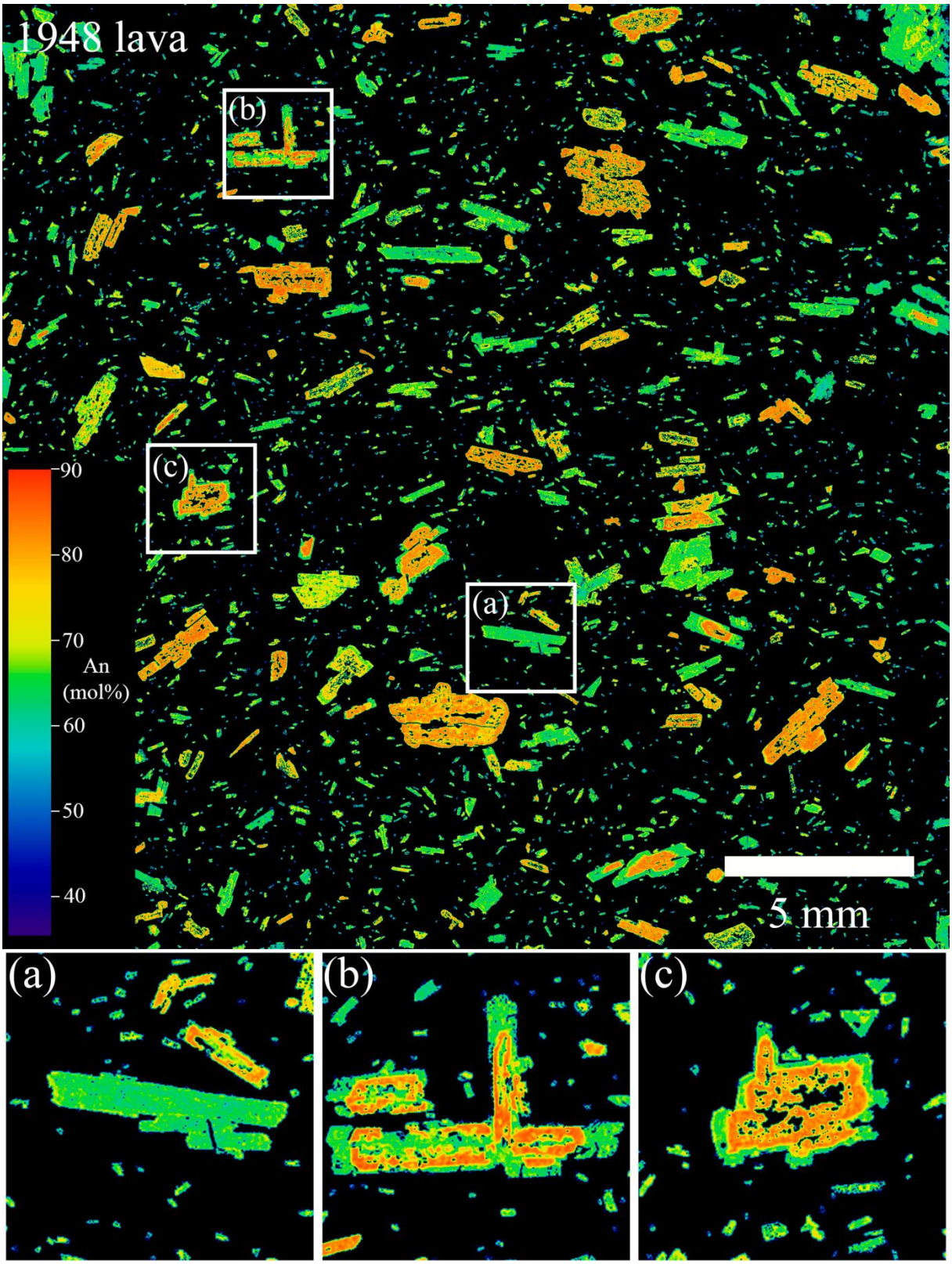

Fig. 3.6. Anorthite calibrated X-Ray map of plagioclase of 1948 lava sample. (a) Example of An-poor phenocryst. (b) Example of a phenocryst with An-poor core, intermediate sieved zone with An-rich compositions and An-poor rim. (c) Example of a phenocryst with sieved core associated with An-rich compositions and An-poor rim.

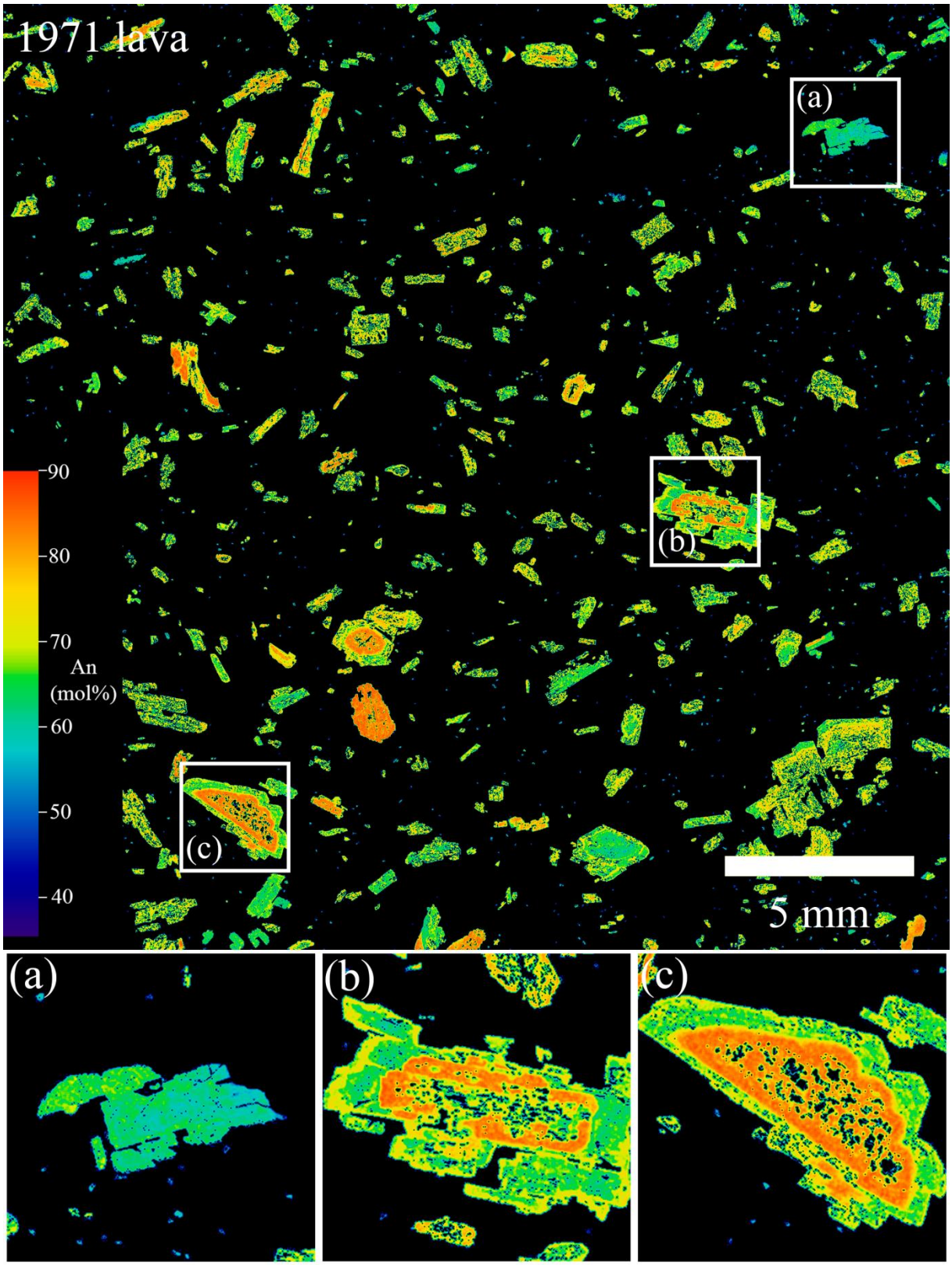

Fig. 3.7. Anorthite calibrated X-Ray map of plagioclase of 1971 lava sample. (a) Example of An-poor phenocryst. (b) Example of a phenocryst with An-poor core, intermediate sieved zone with An-rich compositions and An-poor rim. (c) Example of a phenocryst with sieved core associated with An-rich compositions and An-poor rim.

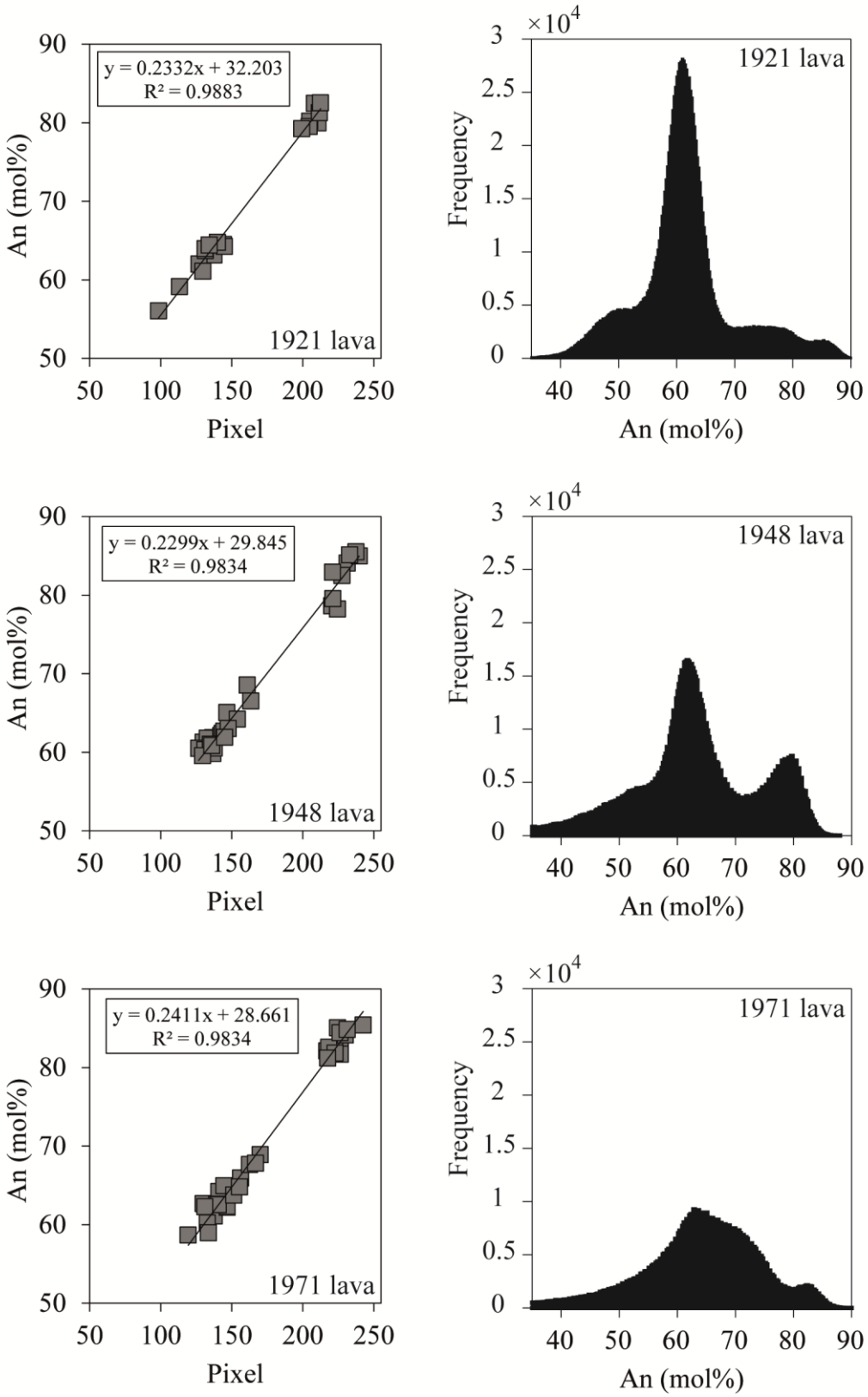

Fig. 3.8. Calibrated plagioclase compositions of the studied lavas. Results of calibration of plagioclase pixels (from the Ca X-ray maps) with An contents measured with EPMA (left) and histograms of frequency of the calibrated An compositions (right).

3.5.2. Mafic mineral compositions and textures

Olivine phenocrysts are anhedral to subhedral (0.05-1.6 mm), usually with resorption textures and slight compositional changes. They appear as isolated crystals or forming clots mainly with clinopyroxenes and/or plagioclases. The forsterite content at the cores and intermediate zones of crystals is slightly different in the three lavas and is positively correlated with the Mg# (Mg# = molar 100×Mg/(Mg+Fe^{2+})) of the host rock (Fig. 3.4b): Fo_{71-78} in 1921 (Mg#: 57), Fo_{76-83} in 1948 (Mg#: 66) and Fo_{74-79} in 1971 (Mg#: 62). Chromium-spinel inclusions are abundant in olivine phenocrysts of 1948 lava samples, less abundant in 1971 and very scarce or absent in 1921 lava samples. This modal variation correlates with the whole-rock Cr content (Fig. 3.2). Available chromium-spinel compositions in 1971 lava have Cr# = 53-62 and Mg# = 26-30 (Morgado *et al.*, 2015). Clinopyroxene phenocrysts are anhedral to subhedral (0.05-2.4 mm) and are always forming clots with olivine and less frequent with plagioclase. Clinopyroxenes of all lava samples have a restricted range of compositions (Wo_{33-43}, En_{47-52}, Fs_{10-15}, Fig. 3.4c) and Mg# (78-87 in 1921, 78-91 in 1948 and 79-86 in 1971, Fig 3.4d). Clinopyroxenes of 1948 lava samples differ from those of the other lava samples because they have a pervasive resorption texture, anhedral zones of orthopyroxene (Wo_{4-5}, En_{74-77}, Fs_{18-22}) and occur as clots with olivine, without plagioclase.

3.6. Thermometry and barometry

The olivine-augite Mg-Fe-exchange geothermometer (Loucks, 1996) and the olivine-clinopyroxene Ca-exchange geobarometer (Köhler & Brey, 1990) were used in 30 olivine-clinopyroxene pairs that occur in two groups of crystal clots: clots of olivine, clinopyroxene and plagioclase (present in all lavas), and clots of olivine and clinopyroxene (present only in the Mg-rich 1948 lava). Details of the calculations are presented in Table 3.4. The equilibrium conditions between olivine and clinopyroxene pairs were tested using Fe/Mg values to determine if both

minerals are in equilibrium with the same melt composition (see Morgado *et al.*, 2015) according to the equations of Grove *et al.* (1997). For the group of ol-cpx-pl clots (Fig. 3.9a, b), similar average temperatures of 1092 ºC (1077-1107 ºC ± 6 ºC for 1921, 1089 ºC ± 6 ºC for 1948, 1077-1099 ºC ± 6 ºC for 1971) were obtained in all lavas (Fig. 3.10a). The group of ol-cpx clots only present in 1948 lava, gave higher temperatures of ~1194 ºC (1190-1200 ºC ± 6 ºC, Fig. 3.9c) except one temperature value of 1174 ºC ± 6 ºC. The Ca-exchange geobarometer gave only positive values in ol-cpx clots (Fig. 3.10b): ~3.3 ± 1.7 kbar (2.9-3.6 ± 1.7 kbar; ~12 km ± 6.17 km) and one pressure value of 0.6 ± 1.7 kbar (2 km ± 6.17 km).

Table 3.4: Thermodynamic variables calculations detail. Temperatures were obtained using the olivine-augite Mg-Fe-exchange geothermometer (Loucks, 1996) and pressures were estimated using the olivine-clinopyroxene Ca-exchange geobarometer (Köhler & Brey, 1990).

Lava	1921	1921	1921	1921	1921
Group of clot	Ol-cpx-pl	Ol-cpx-pl	Ol-cpx-pl	Ol-cpx-pl	Ol-cpx-pl
Ol code	1921-02 - Gl 1-P1	1921-02 - Gl 1-P5	1921-02 - Gl11-P2	1921-02 - Gl 6-P3	1921-02 - Gl 6-P12
Cpx code	1921-02 - Gl 1-P4	1921-02 - Gl 1-P8	1921-02 - Gl11-P1	1921-02 - Gl 6-P2	1921-02 - Gl 6-P9
Fe^{2+} (ol)	0.4993	0.4817	0.4770	0.4627	0.4761
Mg (ol)	1.4841	1.4954	1.5007	1.5094	1.4987
Ca (ol)	0.0072	0.0075	0.0078	0.0079	0.0088
Fe^{2+} (cpx)	0.1808	0.1682	0.1886	0.1697	0.1707
Mg (cpx)	0.9512	0.9178	0.9384	0.9394	0.9382
Ca (cpx)	0.7458	0.7675	0.7498	0.7559	0.7572
(Fe/Mg)ol	0.3364	0.3221	0.3179	0.3066	0.3177
(Fe^{+2}/Mg)aug	0.1901	0.1832	0.2009	0.1806	0.1820
TºC (±6ºC)	1080	1082	1107	1090	1084
DCa	-	-	-	-	-
P kbar (± 1.7kbar)	-	-	-	-	-

Lava	1921	1921	1921	1921	1921
Group of clot	Ol-cpx-pl	Ol-cpx-pl	Ol-cpx-pl	Ol-cpx-pl	Ol-cpx-pl
Ol code	1921-02 - Gl 10-P2	1921-02 - Gl 10-P7	1921-02 - Gl 10-P13	1921-02 - Gl 2-P2	1921-02 - Gl 3-P3
Cpx code	1921-02 - Gl 10-P1	1921-02 - Gl 10-P6	1921-02 - Gl 10-P12	1921-02 - Gl 2-P1	1921-02 - Gl 3-P4
Fe^{2+} (ol)	0.4778	0.4668	0.4746	0.4628	0.4885
Mg (ol)	1.5025	1.5078	1.5032	1.5054	1.4918
Ca (ol)	0.0079	0.0087	0.0084	0.0093	0.0083
Fe^{2+} (cpx)	0.1679	0.1756	0.1826	0.1709	0.1838
Mg (cpx)	0.9475	0.9325	0.9317	0.9234	0.9377
Ca (cpx)	0.7521	0.7683	0.7583	0.7483	0.7520
(Fe/Mg)ol	0.3180	0.3096	0.3157	0.3074	0.3274
(Fe^{+2}/Mg)aug	0.1772	0.1883	0.1960	0.1851	0.1960
TºC (±6ºC)	1077	1098	1103	1095	1094
DCa	-	-	-	-	-
P kbar (± 1.7kbar)	-	-	-	-	-

Lava	1921	1921	1921	1921	1921
Group of clot	Ol-cpx-pl	Ol-cpx-pl	Ol-cpx-pl	Ol-cpx-pl	Ol-cpx-pl
Ol code	1921-02 - Gl 3-P7	1921-02 - Gl 4-P1	1921-02 - Gl 4-P7	1921-02 - Gl 7-P5	1921-02 - Gl 9-P7
Cpx code	1921-02 - Gl 3-P8	1921-02 - Gl 4-P2	1921-02 - Gl 4-P6	1921-02 - Gl 7-P6	1921-02 - Gl 9-P8
Fe^{2+} (ol)	0.5470	0.4705	0.4482	0.4725	0.4804
Mg (ol)	1.4255	1.5041	1.5225	1.5039	1.4984
Ca (ol)	0.0114	0.0073	0.0096	0.0086	0.0083
Fe^{2+} (cpx)	0.2139	0.1774	0.1791	0.1764	0.1959
Mg (cpx)	0.9632	0.9712	0.9803	0.9270	0.9666
Ca (cpx)	0.7186	0.7266	0.7189	0.7656	0.7219
(Fe/Mg)ol	0.3837	0.3128	0.2944	0.3142	0.3206
(Fe^{+2}/Mg)aug	0.2221	0.1827	0.1826	0.1902	0.2026
TºC (±6ºC)	1086	1088	1102	1097	1107
DCa	-	-	-	-	-
P kbar (± 1.7kbar)	-	-	-	-	-

Lava	1921	1921	1948	1948	1948
Group of clot	Ol-cpx-pl	Ol-cpx-pl	Ol-cpx-pl	Ol-cpx	Ol-cpx
Ol code	1921-02 - Pl 4-P19	1921-02 - Mgl 3 - P2	1948-04 - Gl10-P4	1948-04-1-Gl6_2	1948-04-1-Gl5_3
Cpx code	1921-02 - Pl 4-P20	1921-02 - Mgl 3 - P1	1948-04 - Gl10-P3	1948-04-1-Gl6_1	1948-04-1-Gl5_5
Fe^{2+} (ol)	0.4945	0.5154	0.3452	0.3999	0.3564
Mg (ol)	1.4784	1.4582	1.6317	1.5893	1.6065
Ca (ol)	0.0092	0.0091	0.0077	0.0069	0.0067
Fe^{2+} (cpx)	0.1850	0.2114	0.1130	0.2104	0.2092
Mg (cpx)	0.9414	0.9941	0.9127	0.9347	1.0098
Ca (cpx)	0.7603	0.6588	0.8123	0.7557	0.6975
(Fe/Mg)ol	0.3345	0.3534	0.2116	0.2516	0.2218
(Fe^{+2}/Mg)aug	0.1965	0.2126	0.1238	0.2251	0.2072
TºC (±6ºC)	1090	1095	1089	1190	1200
DCa	-	-	-	0.00917	0.00955
P kbar (± 1.7kbar)	-	-	-	2.9	3.4

Lava	1948	1948	1948	1971	1971
Group of clot	Ol-cpx	Ol-cpx	Ol-cpx	Ol-cpx-pl	Ol-cpx-pl
Ol code	1948-04-1-Gl1_3	1948-04-1-Mgl1_3	1948-04-1-Mgl9_1	1971-09 - Gl1-P2	1971-09 - Gl1-P11
Cpx code	1948-04-1-Gl1_1	1948-04-1-Mgl1_1	1948-04-1-Mgl9_3	1971-09 - Gl1-P1	1971-09 - Gl1-P12
Fe^{2+} (ol)	0.4171	0.3493	0.3994	0.4772	0.4643
Mg (ol)	1.5696	1.6293	1.5796	1.5067	1.5114
Ca (ol)	0.0068	0.0070	0.0070	0.0081	0.0075
Fe^{2+} (cpx)	0.2172	0.1674	0.2144	0.1592	0.1629
Mg (cpx)	0.9065	0.9341	0.9260	0.9021	0.9031
Ca (cpx)	0.7566	0.7628	0.7532	0.7766	0.7755
(Fe/Mg)ol	0.2657	0.2144	0.2528	0.3167	0.3072
(Fe^{+2}/Mg)aug	0.2396	0.1792	0.2315	0.1765	0.1804
TºC (±6ºC)	1192	1174	1195	1077	1089
DCa	0.00899	0.00913	0.00935	-	-
P kbar (± 1.7kbar)	3.7	0.6	3.2	-	-

Lava	1971	1971	1971	1971	1971
Group of clot	Ol-cpx-pl	Ol-cpx-pl	Ol-cpx-pl	Ol-cpx-pl	Ol-cpx-pl
Ol code	1971-09 - Gl1-P15	1971-09 - Gl1-P21	1971-09 - Gl1-P23	1971-09 - Gl1-P27	1971-09 - Gl1-P31
Cpx code	1971-09 - Gl1-P16	1971-09 - Gl1-P20	1971-09 - Gl1-P24	1971-09 - Gl1-P28	1971-09 - Gl1-P32
Fe^{2+} (ol)	0.4927	0.4872	0.4917	0.4820	0.4678
Mg (ol)	1.4898	1.4937	1.4886	1.4984	1.5051
Ca (ol)	0.0074	0.0078	0.0083	0.0077	0.0078
Fe^{2+} (cpx)	0.1840	0.1889	0.1828	0.1742	0.1747
Mg (cpx)	0.9111	0.9491	0.9191	0.9338	0.9344
Ca (cpx)	0.7753	0.7148	0.7622	0.7473	0.7550
(Fe/Mg)ol	0.3307	0.3261	0.3303	0.3216	0.3108
(Fe^{+2}/Mg)aug	0.2019	0.1990	0.1989	0.1865	0.1870
TºC (±6ºC)	1099	1098	1095	1086	1095
DCa	-	-	-	-	-
P kbar (± 1.7kbar)	-	-	-	-	-

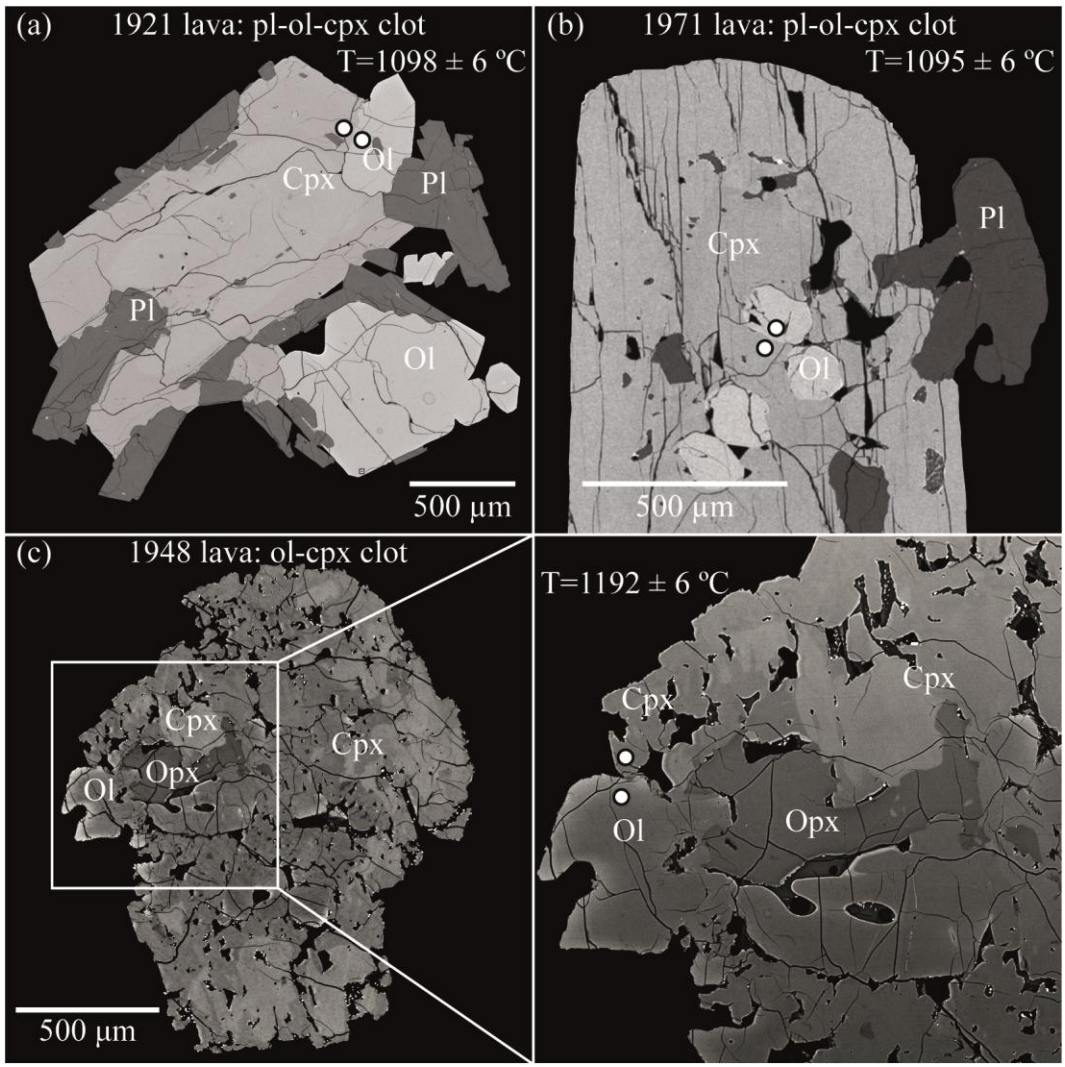

Fig. 3.9. Examples of crystal clots used for thermometric calculations. (a) 1921 lava clot of plagioclase-olivine-clinopyroxene that gave an equilibrium temperature of 1098 ± 6ºC. (b) 1971 lava clot of plagioclase-olivine-clinopyroxene that gave an equilibrium temperature of 1095 ± 6ºC. (c) 1948 lava clot of olivine-clinopyroxene (-orthopyroxene) that gave an equilibrium temperature of 1192 ± 6ºC.

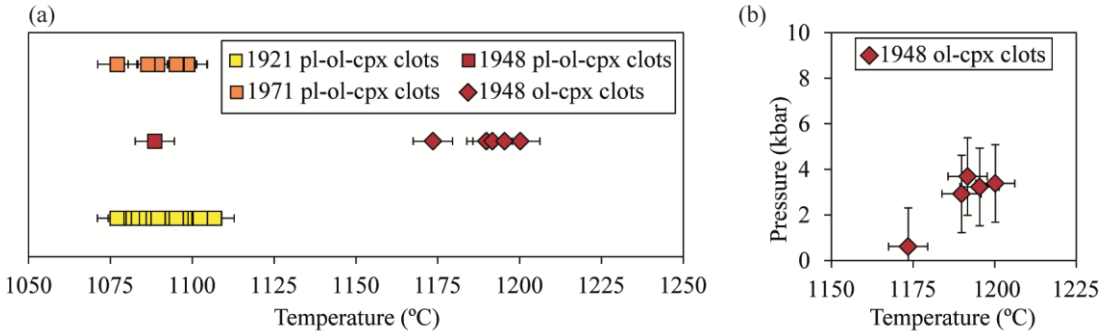

Fig. 3.10. (a) Temperatures calculated for the plagioclase-olivine-clinopyroxene clots of the three studied lavas and for the olivine-clinopyroxene clots only present in 1948 lava. (b) Temperature and pressure obtained only for the olivine-clinopyroxene clots of 1948 lava.

3.7. Discussion

3.7.1. Interpretation of plagioclase compositions and textures

Plagioclase crystals are good tracers of magmatic processes and have been widely used to identify pre-eruptive changes of the magma from which they grew (e.g. Humphreys *et al.*, 2006; Viccaro *et al.*, 2010; Bouvet de Maisonneuve *et al.*, 2013; Cashman and Blundy, 2013). Anorthite content in plagioclase is function of four variables: magma composition, dissolved water content, temperature and pressure (Housh and Luhr, 1991; Nelson and Montana, 1992; Streck, 2008; Lange *et al.*, 2009; Ustunisik *et al.*, 2014; Waters and Lange, 2015). Plagioclase textures could reflect smooth changes in the surrounding magma, if they have continuous, oscillatory zoning patterns; or abrupt changes, if they show disruption in zoning patterns and/or resorption textures. Tsuchiyama (1985) and Nakamura and Shimatika (1998) have experimentally replicated resorption textures by introducing a plagioclase crystal into a melt, which is not in equilibrium. Dissolution occurs if the melt was in equilibrium with a more anorthite rich plagioclase than the added crystal. The resorption textures found in Villarrica are similar to the experimentally reproduced in these studies. In our case we interpret the Villarrica plagioclase crystallization as the result of three steps: (1) Growth of An-poor (An_{57-69}) crystals in a relatively stable reservoir, evidenced by the clean cores and An-poor patches associated with resorption textures; (2) abrupt disequilibrium that generates the partial dissolution textures (boxy or spongy cellular textures) of An-poor plagioclase followed by precipitation of An-rich (An_{76-89}) zones; (3) restoration to the initial conditions giving rise to An-poor clean oscillatory zoned rims and abundant small An-poor crystals. Despite the sequence of crystallization been the same for the three studied lavas, subtle differences in An-rich/An-poor ratios are observed.

In order to constrain the thermodynamic conditions of plagioclase crystallization of each step, we use MELTS (Asimow & Ghiorso, 1998; Ghiorso & Sack, 1995) based on two assumptions: (1) closed system (i.e., constant bulk composition) and (2) temperatures of An-poor plagioclase crystallization correspond to those obtained for An-poor plagioclase-olivine-clinopyroxene clots (~1092 ºC). We justify the first assumption because of the limited compositional range in historical lavas of Villarrica and the results of Fe vs. An contents (Fig. 3.4a; slightly negative correlation) interpreted as the result of thermal mixing in a closed system, as suggested by Ruprecht and Wörner (2007). We use the most primitive available Villarrica lava sample (V2-8; Hickey-Vargas *et al.*, 1989) as the initial liquid composition to simulate the studied lavas, which are restricted to a short compositional range (51.7-52.4 wt. % SiO_2, 5.1-7.2 wt. % MgO, see Table 3.2). We assume quartz-fayalite-magnetite (QFM) buffer conditions, as it was suggested by Lohmar *et al*., (2012), and a pressure of 0.5 kbar, consistent with previous estimations (Lohmar *et al*., 2012; Morgado *et al*., 2015). Three scenarios are likely to reproduce the changes from ~An_{60} to ~An_{80} and the subsequent restoration to the An-poor compositions. The first scenario includes a heating (thermal mixing) of 94 ºC at constant dissolved water of 0.5 wt. % (Scenario 1, Fig. 3.11). It interesting to note that the ΔT estimated in this scenario is similar to the ΔT between the two groups of crystal clots (~100°C). After the restoration of the initial conditions, An-poor plagioclase compositions are reproduced. A second scenario that could also generate An_{80} plagioclase, considers a less intense heating, but small water addition, leading to conditions of magmatic disequilibrium (Scenario 2, Fig. 3.11). The third scenario considers an even less intense heating accompanied with a greater water addition. In this case, the restoration to the initial temperature would generate compositions out of the range of An-poor plagioclase compositions (Scenario 3, Fig. 3.11). Despite the first two scenarios are likely to occur, the incorporation of volatiles, without significant changes in the bulk composition, would allow

reaching the more anorthitic plagioclase compositions more efficiently. Although decompression under H_2O-undersaturated conditions could explain the change from An-poor to An-rich plagioclases, the restoration to the initial higher-pressure conditions (under which the An-poor rims would form), appears to be geologically unrealistic if a lithostatic pressure-dominated process is considered. We favour a recharge of the Villarrica reservoir by magma of similar bulk composition, but hotter and richer in water, as a mechanism to explain the combined processes of heating and subtle water enrichment.

If we assume that the An-rich compositions represent the crystallization conditions driven by the interaction of the reservoir with a new hot magma, then the among-lava variations of An-rich/An-poor modal ratio could be function of the time spent in the interactions. Thus, higher An-rich/An-poor modal ratio (as it is observed in the most primitive 1948 lava; Fig. 3.5) would imply a longer time of interaction with the hot magma allowing more An-rich plagioclase formation and An-poor plagioclase dissolution.

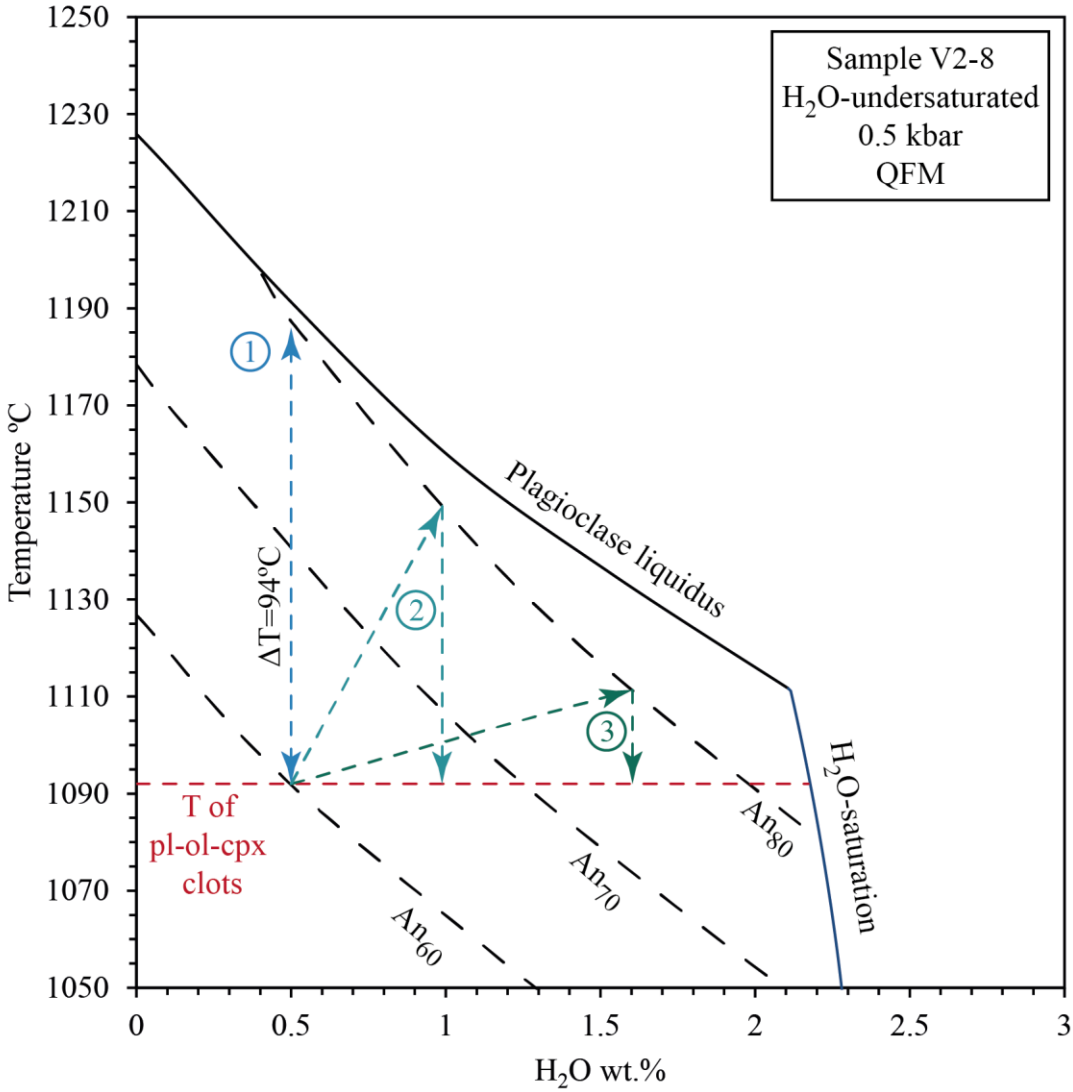

Fig. 3.11. Plagioclase equilibrium compositions as function of temperature and water content obtained by MELTS. Composition of the initial melt, pressure and fO_2 correspond to the bulk composition of the sample V2-8 (Hickey-Vargas *et al.*, 1989), 0.5 kbar and QFM buffer, respectively. Three possible scenarios to reproduce the changes from An-poor to An-rich and a restoration of An-poor compositions are shown. The temperature of plagioclase-olivine-clinopyroxene clots is assumed to be the temperature of An-poor crystallization and is shown in red dashed line.

3.7.2. Magma recharge of the Villarrica reservoir

Despite the narrow whole-rock compositional range (around 52 wt. % SiO_2) in the studied Villarrica 20th century lavas suggests a chemically closed magmatic system, the slight variations in compatible (MgO, Ni, Cr) and incompatible (K_2O, Na_2O, Ba) elements could be evidence of slight compositional changes. We observe variations in MgO content (in order of increasing primitive character: 1921, 1971 and 1948) that positively correlate with some mineral compositions and textures, such as the An-rich/An-poor modal ratio, Fo contents and abundance of chromium-spinel inclusions in olivine. In addition, the most primitive lava (1948) presents the highest mafic minerals/plagioclases ratios, Mg# in pyroxenes (Fig. 3.4d) and temperatures. We suggest that these variations could indicate some degrees of interaction between the reservoir and the recharging hot and more primitive magmas (compositional mixing). Those 1948 olivine-clinopyroxene clots recording the highest P-T conditions (Table 3.4) could be testimonies of minerals dragged from the deep source of the recharging magma.

The apparent contradiction between a closed system (thermal mixing), supported by thermodynamic models, and an open system (compositional mixing), supported by the subtle compositional variations among the studied lavas, can be understood as a result of cryptic magma recharge, which corresponds to the interaction between pulses of magma that have similar anhydrous bulk compositions, but different volatile contents (Humphreys *et al.*, 2006). Thus, unlike the mixing of two contrasting magma, the cryptic mixing would be more difficult to detect (e.g. D'Lemos, 1996; de Silva *et al.*, 2008). Considering the existence of a mushy zone at the lower parts of a reservoir, as it was shown by Gutiérrez and Parada (2010), a rheological barrier to a new magma input is expected, except for a cryptic upward volatile migration from underplated mafic magmas. This advection would contribute to a more efficient heat transfer and distribution than heat conduction alone (Bachmann and Bergantz's 2006) and is consistent with

the proposed scenario 2 (Fig. 3.11), where increasing volatile contents also reproduce the An-rich plagioclase formation. The cryptic mixing has been identified mainly in intermediate to silicic systems, as in the 2000 andesites of Shiveluch Volcano, Kamchatka (Humphreys *et al.*, 2006), in the andesitic lavas of the El Misti Volcano, Peru (Ruprecht & Wörner, 2007), in andesites of Mt Taranaki, New Zealand (Turner *et al.*, 2008) and in the 1600 explosive dacitic eruption of Huaynaputina, Peru (de Silva *et al.*, 2008). Furthermore, Mount St. Helens dacitic system is understood as physically open to multiple inputs of pulses of broadly similar H_2O-rich magmas (Cashman & Blundy, 2013). Less evidence of cryptic mixing has been observed in basaltic systems, as in the trachybasalts of Mt. Etna Volcano, Italy (Viccaro *et al.*, 2016, 2010) and the high-alumina basalts of Barren Island Volcano (Renjith, 2014).

3.7.3. Final comments

Despite the limited number of studied 20th century lavas, the observed increase in the primitive character seems to be negatively correlated with the intensity of the respective eruptions. The 1948 lava is the most primitive and was produced during the most explosive Villarrica eruption of the 20th century, which lasted 3.5 months and generated columns of up to 8 km (Moreno and Clavero, 2006). The 1971 lava is less primitive and was produced in a less intense eruption, with columns of up to 3 km and an intense effusion of lava during its paroxysmal phase (Moreno and Clavero, 2006). The 1921 lava is the most differentiated and was produced during the less intense eruption, with scarce emission of pyroclasts (Petit-Breuilh, 1994) and generated pahoehoe lava morphologies, which are commonly associated with small eruption rates. The mentioned negative correlation, which is the opposite to the commonly expected, has been identified elsewhere at different time scales: at short term, the correlation has been detected in volcanic materials of a single eruption (e.g. Sides *et al.*, 2014; Taddeucci *et al.*, 2015), and at medium term, is recorded over a period of several successive eruptions (e.g.

Newhall, 1979; Baker and Holland, 1973). We speculate that the time of interaction between the recharge magma and the reservoir could play a key role in the eruptive intensities. A longer interaction could produce more mafic hybrid magma and cause a higher volatile influx from the injected magma causing higher intensity of the resulting eruption.

3.8. Conclusions

The studied lavas of the Villarrica Volcano erupted in the 20th century, record similar pre-eruptive processes that include heating and water addition. A heating (thermal mixing) of about 100 °C (from ~1090 to ~1190 °C) at ~0.5 kbar, is necessary to reproduce the observed An-rich plagioclase around resorbed An-poor cores. However, incorporation of small amounts of volatiles and hot mafic magma (cryptic mixing) into the reservoir is likely to occur and could also explain the resorption and modification of plagioclase composition. In this scenario, a longer interaction of the hot magma with the reservoir could explain the highest An-rich/An-poor modal content ratios in the more mafic, hotter and volatile-rich hybrid magma (1948 lava) that ultimately resulted in the highest intensity eruption.

Acknowledgments

This project was mainly funded by CONICYT-FONDAP project 15090013 “Andean Geothermal Center of Excellence” (CEGA) and the Department of Geology of the University of Chile. C.P. acknowledges the financial support of “Departamento de Postgrado y Postítulo de la Vicerrectoría de Asuntos Académicos” of the University of Chile for a short internship at the School of Earth Sciences of the University of Bristol. Participation of C.C. and E.M were also supported by CONICYT MSc fellowship (22130368, CC) and CONICYT PhD fellowships (72160339, C.C.; 72160268, E.M.). Special thanks to Angelo Castruccio, Claudia Cannatelli, Katharine Cashman and Alison Rust for valuable suggestions. Thanks to Stuart Kearns and

Benjamin Buse who provided great assistance with EPMA at the University of Bristol. Thanks to Joe Pickles for his help with EPMA at the University of Exeter.

References

Asimow, P. D., & Ghiorso, M. S. (1998). Algorithmic modifications extending MELTS to calculate subsolidus phase relations. *American Mineralogist*, *83*(9–10), 1127–1132. https://doi.org/10.2138/am-1998-9-1022

Bachmann, O., & Bergantz, G. W. (2006). Gas percolation in upper-crustal silicic crystal mushes as a mechanism for upward heat advection and rejuvenation of near-solidus magma bodies. *Journal of Volcanology and Geothermal Research*, *149*(1–2), 85–102. https://doi.org/10.1016/j.jvolgeores.2005.06.002

Bertin, D., Amigo, A., & Bertin, L. (2015). Erupción del volcán Villarrica 2015: Productos emitidos y volumen involucrado. In *14º Congreso Geológico Chileno* (Vol. 3, pp. 249–251).

Bouvet de Maisonneuve, C., Dungan, M. A., Bachmann, O., & Burgisser, A. (2013). Petrological insights into shifts in eruptive styles at Volcán Llaima (Chile). *Journal of Petrology*, *54*(2), 393–420. https://doi.org/10.1093/petrology/egs073

Cashman, K., & Blundy, J. (2013). Petrological cannibalism: The chemical and textural consequences of incremental magma body growth. *Contributions to Mineralogy and Petrology*, *166*(3), 703–729. https://doi.org/10.1007/s00410-013-0895-0

Cembrano, J., Hervé, F., & Lavenu, A. (1996). The Liquiñe Ofqui fault zone: a long-lived intra-arc fault system in southern Chile. *Tectonophysics*, *259*(1–3), 55–66. https://doi.org/10.1016/0040-1951(95)00066-6

Clavero, J., & Moreno, H. (1994). Ignimbritas Licán y Pucón: Evidencias de erupciones explosivas andesítico-basálticas postglaciales del Volcán Villarrica, Andes del Sur, 39°25′S. *Actas VII Congreso Geológico Chileno*, 250–254.

D'Lemos, R. S. (1996). Mixing between granitic and dioritic crystal mushes, Guernsey, Channel Island, UK. *Lithos*, *38*, 233–257. https://doi.org/10.1016/0024-4937(96)00007-2

de Silva, S., Salas, G., & Schubring, S. (2008). Triggering explosive eruptions-The case for silicic magma recharge at Huaynaputina, southern Peru. *Geology*, *36*(5), 387–390. https://doi.org/10.1130/G24380A.1

Droop T.,R., G. (1987). A General Equation for Estimating Fe3+ Concentrations in Ferromagnesian Silicates and Oxides from Microprobe Analyses, Using Stoichiometric Criteria. *Mineralogical Magazine*, *51*(361), 431–435. https://doi.org/10.1180/minmag.1987.051.361.10

Ghiorso, M. S., & Sack, R. O. (1995). Chemical mass transfer in magmatic processes IV. A revised and internally consistent thermodynamic model for the interpolation and extrapolation of liquid-solid equilibria in magmatic systems at elevated temperatures and pressures. *Contributions to Mineralogy and Petrology*, *119*(2–3), 197–212. https://doi.org/10.1007/BF00307281

Grove, T. L., Donnelly-Nolan, J. M., & Housh, T. (1997). Magmatic processes that generated the rhyolite of Glass Mountain, Medicine Lake volcano, N. California. *Contributions to Mineralogy and Petrology*, *127*, 205–223. https://doi.org/10.1007/s004100050276

Gutiérrez, F., & Parada, M. A. (2010). Numerical modeling of time-dependent fluid dynamics and differentiation of a shallow basaltic magma chamber. *Journal of Petrology*, *51*(3), 731–

762. https://doi.org/10.1093/petrology/egp101

Hickey-Vargas, R., Roa, H. M., Escobar, L. L., & Frey, F. A. (1989). Geochemical variations in Andean basaltic and silicic lavas from the Villarrica-Lanin volcanic chain (39.5° S): an evaluation of source heterogeneity, fractional crystallization and crustal assimilation. *Contributions to Mineralogy and Petrology*, *103*(3), 361–386. https://doi.org/10.1007/BF00402922

Housh, T. B., & Luhr, J. F. (1991). Plagioclase-melt equilibria in hydrous systems. *American Mineralogist*, *76*(3–4), 477–492.

Humphreys, M. C. S., Blundy, J. D., & Sparks, R. S. J. (2006). Magma evolution and open-system processes at Shiveluch Volcano: Insights from phenocryst zoning. *Journal of Petrology*, *47*(12), 2303–2334. https://doi.org/10.1093/petrology/egl045

Köhler, T. P., & Brey, G. P. (1990). Calcium exchange between olivine and clinopyroxene calibrated as a geothermobarometer for natural peridotites from 2 to 60 kb with applications. *Geochimica et Cosmochimica Acta*, *54*(9), 2375–2388. https://doi.org/10.1016/0016-7037(90)90226-B

Lange, R. A., Frey, H. M., & Hector, J. (2009). A thermodynamic model for the plagioclase-liquid hygrometer/thermometer. *American Mineralogist*, *94*(4), 494–506. https://doi.org/10.2138/am.2009.3011

Le Bas, M. J., Le Maitre, R. W., Streckeisen, A., & Zanettin, B. (1986). A chemical classification of volcanic rocks based on the total alkali silica diagram. *Journal of Petrology*, *27*(3), 745–750. https://doi.org/10.1093/petrology/27.3.745

Lohmar, S. (2008). *Petrología de las Ignimbritas Licán y Pucón (Volcán Villarrica) y Cutacautín (Volcán Llaima) en los Andes del Sur de Chile*. *PhD Thesis*. Université Blaise Pascal (France) - Universidad de Chile (Santiago, Chile).

Lohmar, S., Parada, M., Gutiérrez, F., Robin, C., & Gerbe, M. C. (2012). Mineralogical and numerical approaches to establish the pre-eruptive conditions of the mafic Licán Ignimbrite, Villarrica Volcano (Chilean Southern Andes). *Journal of Volcanology and Geothermal Research*, *235–236*, 55–69. https://doi.org/10.1016/j.jvolgeores.2012.05.006

López-Escobar, L., Cembrano, J., & Moreno, H. (1995). Geochemistry and tectonics of the Chilean Southern Andes basaltic Quaternary volcanism (37-46^{o}S). *Revista Geológica de Chile*, *22*(2), 219–234.

Loucks, R. R. (1996). A precise olivine-augite Mg-Fe-exehange geothermometer. *Contributions to Mineralogy and Petrology*, *125*(2–3), 140–150. https://doi.org/10.1007/s004100050211

Moreno, H., & Clavero, J. (2006). Geología del volcán Villarrica, Regiones de la Araucanía y de los Lagos. Servicio Nacional de Geología y Minería. *Carta Geológica de Chile, Serie Geología Básica*, *98*.

Moreno, H., & Clavero, J. (2006). Geología del volcán Villarrica, Regiones de la Araucanía y de los Lagos. Servicio Nacional de Geología y Minería. *Carta Geológica de Chile, Serie Geología Básica*.

Morgado, E., Parada, M. A., Contreras, C., Castruccio, A., Gutiérrez, F., & McGee, L. E. (2015). Contrasting records from mantle to surface of Holocene lavas of two nearby arc volcanic complexes: Caburgua-Huelemolle Small Eruptive Centers and Villarrica Volcano, Southern Chile. *Journal of Volcanology and Geothermal Research*, *306*, 1–16.

https://doi.org/10.1016/j.jvolgeores.2015.09.023

Nakamura, M., & Shimatika, S. (1998). Dissolution origin and syn-entrapment compositional changes of melt inclusions in plagioclase. *Earth and Planetary Science Letters*, *161*(1–4), 119–133. Retrieved from http://www.sciencedirect.com/science/article/B6V61-3V72DR0-2R/2/256c1872cb9d3914948debc7a73e672a

Nelson, S. T., & Montana, A. (1992). Sieve-textured plagioclase in volcanic rocks produced by rapid decompression. *American Mineralogist*, *77*(11–12), 1242–1249.

Newhall, C. G. (1979). Temporal variation in the lavas of Mayon volcano, Philippines. *Journal of Volcanology and Geothermal Research*, *6*(1–2), 61–83. https://doi.org/10.1016/0377-0273(79)90047-7

Petit-Breuilh, M. E. (1994). Contribución al conocimiento de la cronología eruptiva histórica del Volcán Villarrica, 1558-1985. *Revista Frontera*, *13*, 71–99.

Renjith, M. L. (2014). Micro-textures in plagioclase from 1994-1995 eruption, Barren Island Volcano: Evidence of dynamic magma plumbing system in the Andaman subduction zone. *Geoscience Frontiers*, *5*(1), 113–126. https://doi.org/10.1016/j.gsf.2013.03.006

Roduit, N. (2007). JMicroVision : un logiciel d'analyse d'images pétrographiques polyvalent. *Uiniversité de Genève*, 116.

Ruprecht, P., & Wörner, G. (2007). Variable regimes in magma systems documented in plagioclase zoning patterns: El Misti stratovolcano and Andahua monogenetic cones. *Journal of Volcanology and Geothermal Research*, *165*(3–4), 142–162. https://doi.org/10.1016/j.jvolgeores.2007.06.002

Sides, I., Edmonds, M., Maclennan, J., Houghton, B. F., Swanson, D. A., & Steele-MacInnis, M. J. (2014). Magma mixing and high fountaining during the 1959 K īlauea Iki eruption, Hawai'i. *Earth and Planetary Science Letters*, *400*, 102–112. https://doi.org/10.1016/j.epsl.2014.05.024

Stern, C. R., Moreno, H., López-Escobar, L., Clavero, J. E., Lara, L. E., Naranjo, J. a., … Skewes, M. A. (2007). Chilean volcanoes. In T. Moreno & W. Gibbons (Eds.), *The Geology of Chile* (pp. 147–178). Geological Society of London. Retrieved from https://doi.org/10.1144/GOCH.5

Streck, M. J. (2008). Mineral Textures and Zoning as Evidence for Open System Processes. *Reviews in Mineralogy and Geochemistry*, *69*(1), 595–622. https://doi.org/10.2138/rmg.2008.69.15

Taddeucci, J., Edmonds, M., Houghton, B., James, M. R., & Vergniolle, S. (2015). *Hawaiian and Strombolian Eruptions*. *The Encyclopedia of Volcanoes* (Second Edi). Elsevier Inc. https://doi.org/10.1016/B978-0-12-385938-9.00027-4

Tsuchiyama, A. (1985). Dissolution kinetics of plagioclase in the melt of the system diopside-albite-anorthite, and origin of dusty plagioclase in andesites. *Contributions to Mineralogy and Petrology*, *89*(1), 1–16. https://doi.org/10.1007/BF01177585

Turner, M. B., Cronin, S. J., Smith, I. E., Stewart, R. B., & Neall, V. E. (2008). Eruption episodes and magma recharge events in andesitic systems: Mt Taranaki, New Zealand. *Journal of Volcanology and Geothermal Research*, *177*(4), 1063–1076. https://doi.org/10.1016/j.jvolgeores.2008.08.001

Ustunisik, G., Kilinc, A., & Nielsen, R. L. (2014). New insights into the processes controlling

compositional zoning in plagioclase. *Lithos*, *200–201*(1), 80–93. https://doi.org/10.1016/j.lithos.2014.03.021

Van Daele, M., Moernaut, J., Silversmit, G., Schmidt, S., Fontijn, K., Heirman, K., … De Batist, M. (2014). The 600 yr eruptive history of Villarrica Volcano (Chile) revealed by annually laminated lake sediments. *Bulletin of the Geological Society of America*, *126*(3–4), 481–498. https://doi.org/10.1130/B30798.1

Viccaro, M., Barca, D., Bohrson, W. A., D'Oriano, C., Giuffrida, M., Nicotra, E., & Pitcher, B. W. (2016). Crystal residence times from trace element zoning in plagioclase reveal changes in magma transfer dynamics at Mt. Etna during the last 400 years. *Lithos*, *248–251*, 309–323. https://doi.org/10.1016/j.lithos.2016.02.004

Viccaro, M., Giacomoni, P. P., Ferlito, C., & Cristofolini, R. (2010). Dynamics of magma supply at Mt. Etna volcano (Southern Italy) as revealed by textural and compositional features of plagioclase phenocrysts. *Lithos*, *116*(1–2), 77–91. https://doi.org/10.1016/j.lithos.2009.12.012

Waters, L. E., & Lange, R. A. (2015). An updated calibration of the plagioclase-liquid hygrometer-thermometer applicable to basalts through rhyolites. *American Mineralogist*, *100*(10), 2172–2184. https://doi.org/10.2138/am-2015-5232

Witter, J. B., Kress, V. C., Delmelle, P., & Stix, J. (2004). Volatile degassing, petrology, and magma dynamics of the Villarrica Lava Lake, Southern Chile. *Journal of Volcanology and Geothermal Research*, *134*(4), 303–337. https://doi.org/10.1016/j.jvolgeores.2004.03.002

Appendix 1. Supplementary data

Table A.1. Whole rock geochemistry data from the 3 studied lavas of Villarrica Volcano.

Lava	Detection limit	1921	1921	1921	1921	1921	1921
Code		1921 D04	R1921 06	1921 02	1921 03	1921 04	1921 08
SiO_2 (wt. %)	0.01 (%)	52.15	52.49	52.25	52.32	52.29	52.43
TiO_2 (wt. %)	0.001 (%)	1.250	1.254	1.255	1.232	1.296	1.304
Al_2O_3 (wt. %)	0.01 (%)	16.98	16.72	17.00	17.04	16.73	16.62
Fe_2O_3 (wt. %)	0.01 (%)	3.61	3.60	3.19	3.29	2.46	3.39
FeO (wt. %)	0.1 (%)	6.77	6.67	7.18	6.87	8.10	7.11
MnO (wt. %)	0.001 (%)	0.163	0.162	0.161	0.157	0.162	0.163
MgO (wt. %)	0.01 (%)	5.4	5.4	5.4	5.3	5.3	5.3
CaO (wt. %)	0.01 (%)	9.63	9.64	9.50	9.61	9.49	9.48
Na_2O (wt. %)	0.01 (%)	3.02	3.03	3.06	3.09	3.07	3.10
K_2O (wt. %)	0.01 (%)	0.757	0.756	0.768	0.767	0.781	0.790
P_2O_5 (wt. %)	0.01 (%)	0.309	0.269	0.263	0.269	0.277	0.286
LOI		-0.23	-0.40	-0.41	-0.45	-0.45	-0.46
total		100.20	100.10	98.49	99.92	100.70	100.80
Sc (ppm)	1 (ppm)	34	34	34	34	35	35
Be (ppm)	1 (ppm)	1	1	1	1	1	1
V (ppm)	5 (ppm)	306	308	304	305	323	329
Cr (ppm)	20 (ppm)	110	110	110	110	120	100
Co (ppm)	1 (ppm)	29	29	30	29	30	30
Ni (ppm)	20 (ppm)	50	40	50	50	50	40
Cu (ppm)	10 (ppm)	120	130	130	130	130	130
Zn (ppm)	30 (ppm)	90	80	100	90	120	90
Ga (ppm)	1 (ppm)	19	19	20	19	19	19
Ge (ppm)	1 (ppm)	2	2	2	2	2	2
As (ppm)	5 (ppm)	8	7	9	8	8	7
Rb (ppm)	2 (ppm)	18	17	18	18	18	18
Sr (ppm)	2 (ppm)	425	423	417	428	421	415
Y (ppm)	2 (ppm)	24	24	24	23	26	25
Zr (ppm)	4 (ppm)	101	104	100	100	106	106
Nb (ppm)	1 (ppm)	2	2	2	2	2	2
Ag (ppm)	0.5 (ppm)	0.8	0.6	0.8	0.8	0.8	0.8
Cs (ppm)	0.5 (ppm)	1.6	1.6	1.6	1.6	1.7	1.7
Ba (ppm)	3 (ppm)	233	236	232	233	241	244
La (ppm)	0.1 (ppm)	9.3	10.1	9.4	9.3	9.9	10
Ce (ppm)	0.1 (ppm)	22.3	23.6	23.1	22.4	23.8	23.6
Pr (ppm)	0.05 (ppm)	3.15	3.32	3.29	3.24	3.42	3.44
Nd (ppm)	0.1 (ppm)	14.7	15.3	15.5	15	15.8	15.8
Sm (ppm)	0.1 (ppm)	3.7	4.1	3.9	3.9	4.2	4.2
Eu (ppm)	0.05 (ppm)	1.11	1.09	1.14	1.05	1.12	1.16
Gd (ppm)	0.1 (ppm)	4.1	4.5	4.1	4.2	4.2	4.5
Tb (ppm)	0.1 (ppm)	0.7	0.7	0.7	0.7	0.7	0.8
Dy (ppm)	0.1 (ppm)	4.1	4.3	4.2	4.2	4.6	4.6
Ho (ppm)	0.1 (ppm)	0.9	0.9	0.9	0.9	0.9	0.9
Er (ppm)	0.1 (ppm)	2.6	2.6	2.6	2.5	2.6	2.7
Tm (ppm)	0.05 (ppm)	0.4	0.39	0.4	0.39	0.43	0.42
Yb (ppm)	0.1 (ppm)	2.4	2.8	2.6	2.5	2.7	2.7
Lu (ppm)	0.04 (ppm)	0.36	0.38	0.38	0.38	0.38	0.39
Hf (ppm)	0.2 (ppm)	2.5	2.5	2.5	2.4	2.7	2.6
Pb (ppm)	5 (ppm)	8	8	8	8	8	8
Th (ppm)	0.1 (ppm)	1.7	1.8	1.6	1.6	1.7	1.7
U (ppm)	0.1 (ppm)	0.5	0.6	0.5	0.6	0.6	0.6

Lava	1921	1948	1948	1948	1948	1948
Code	1921 05	1948 09	1948 04	1948 05	1948 06	1948 07
SiO_2 (wt. %)	52.36	51.72	51.65	51.67	52.05	51.98
TiO_2 (wt. %)	1.326	1.084	1.095	1.098	1.082	1.085
Al_2O_3 (wt. %)	16.65	16.36	16.36	16.45	16.27	16.34
Fe_2O_3 (wt. %)	3.23	4.64	3.94	3.81	4.04	3.58
FeO (wt. %)	7.31	5.59	6.39	6.60	6.02	6.45
MnO (wt. %)	0.164	0.157	0.156	0.158	0.156	0.156
MgO (wt. %)	5.3	7.1	7.1	7.0	6.9	7.0
CaO (wt. %)	9.46	9.59	9.58	9.46	9.66	9.65
Na_2O (wt. %)	3.11	2.90	2.89	2.88	2.95	2.93
K_2O (wt. %)	0.790	0.619	0.629	0.630	0.622	0.625
P_2O_5 (wt. %)	0.276	0.210	0.220	0.210	0.211	0.202
LOI	-0.48	-0.56	-0.52	-0.52	-0.47	-0.47
total	100.80	99.53	99.56	99.51	99.27	98.71
Sc (ppm)	35	33	33	33	33	33
Be (ppm)	1	1	1	1	1	1
V (ppm)	327	290	294	295	290	287
Cr (ppm)	110	310	310	330	300	290
Co (ppm)	29	33	33	34	33	33
Ni (ppm)	40	100	100	110	110	100
Cu (ppm)	150	130	130	140	130	120
Zn (ppm)	100	80	80	90	90	90
Ga (ppm)	20	17	18	18	19	17
Ge (ppm)	2	2	1	2	2	2
As (ppm)	8	8	8	9	8	8
Rb (ppm)	18	14	15	15	15	14
Sr (ppm)	431	375	381	375	371	384
Y (ppm)	25	22	21	22	20	21
Zr (ppm)	107	84	85	84	85	83
Nb (ppm)	2	1	2	2	1	1
Ag (ppm)	0.7	3.8	0.7	0.6	0.6	0.6
Cs (ppm)	1.7	1.4	1.4	1.4	1.5	1.4
Ba (ppm)	243	186	187	185	185	184
La (ppm)	9.7	6.9	6.9	6.9	6.8	6.7
Ce (ppm)	23.3	17	16.6	17.4	17.1	16.4
Pr (ppm)	3.34	2.53	2.53	2.52	2.59	2.44
Nd (ppm)	15.7	11.7	11.7	11.9	12.1	11.4
Sm (ppm)	4.3	3.3	3.3	3.2	3.4	3.3
Eu (ppm)	1.15	0.95	0.92	1	0.93	0.9
Gd (ppm)	4.4	3.5	3.5	3.5	3.7	3.4
Tb (ppm)	0.7	0.6	0.6	0.6	0.6	0.6
Dy (ppm)	4.6	3.7	3.8	3.8	3.8	3.6
Ho (ppm)	0.9	0.8	0.8	0.8	0.8	0.8
Er (ppm)	2.7	2.3	2.3	2.2	2.2	2.3
Tm (ppm)	0.41	0.36	0.36	0.36	0.35	0.34
Yb (ppm)	2.5	2.3	2.2	2.3	2.3	2.1
Lu (ppm)	0.39	0.35	0.34	0.33	0.35	0.31
Hf (ppm)	2.8	2.1	2.2	2.1	2.2	2
Pb (ppm)	8	6	7	7	7	6
Th (ppm)	1.8	1.2	1.2	1.2	1.2	1.1
U (ppm)	0.6	0.5	0.4	0.4	0.4	0.4

Lava	1948	1948	1948	1948	1948	1948
Code	1948 08	1948 10	1948 11	1948 12	1948 N1	1948 01
SiO_2 (wt. %)	52.38	51.87	52.03	52.25	51.61	51.68
TiO_2 (wt. %)	1.099	1.099	1.086	1.111	1.098	1.089
Al_2O_3 (wt. %)	16.23	16.57	16.30	15.95	16.28	16.37
Fe_2O_3 (wt. %)	3.28	3.57	2.94	5.81	4.09	3.55
FeO (wt. %)	6.67	6.47	7.04	4.25	6.23	6.68
MnO (wt. %)	0.155	0.156	0.155	0.159	0.157	0.156
MgO (wt. %)	6.9	7.0	7.0	7.0	7.2	7.2
CaO (wt. %)	9.54	9.53	9.63	9.73	9.59	9.58
Na_2O (wt. %)	2.94	2.89	2.94	2.92	2.88	2.91
K_2O (wt. %)	0.637	0.627	0.623	0.627	0.623	0.618
P_2O_5 (wt. %)	0.219	0.212	0.231	0.202	0.211	0.209
LOI	-0.43	-0.45	-0.48	-0.38	-0.46	-0.46
total	100.00	98.43	98.97	98.45	99.06	99.82
Sc (ppm)	34	33	33	34	33	33
Be (ppm)	1	1	< 1	1	1	< 1
V (ppm)	300	286	289	292	293	292
Cr (ppm)	290	310	250	310	320	280
Co (ppm)	33	33	33	33	35	34
Ni (ppm)	100	100	100	100	110	100
Cu (ppm)	130	140	130	120	130	130
Zn (ppm)	100	90	80	80	90	80
Ga (ppm)	18	18	18	18	18	18
Ge (ppm)	2	2	2	1	2	2
As (ppm)	8	9	8	8	9	9
Rb (ppm)	15	15	15	15	15	14
Sr (ppm)	382	377	383	373	374	375
Y (ppm)	22	21	21	22	21	20
Zr (ppm)	88	84	83	86	84	84
Nb (ppm)	1	1	1	1	1	1
Ag (ppm)	0.6	1.3	0.8	0.8	0.6	0.6
Cs (ppm)	1.5	1.4	1.4	1.4	1.5	1.4
Ba (ppm)	193	185	187	190	185	186
La (ppm)	7.3	7.1	6.9	7.1	6.9	6.9
Ce (ppm)	18	17.1	16.8	17.4	17.1	17
Pr (ppm)	2.62	2.53	2.48	2.65	2.54	2.56
Nd (ppm)	12.6	11.8	11.6	12.2	12.2	12.2
Sm (ppm)	3.5	3.3	3.2	3.3	3.3	3.5
Eu (ppm)	1.01	0.96	0.96	0.87	0.94	1.01
Gd (ppm)	3.7	3.6	3.6	3.7	3.7	3.7
Tb (ppm)	0.6	0.6	0.6	0.6	0.6	0.6
Dy (ppm)	3.9	3.7	3.7	4	3.7	3.8
Ho (ppm)	0.8	0.8	0.8	0.8	0.8	0.8
Er (ppm)	2.4	2.3	2.4	2.3	2.3	2.2
Tm (ppm)	0.35	0.35	0.37	0.35	0.36	0.34
Yb (ppm)	2.2	2.2	2.3	2.2	2.3	2.2
Lu (ppm)	0.32	0.34	0.34	0.35	0.33	0.33
Hf (ppm)	2.2	2.2	2	2.2	2	2.1
Pb (ppm)	7	7	7	7	7	7
Th (ppm)	1.3	1.3	1.2	1.2	1.2	1.2
U (ppm)	0.4	0.4	0.4	0.4	0.4	0.4

Lava	1948	1971	1971	1971	1971	1971
Code	1948 02	RC 1971	RM 1971	RMII 1971	1971 N1	1971 N2
SiO_2 (wt. %)	51.77	52.42	51.97	52.21	52.15	52.17
TiO_2 (wt. %)	1.088	1.112	1.133	1.126	1.118	1.108
Al_2O_3 (wt. %)	16.32	16.66	16.80	16.75	16.82	16.80
Fe_2O_3 (wt. %)	3.45	3.77	4.06	3.59	4.04	3.83
FeO (wt. %)	6.79	6.07	6.07	6.47	5.97	6.11
MnO (wt. %)	0.157	0.153	0.156	0.154	0.153	0.153
MgO (wt. %)	7.1	6.2	6.3	6.2	6.2	6.2
CaO (wt. %)	9.62	9.67	9.66	9.59	9.62	9.70
Na_2O (wt. %)	2.92	3.04	3.01	3.04	3.04	3.06
K_2O (wt. %)	0.619	0.637	0.636	0.637	0.637	0.641
P_2O_5 (wt. %)	0.220	0.219	0.219	0.219	0.229	0.200
LOI	-0.49	-0.45	-0.47	-0.48	-0.48	-0.52
total	99.63	99.99	100.10	99.95	99.99	99.29
Sc (ppm)	33	32	32	32	31	32
Be (ppm)	1	1	1	1	1	1
V (ppm)	293	293	292	294	289	292
Cr (ppm)	330	170	170	180	180	170
Co (ppm)	34	29	31	30	31	31
Ni (ppm)	100	70	80	70	70	70
Cu (ppm)	130	240	130	130	130	130
Zn (ppm)	80	80	100	80	80	100
Ga (ppm)	18	18	19	18	18	19
Ge (ppm)	2	1	2	2	2	2
As (ppm)	8	9	9	9	9	9
Rb (ppm)	15	14	15	14	14	15
Sr (ppm)	379	427	425	423	421	423
Y (ppm)	20	21	22	21	21	20
Zr (ppm)	84	86	85	86	86	84
Nb (ppm)	1	1	1	1	1	1
Ag (ppm)	0.7	0.7	0.6	0.6	0.8	0.7
Cs (ppm)	1.4	1.4	1.5	1.4	1.4	1.4
Ba (ppm)	186	201	200	199	201	199
La (ppm)	7.2	7	7.2	7.2	7.2	7.3
Ce (ppm)	17.2	17.4	17.7	17.7	17.5	17.9
Pr (ppm)	2.54	2.51	2.59	2.62	2.6	2.65
Nd (ppm)	12.3	12.3	13.2	12.5	12.3	12.6
Sm (ppm)	3.3	3.4	3.3	3.3	3.6	3.3
Eu (ppm)	0.93	0.95	0.98	0.97	0.96	0.97
Gd (ppm)	3.7	3.6	3.8	3.6	3.6	3.8
Tb (ppm)	0.6	0.6	0.6	0.6	0.6	0.6
Dy (ppm)	3.7	3.7	3.8	3.7	3.6	3.7
Ho (ppm)	0.8	0.8	0.8	0.8	0.8	0.8
Er (ppm)	2.3	2.2	2.2	2.3	2.4	2.3
Tm (ppm)	0.36	0.35	0.34	0.35	0.37	0.37
Yb (ppm)	2.3	2.3	2.3	2.2	2.3	2.3
Lu (ppm)	0.33	0.33	0.34	0.32	0.32	0.33
Hf (ppm)	2.1	2.2	2	2.1	2.3	2.1
Pb (ppm)	6	7	7	7	7	7
Th (ppm)	1.2	1.2	1.2	1.1	1.2	1.1
U (ppm)	0.5	0.4	0.5	0.4	0.4	0.4

Lava	1971	1971	1971	1971	1971	1971
Code	1971 02	1971 03	1971 N6	R1971 DM	R1971 DV	1971 04
SiO_2 (wt. %)	52.58	52.24	52.23	52.05	52.21	52.26
TiO_2 (wt. %)	1.118	1.138	1.092	1.125	1.140	1.116
Al_2O_3 (wt. %)	16.58	16.65	16.56	16.65	16.73	16.76
Fe_2O_3 (wt. %)	3.38	3.34	3.01	2.32	4.59	3.34
FeO (wt. %)	6.43	6.78	7.12	8.11	5.55	6.74
MnO (wt. %)	0.154	0.156	0.155	0.155	0.155	0.154
MgO (wt. %)	6.2	6.2	6.3	6.1	6.2	6.1
CaO (wt. %)	9.68	9.61	9.65	9.66	9.63	9.66
Na_2O (wt. %)	3.02	3.01	3.02	3.00	3.01	3.04
K_2O (wt. %)	0.643	0.638	0.633	0.631	0.635	0.644
P_2O_5 (wt. %)	0.218	0.229	0.208	0.220	0.202	0.211
LOI	-0.45	-0.50	-0.61	-0.56	-0.41	-0.54
total	100.60	99.76	100.60	99.34	98.73	98.85
Sc (ppm)	32	32	32	31	32	32
Be (ppm)	1	1	1	< 1	1	1
V (ppm)	297	292	297	292	287	290
Cr (ppm)	190	180	190	180	180	180
Co (ppm)	30	31	31	32	30	30
Ni (ppm)	70	70	90	80	70	70
Cu (ppm)	130	140	130	130	120	130
Zn (ppm)	80	90	80	90	90	80
Ga (ppm)	19	18	19	20	18	19
Ge (ppm)	2	2	1	2	2	1
As (ppm)	9	9	8	11	7	8
Rb (ppm)	15	14	14	14	14	15
Sr (ppm)	424	421	414	424	417	418
Y (ppm)	22	21	22	22	21	22
Zr (ppm)	87	86	85	85	85	86
Nb (ppm)	2	1	1	1	1	1
Ag (ppm)	0.7	0.7	0.7	0.6	0.5	0.5
Cs (ppm)	1.5	1.4	1.4	1.5	1.5	1.4
Ba (ppm)	202	199	201	196	197	198
La (ppm)	7.2	7	6.9	7.3	7	7.1
Ce (ppm)	17.7	17.3	17.5	18	17.3	17.5
Pr (ppm)	2.66	2.57	2.56	2.58	2.62	2.61
Nd (ppm)	12.6	12.5	12	12.7	12.5	12.4
Sm (ppm)	3.4	3.3	3.4	3.4	3.2	3.5
Eu (ppm)	0.94	0.99	0.97	0.98	0.93	0.99
Gd (ppm)	3.6	3.6	3.6	3.6	3.5	3.6
Tb (ppm)	0.6	0.6	0.6	0.6	0.6	0.6
Dy (ppm)	3.8	3.8	3.7	3.6	3.6	3.8
Ho (ppm)	0.8	0.8	0.8	0.8	0.8	0.8
Er (ppm)	2.4	2.3	2.3	2.3	2.4	2.4
Tm (ppm)	0.36	0.34	0.37	0.35	0.37	0.36
Yb (ppm)	2.3	2.2	2.4	2.2	2.3	2.2
Lu (ppm)	0.32	0.33	0.34	0.33	0.32	0.33
Hf (ppm)	2.1	2.2	2.3	2.2	2.1	2.1
Pb (ppm)	7	8	6	7	6	7
Th (ppm)	1.2	1.1	1.2	1.2	1.2	1.2
U (ppm)	0.4	0.4	0.4	0.4	0.4	0.4

Lava	1971	1971	1971	1971	1971	1971
Code	R1971 04	1971 N5	1971 N4	1971 05	RM 1971 05	1971 07
SiO_2 (wt. %)	52.48	52.58	52.60	52.21	52.38	53.12
TiO_2 (wt. %)	1.163	1.148	1.095	1.128	1.147	1.132
Al_2O_3 (wt. %)	16.61	16.56	16.42	16.93	16.74	16.77
Fe_2O_3 (wt. %)	3.64	3.83	3.21	3.72	3.79	3.56
FeO (wt. %)	6.43	6.13	6.64	6.41	6.31	6.03
MnO (wt. %)	0.155	0.156	0.155	0.154	0.153	0.153
MgO (wt. %)	6.1	6.0	6.3	6.0	6.0	6.0
CaO (wt. %)	9.52	9.65	9.67	9.46	9.60	9.32
Na_2O (wt. %)	3.05	3.06	3.01	3.15	3.01	3.06
K_2O (wt. %)	0.653	0.663	0.644	0.621	0.641	0.662
P_2O_5 (wt. %)	0.228	0.221	0.231	0.227	0.240	0.207
LOI	-0.51	-0.49	-0.48	-0.54	-0.33	-0.44
total	100.60	99.06	98.91	100.90	99.57	100.80
Sc (ppm)	33	32	31	32	32	33
Be (ppm)	1	1	1	1	1	1
V (ppm)	300	300	292	297	293	294
Cr (ppm)	180	160	190	190	170	190
Co (ppm)	30	29	32	31	30	31
Ni (ppm)	70	60	70	80	70	70
Cu (ppm)	130	120	130	140	130	130
Zn (ppm)	80	80	90	100	80	90
Ga (ppm)	18	18	19	19	18	19
Ge (ppm)	2	2	2	2	1	2
As (ppm)	8	7	9	17	8	9
Rb (ppm)	14	14	14	15	14	15
Sr (ppm)	428	420	406	432	420	427
Y (ppm)	22	23	21	22	22	23
Zr (ppm)	90	88	85	89	86	89
Nb (ppm)	1	1	1	1	1	2
Ag (ppm)	0.6	0.6	0.6	0.6	0.6	0.6
Cs (ppm)	1.4	1.5	1.5	1.5	1.4	1.5
Ba (ppm)	205	203	198	199	199	204
La (ppm)	7.5	7.1	7.3	7.9	6.9	8.1
Ce (ppm)	18.3	17.7	17.7	18.9	17.4	18.8
Pr (ppm)	2.62	2.63	2.57	2.68	2.54	2.74
Nd (ppm)	12.4	12.4	12.3	12.8	11.8	12.5
Sm (ppm)	3.5	3.4	3.4	3.4	3.5	3.5
Eu (ppm)	1.04	0.99	1	0.96	1.01	0.98
Gd (ppm)	3.7	3.6	3.5	3.7	3.6	3.6
Tb (ppm)	0.6	0.6	0.6	0.6	0.6	0.6
Dy (ppm)	4	3.9	3.9	3.8	3.8	3.9
Ho (ppm)	0.8	0.8	0.8	0.8	0.8	0.8
Er (ppm)	2.3	2.3	2.3	2.4	2.3	2.3
Tm (ppm)	0.36	0.36	0.34	0.36	0.35	0.35
Yb (ppm)	2.3	2.3	2.2	2.3	2.3	2.2
Lu (ppm)	0.34	0.33	0.33	0.33	0.34	0.33
Hf (ppm)	2.1	2.2	2.2	2	2.2	2.3
Pb (ppm)	7	7	7	38	7	7
Th (ppm)	1.2	1.2	1.2	1.3	1.2	1.1
U (ppm)	0.4	0.4	0.4	0.5	0.4	0.4

Lava	1971	1971	1971	1971	1971	1971
Code	1971 08	1971 09	1971 10 M1	1971 10 M2	1971 11	1971 12
SiO_2 (wt. %)	52.14	52.41	52.42	52.32	52.14	52.36
TiO_2 (wt. %)	1.126	1.112	1.128	1.131	1.123	1.119
Al_2O_3 (wt. %)	16.74	16.69	16.84	16.87	17.03	16.91
Fe_2O_3 (wt. %)	3.45	3.31	3.20	3.91	3.02	3.10
FeO (wt. %)	6.77	6.69	6.66	5.98	6.97	6.82
MnO (wt. %)	0.156	0.154	0.155	0.154	0.154	0.152
MgO (wt. %)	6.1	6.1	6.0	6.0	6.0	6.0
CaO (wt. %)	9.60	9.60	9.66	9.65	9.67	9.60
Na_2O (wt. %)	3.03	3.06	3.04	3.06	3.07	3.08
K_2O (wt. %)	0.647	0.649	0.646	0.647	0.647	0.652
P_2O_5 (wt. %)	0.212	0.230	0.232	0.229	0.219	0.227
LOI	-0.54	-0.51	-0.47	-0.49	-0.55	-0.61
total	98.35	99.60	98.57	99.92	99.92	100.60
Sc (ppm)	32	32	32	32	32	32
Be (ppm)	1	1	1	1	1	1
V (ppm)	290	293	291	295	300	298
Cr (ppm)	180	190	180	170	160	160
Co (ppm)	31	31	30	30	30	31
Ni (ppm)	80	70	70	70	70	60
Cu (ppm)	130	130	130	130	130	130
Zn (ppm)	90	80	90	80	80	90
Ga (ppm)	19	19	18	18	18	18
Ge (ppm)	2	2	2	1	1	1
As (ppm)	7	9	8	8	8	7
Rb (ppm)	15	15	14	14	14	15
Sr (ppm)	412	420	420	429	434	433
Y (ppm)	22	22	22	22	21	21
Zr (ppm)	86	87	86	86	87	88
Nb (ppm)	1	1	1	1	3	3
Ag (ppm)	< 0.5	0.7	0.7	0.6	0.5	< 0.5
Cs (ppm)	1.5	1.4	1.5	1.5	1.6	1.7
Ba (ppm)	197	200	199	202	201	203
La (ppm)	7.4	7.3	7.2	7.2	8.5	8.3
Ce (ppm)	17.9	17.8	17.8	17.7	20.5	20
Pr (ppm)	2.67	2.64	2.67	2.56	2.83	2.78
Nd (ppm)	13	12.5	12.3	12.1	13.3	13.4
Sm (ppm)	3.4	3.6	3.5	3.5	3.5	3.5
Eu (ppm)	1	1.02	0.99	0.96	1.08	1.05
Gd (ppm)	3.8	3.9	3.7	3.5	3.5	3.7
Tb (ppm)	0.6	0.7	0.6	0.6	0.6	0.6
Dy (ppm)	3.9	3.8	3.8	3.8	3.9	3.8
Ho (ppm)	0.8	0.8	0.8	0.8	0.8	0.8
Er (ppm)	2.3	2.3	2.3	2.3	2.3	2.3
Tm (ppm)	0.36	0.35	0.36	0.36	0.38	0.35
Yb (ppm)	2.2	2.3	2.3	2.2	2.4	2.2
Lu (ppm)	0.33	0.35	0.33	0.33	0.35	0.33
Hf (ppm)	2.2	2.1	2.1	2.2	2.1	2.1
Pb (ppm)	7	7	7	7	8	8
Th (ppm)	1.2	1.2	1.2	1.2	1.4	1.4
U (ppm)	0.5	0.4	0.4	0.4	0.5	0.5

Lava	1971	1971	1971	1971
Code	1971 13	1971 30	1971 29	1971 28
SiO_2 (wt. %)	51.95	52.68	52.75	52.24
TiO_2 (wt. %)	1.123	1.127	1.094	1.121
Al_2O_3 (wt. %)	17.12	16.69	17.30	17.15
Fe_2O_3 (wt. %)	3.34	2.82	2.84	3.79
FeO (wt. %)	6.81	7.07	6.80	6.13
MnO (wt. %)	0.155	0.153	0.149	0.152
MgO (wt. %)	6.1	6.0	5.7	5.8
CaO (wt. %)	9.46	9.58	9.43	9.60
Na_2O (wt. %)	3.07	3.07	3.09	3.10
K_2O (wt. %)	0.651	0.647	0.651	0.652
P_2O_5 (wt. %)	0.237	0.179	0.207	0.217
LOI	-0.56	-0.55	-0.59	-0.48
total	100.70	99.93	100.80	100.70
Sc (ppm)	33	33	32	32
Be (ppm)	1	1	1	1
V (ppm)	298	292	290	300
Cr (ppm)	160	170	150	160
Co (ppm)	30	31	29	31
Ni (ppm)	60	70	60	60
Cu (ppm)	130	130	130	140
Zn (ppm)	90	90	90	140
Ga (ppm)	17	18	18	18
Ge (ppm)	2	1	1	2
As (ppm)	7	7	8	7
Rb (ppm)	14	15	14	15
Sr (ppm)	431	428	438	430
Y (ppm)	22	22	22	21
Zr (ppm)	88	87	87	89
Nb (ppm)	3	2	2	3
Ag (ppm)	0.5	0.5	0.7	0.6
Cs (ppm)	1.7	1.7	1.6	1.6
Ba (ppm)	204	198	202	204
La (ppm)	8.2	8	8	9.1
Ce (ppm)	19.9	19.7	19.6	21.4
Pr (ppm)	2.77	2.72	2.72	2.88
Nd (ppm)	13	13.3	13.1	13.8
Sm (ppm)	3.6	3.6	3.4	3.8
Eu (ppm)	1.08	1.03	1.11	1.06
Gd (ppm)	3.6	3.7	3.5	3.8
Tb (ppm)	0.6	0.7	0.6	0.7
Dy (ppm)	3.9	3.9	3.8	4
Ho (ppm)	0.8	0.8	0.8	0.8
Er (ppm)	2.3	2.3	2.3	2.4
Tm (ppm)	0.34	0.35	0.35	0.36
Yb (ppm)	2.2	2.2	2.3	2.3
Lu (ppm)	0.34	0.35	0.35	0.35
Hf (ppm)	2.2	2.2	2.2	2.2
Pb (ppm)	9	8	8	11
Th (ppm)	1.4	1.3	1.3	1.4
U (ppm)	0.4	0.5	0.4	0.5

Table A.2. EPMA of plagioclase phenocrysts chemistry. Analysis performed at University of Exeter (UoE) and University of Bristol (UoB).

Lava		1921	1921	1921	1921	1921
Point		1921-Pl4_1	1921-Pl4_2	1921-Pl4_3	1921-Pl4_4	1921-Pl4_6
Laboratory	Detection limit	UoE	UoE	UoE	UoE	UoE
Na2O (wt. %)	0.01 (%)	3.93	3.93	2.01	2.09	3.48
FeO (wt. %)	0.02 (%)	0.675	0.743	0.660	0.547	0.657
CaO (wt. %)	0.01 (%)	12.86	13.04	16.50	16.27	13.68
Al2O3 (wt. %)	0.01 (%)	28.45	28.38	31.76	31.60	29.32
K2O (wt. %)	0.005 (%)	0.162	0.178	0.071	0.082	0.139
MgO (wt. %)	0.01 (%)	0.181	0.181	0.120	0.122	0.188
SiO2 (wt. %)	0.02 (%)	52.18	52.31	47.74	47.99	50.76
TiO2 (wt. %)	0.01 (%)					
Total		98.65	98.85	98.95	98.81	98.35
Al (%)		15.06	15.02	16.81	16.72	15.52
Fe (ppm)		5244	5773	5127	4249	5110
Ti (ppm)						
Mg (ppm)		1090	1089	722	733	1134
XAn		63.54	63.79	81.42	80.58	67.67
XAb		35.50	35.17	18.15	18.93	31.50
XOr		0.96	1.05	0.42	0.49	0.83
Compositional group		An-poor	An-poor	An-rich	An-rich	An-poor

Lava	1921	1921	1921	1921	1921	1921
Point	1921-Pl4_7	1921-05-1__12	1921-05-1__13	1921-02 - Gl 1-P9	1921-02 - Gl 1-P10	1921-02 - Gl 1-P11
Laboratory	UoE	UoE	UoE	UoB	UoB	UoB
Na2O (wt. %)	4.35	1.75	3.84	2.22	2.16	2.30
FeO (wt. %)	0.941	0.680	0.732	0.676	0.618	0.630
CaO (wt. %)	12.12	16.94	13.11	16.60	16.38	16.75
Al2O3 (wt. %)	27.83	31.89	28.59	32.34	32.35	32.87
K2O (wt. %)	0.237	0.031	0.072	0.069	0.070	0.075
MgO (wt. %)	0.215	0.096	0.184	0.114	0.112	0.122
SiO2 (wt. %)	53.11	46.86	52.37	46.94	47.42	48.15
TiO2 (wt. %)		0.049	0.076	0.010	0.029	0.034
Total	99.05	98.38	98.97	98.99	99.18	100.94
Al (%)	14.73	16.88	15.13	17.11	17.12	17.40
Fe (ppm)	7315	5287	5690	5252	4807	4900
Ti (ppm)		292	456	63	174	201
Mg (ppm)	1293	580	1108	690	673	736
XAn	59.51	83.95	64.88	79.97	80.19	79.52
XAb	39.09	15.88	34.71	19.63	19.40	20.04
XOr	1.40	0.18	0.42	0.40	0.41	0.43
Compositional group	An-poor	An-rich	An-poor	An-rich	An-rich	An-rich

Lava	1921	1921	1921	1921	1921	1921
Point	1921-02 - Gl 1-P13	1921-02 - Gl 1-P14	1921-02 - Gl 1-P15	1921-02 - Gl 1-P16	1921-02 - Gl 1-P12	1921-02 - Gl11-P5
Laboratory	UoB	UoB	UoB	UoB	UoB	UoB
Na2O (wt. %)	4.08	3.85	4.16	4.49	3.97	4.15
FeO (wt. %)	0.731	0.699	0.723	1.030	0.746	0.804
CaO (wt. %)	13.17	13.23	12.82	12.24	13.46	13.12
Al2O3 (wt. %)	29.56	29.49	29.54	28.46	30.21	29.65
K2O (wt. %)	0.166	0.183	0.186	0.189	0.177	0.163
MgO (wt. %)	0.214	0.197	0.191	0.178	0.182	0.200
SiO2 (wt. %)	52.41	51.06	52.75	52.99	52.53	52.62
TiO2 (wt. %)	0.055	0.062	0.048	0.072	0.080	0.059
Total	100.41	98.79	100.44	99.69	101.39	100.79
Al (%)	15.65	15.61	15.63	15.06	15.99	15.69
Fe (ppm)	5684	5433	5618	8008	5800	6252
Ti (ppm)	331	374	286	434	480	353
Mg (ppm)	1291	1188	1152	1071	1096	1204
XAn	63.15	64.50	62.01	59.12	64.25	62.69
XAb	35.89	34.42	36.90	39.78	34.73	36.37
XOr	0.96	1.07	1.08	1.10	1.02	0.94
Compositional group	An-poor	An-poor	An-poor	An-poor	An-poor	An-poor

Lava	1921	1921	1921	1921	1921	1921
Point	1921-02 - Gl11-P6	1921-02 - Gl11-P7	1921-02 - Gl11-P8	1921-02 - Gl11-P10	1921-02 - Gl11-P12	1921-02 - Gl 6-P13
Laboratory	UoB	UoB	UoB	UoB	UoB	UoB
Na2O (wt. %)	4.01	3.74	4.86	4.31	4.24	4.17
FeO (wt. %)	0.718	0.722	0.976	0.707	0.749	1.072
CaO (wt. %)	13.27	13.87	11.80	12.31	12.99	12.45
Al2O3 (wt. %)	29.74	30.38	28.50	28.77	29.66	29.02
K2O (wt. %)	0.167	0.161	0.238	0.180	0.192	0.186
MgO (wt. %)	0.164	0.191	0.178	0.198	0.198	0.191
SiO2 (wt. %)	52.34	52.02	54.52	52.60	53.42	52.60
TiO2 (wt. %)	0.045	0.031	0.078	0.080	0.082	0.067
Total	100.48	101.12	101.17	99.21	101.53	99.76
Al (%)	15.74	16.08	15.08	15.23	15.69	15.36
Fe (ppm)	5584	5614	7584	5495	5819	8332
Ti (ppm)	270	187	468	481	489	402
Mg (ppm)	990	1149	1075	1191	1191	1152
XAn	63.72	66.29	56.22	60.29	61.91	61.30
XAb	35.32	32.78	42.41	38.65	36.98	37.60
XOr	0.97	0.93	1.37	1.06	1.11	1.10
Compositional group	An-poor	An-poor	An-poor	An-poor	An-poor	An-poor

Lava	1921	1921	1921	1921	1921	1921
Point	1921-02 - Gl 10-P3	1921-02 - Gl 10-P8	1921-02 - Gl 10-P9	1921-02 - Gl 10-P16	1921-02 - Gl 10-P17	1921-02 - Gl 10-P18
Laboratory	UoB	UoB	UoB	UoB	UoB	UoB
Na2O (wt. %)	4.27	4.61	4.17	4.25	4.22	4.07
FeO (wt. %)	0.812	1.078	0.906	0.719	0.721	0.745
CaO (wt. %)	12.76	12.08	12.76	12.72	12.79	12.85
Al2O3 (wt. %)	29.09	28.34	29.02	28.93	28.65	29.09
K2O (wt. %)	0.174	0.199	0.184	0.183	0.178	0.177
MgO (wt. %)	0.200	0.190	0.181	0.192	0.204	0.187
SiO2 (wt. %)	52.38	53.01	52.59	52.29	52.35	51.82
TiO2 (wt. %)	0.034	0.068	0.069	0.073	0.066	0.065
Total	99.73	99.59	99.89	99.36	99.20	99.02
Al (%)	15.40	15.00	15.36	15.31	15.16	15.40
Fe (ppm)	6315	8380	7046	5591	5608	5794
Ti (ppm)	204	410	411	437	395	387
Mg (ppm)	1206	1147	1092	1157	1230	1130
XAn	61.31	58.12	61.88	61.38	61.69	62.59
XAb	37.68	40.72	37.04	37.55	37.28	36.37
XOr	1.01	1.15	1.08	1.07	1.04	1.04
Compositional group	An-poor	An-poor	An-poor	An-poor	An-poor	An-poor

Lava	1921	1921	1921	1921	1921	1921
Point	1921-02 - Gl 10-P19	1921-02 - Gl 10-P20	1921-02 - Gl 10-P21	1921-02 - Gl 10-P22	1921-02 - Gl 2-P5	1921-02 - Gl 2-P6
Laboratory	UoB	UoB	UoB	UoB	UoB	UoB
Na2O (wt. %)	4.02	4.17	3.83	4.19	1.87	3.68
FeO (wt. %)	0.726	0.735	0.755	0.826	0.590	0.662
CaO (wt. %)	13.06	12.54	13.18	12.75	16.85	13.43
Al2O3 (wt. %)	29.15	28.69	29.39	29.01	32.80	29.52
K2O (wt. %)	0.173	0.160	0.166	0.192	0.052	0.140
MgO (wt. %)	0.195	0.206	0.165	0.193	0.160	0.176
SiO2 (wt. %)	51.97	53.20	52.21	52.41	46.75	51.42
TiO2 (wt. %)	0.071	0.074	0.035	0.073	0.004	0.058
Total	99.40	99.79	99.77	99.65	99.08	99.09
Al (%)	15.43	15.18	15.55	15.35	17.36	15.62
Fe (ppm)	5643	5713	5869	6421	4588	5144
Ti (ppm)	425	445	208	435	21	349
Mg (ppm)	1175	1245	996	1163	967	1062
XAn	63.31	61.59	64.63	61.71	82.86	66.06
XAb	35.68	37.47	34.39	37.17	16.83	33.11
XOr	1.01	0.95	0.98	1.12	0.31	0.83
Compositional group	An-poor	An-poor	An-poor	An-poor	An-rich	An-poor

Lava	1921	1921	1921	1921	1921	1921
Point	1921-02 - Gl 2-P7	1921-02 - Gl 2-P8	1921-02 - Mgl1-P3	1921-02 - Gl 3-P11	1921-02 - Gl 3-P12	1921-02 - Gl 7-P3
Laboratory	UoB	UoB	UoB	UoB	UoB	UoB
Na2O (wt. %)	2.16	4.60	4.22	4.25	4.63	4.26
FeO (wt. %)	0.581	1.095	0.789	0.954	0.924	0.680
CaO (wt. %)	16.22	11.67	12.71	12.55	12.07	12.49
Al2O3 (wt. %)	32.07	27.95	29.01	28.95	28.39	28.60
K2O (wt. %)	0.074	0.221	0.187	0.187	0.225	0.192
MgO (wt. %)	0.113	0.192	0.170	0.159	0.194	0.188
SiO2 (wt. %)	47.69	53.36	52.64	52.10	53.46	52.49
TiO2 (wt. %)	0.031	0.082	0.057	0.067	0.063	0.057
Total	98.95	99.17	99.79	99.23	99.97	99.00
Al (%)	16.97	14.79	15.35	15.32	15.03	15.14
Fe (ppm)	4520	8511	6134	7419	7182	5286
Ti (ppm)	185	489	345	400	378	344
Mg (ppm)	683	1159	1027	957	1171	1133
XAn	80.00	57.30	61.48	61.02	57.94	60.83
XAb	19.55	41.40	37.43	37.89	40.76	38.04
XOr	0.44	1.31	1.09	1.09	1.30	1.12
Compositional group	An-rich	An-poor	An-poor	An-poor	An-poor	An-poor

Lava	1921	1921	1921	1921	1921	1921
Point	1921-02 - Gl 7-P2	1921-02 - Gl 7-P4	1921-02 - Gl 9-P1	1921-02 - Gl 9-P2	1921-02 - Gl 9-P3	1921-02 - Gl 9-P4
Laboratory	UoB	UoB	UoB	UoB	UoB	UoB
Na2O (wt. %)	4.10	4.01	1.78	4.34	4.19	4.48
FeO (wt. %)	0.776	0.754	0.677	0.738	0.708	0.915
CaO (wt. %)	12.84	13.00	16.97	12.40	12.70	12.34
Al2O3 (wt. %)	28.73	29.23	32.81	28.63	29.02	28.54
K2O (wt. %)	0.173	0.164	0.073	0.185	0.186	0.209
MgO (wt. %)	0.191	0.194	0.102	0.175	0.233	0.141
SiO2 (wt. %)	52.43	51.93	46.79	52.89	52.99	52.55
TiO2 (wt. %)	0.046	0.045	0.015	0.062	0.069	0.080
Total	99.30	99.35	99.24	99.44	100.11	99.28
Al (%)	15.21	15.47	17.36	15.15	15.36	15.10
Fe (ppm)	6030	5863	5259	5739	5502	7109
Ti (ppm)	276	272	89	374	416	477
Mg (ppm)	1154	1170	616	1057	1405	850
XAn	62.46	63.25	83.49	60.28	61.67	59.26
XAb	36.53	35.78	16.08	38.63	37.24	39.53
XOr	1.01	0.96	0.43	1.09	1.09	1.21
Compositional group	An-poor	An-poor	An-rich	An-poor	An-poor	An-poor

Lava	1921	1921	1921	1921	1921	1921
Point	1921-02 - Pl 5-P1	1921-02 - Pl 5-P2	1921-02 - Pl 5-P3	1921-02 - Pl 5-P4	1921-02 - Pl 5-P5	1921-02 - Pl 5-P6
Laboratory	UoB	UoB	UoB	UoB	UoB	UoB
Na2O (wt. %)	1.53	1.23	1.25	1.32	1.74	4.20
FeO (wt. %)	0.515	0.496	0.527	0.484	0.506	0.693
CaO (wt. %)	17.84	18.16	18.02	18.17	17.28	12.78
Al2O3 (wt. %)	34.06	34.12	33.91	34.02	33.22	29.09
K2O (wt. %)	0.032	0.040	0.041	0.029	0.033	0.157
MgO (wt. %)	0.078	0.110	0.109	0.097	0.136	0.159
SiO2 (wt. %)	45.84	45.45	45.24	45.63	46.28	52.60
TiO2 (wt. %)	0.008	0.014	0.003	0.016	0.010	0.072
Total	99.91	99.65	99.16	99.79	99.21	99.76
Al (%)	18.02	18.06	17.95	18.01	17.58	15.39
Fe (ppm)	4001	3853	4098	3761	3932	5390
Ti (ppm)	49	84	19	96	59	431
Mg (ppm)	469	664	656	586	821	957
XAn	86.26	88.70	88.48	88.07	84.23	61.88
XAb	13.55	11.06	11.27	11.76	15.58	37.20
XOr	0.19	0.24	0.24	0.17	0.19	0.92
Compositional group	An-rich	An-rich	An-rich	An-rich	An-rich	An-poor

Lava	1921	1921	1921	1921	1921	1921
Point	1921-02 - Pl 5-P7	1921-02 - Pl 5-P8	1921-02 - Pl 5-P9	1921-02 - Pl 5-P10	1921-02 - Pl 4-P10	1921-02 - Pl 4-P9
Laboratory	UoB	UoB	UoB	UoB	UoB	UoB
Na2O (wt. %)	3.89	3.77	4.04	4.06	2.30	1.89
FeO (wt. %)	0.677	0.619	0.711	0.706	0.701	0.644
CaO (wt. %)	13.07	13.88	12.79	13.06	16.42	16.66
Al2O3 (wt. %)	29.22	30.21	29.14	29.54	32.58	32.45
K2O (wt. %)	0.159	0.138	0.171	0.185	0.061	0.063
MgO (wt. %)	0.157	0.137	0.195	0.192	0.148	0.142
SiO2 (wt. %)	52.10	51.54	52.40	51.87	47.07	47.05
TiO2 (wt. %)	0.063	0.041	0.051	0.055	0.019	0.035
Total	99.35	100.35	99.51	99.67	99.31	98.94
Al (%)	15.47	15.99	15.42	15.63	17.24	17.17
Fe (ppm)	5259	4811	5524	5489	5447	5007
Ti (ppm)	379	246	304	332	116	207
Mg (ppm)	950	825	1174	1156	890	856
XAn	64.12	66.21	62.73	63.01	79.24	82.46
XAb	34.94	33.00	36.26	35.92	20.40	17.17
XOr	0.94	0.79	1.01	1.08	0.36	0.38
Compositional group	An-poor	An-poor	An-poor	An-poor	An-rich	An-rich

Lava	1921	1921	1921	1921	1921	1921
Point	1921-02 - Pl 4-P11	1921-02 - Pl 4-P12	1921-02 - Pl 4-P13	1921-02 - Pl 4-P14	1921-02 - Pl 4-P15	1921-02 - Pl 4-P16
Laboratory	UoB	UoB	UoB	UoB	UoB	UoB
Na2O (wt. %)	2.08	1.89	3.99	3.85	3.98	4.86
FeO (wt. %)	0.641	0.612	0.706	0.756	0.665	0.617
CaO (wt. %)	16.87	16.82	13.20	13.36	13.28	11.69
Al2O3 (wt. %)	32.77	32.51	29.43	29.71	29.60	28.06
K2O (wt. %)	0.051	0.082	0.171	0.166	0.154	0.220
MgO (wt. %)	0.144	0.119	0.176	0.190	0.193	0.205
SiO2 (wt. %)	46.95	47.06	52.07	51.28	51.82	53.88
TiO2 (wt. %)	0.007	0.028	0.062	0.052	0.037	0.079
Total	99.54	99.13	99.81	99.37	99.74	99.63
Al (%)	17.35	17.21	15.57	15.72	15.67	14.85
Fe (ppm)	4983	4761	5484	5878	5170	4796
Ti (ppm)	43	169	373	312	225	474
Mg (ppm)	867	717	1064	1147	1163	1235
XAn	81.26	82.52	63.71	64.77	63.98	56.04
XAb	18.45	17.00	35.29	34.26	35.13	42.68
XOr	0.30	0.49	1.00	0.97	0.89	1.27
Compositional group	An-rich	An-rich	An-poor	An-poor	An-poor	An-poor

Lava	1921	1921	1921	1921	1921	1921
Point	1921-02 - Pl 4-P17	1921-02 - Pl 4-P18	1921-02 - Pl 6-P1	1921-02 - Pl 6-P2	1921-02 - Pl 6-P3	1921-02 - Pl 6-P4
Laboratory	UoB	UoB	UoB	UoB	UoB	UoB
Na2O (wt. %)	3.93	4.30	1.25	1.31	1.51	4.06
FeO (wt. %)	0.652	0.782	0.588	0.518	0.541	0.677
CaO (wt. %)	13.40	12.79	18.31	18.30	17.39	12.87
Al2O3 (wt. %)	29.53	29.06	34.16	34.36	33.64	29.16
K2O (wt. %)	0.160	0.213	0.021	0.044	0.047	0.168
MgO (wt. %)	0.194	0.165	0.065	0.092	0.096	0.184
SiO2 (wt. %)	51.76	52.48	45.33	45.04	45.52	52.24
TiO2 (wt. %)	0.054	0.070	0.012	0.010	0.018	0.049
Total	99.69	99.87	99.78	99.68	98.78	99.41
Al (%)	15.63	15.38	18.08	18.18	17.80	15.43
Fe (ppm)	5071	6079	4571	4023	4208	5263
Ti (ppm)	323	420	72	61	108	294
Mg (ppm)	1171	995	393	553	580	1112
XAn	64.42	61.08	88.76	88.17	86.04	62.75
XAb	34.65	37.69	11.12	11.57	13.68	36.26
XOr	0.93	1.23	0.12	0.26	0.28	0.99
Compositional group	An-poor	An-poor	An-rich	An-rich	An-rich	An-poor

Lava	1921	1921	1921	1921	1921	1921
Point	1921-02 - Pl 6-P5	1921-02 - Pl 6-P6	1921-02 - Pl 7-P2	1921-02 - Pl 7-P3	1921-02 - Pl 7-P4	1921-02 - Pl 7-P5
Laboratory	UoB	UoB	UoB	UoB	UoB	UoB
Na2O (wt. %)	4.12	4.26	4.10	4.08	4.01	4.62
FeO (wt. %)	0.735	0.798	0.690	0.724	0.680	0.921
CaO (wt. %)	12.94	12.40	12.81	12.87	13.35	11.58
Al2O3 (wt. %)	29.14	29.02	28.92	29.09	29.52	27.57
K2O (wt. %)	0.189	0.181	0.187	0.153	0.161	0.225
MgO (wt. %)	0.193	0.170	0.177	0.197	0.198	0.208
SiO2 (wt. %)	52.13	52.46	52.61	52.18	52.08	53.56
TiO2 (wt. %)	0.064	0.040	0.068	0.056	0.067	0.088
Total	99.52	99.33	99.59	99.40	100.07	98.78
Al (%)	15.42	15.36	15.30	15.40	15.62	14.59
Fe (ppm)	5714	6200	5366	5628	5288	7161
Ti (ppm)	385	237	407	336	399	528
Mg (ppm)	1162	1028	1066	1187	1191	1252
XAn	62.44	60.72	62.35	62.67	63.91	57.04
XAb	36.45	38.21	36.55	36.43	35.16	41.62
XOr	1.10	1.07	1.10	0.90	0.93	1.34
Compositional group	An-poor	An-poor	An-poor	An-poor	An-poor	An-poor

Lava	1921	1921	1921	1921	1921	1948
Point	1921-02 - Pl 3-P1	1921-02 - Pl 3-P2	1921-02 - Pl 3-P3	1921-02 - Pl 3-P4	1921-02 - Pl 3-P5	1948-04-1-Pl15_4
Laboratory	UoB	UoB	UoB	UoB	UoB	UoE
Na2O (wt. %)	4.18	4.04	4.03	4.15	4.22	2.23
FeO (wt. %)	0.771	0.770	0.815	0.762	0.661	0.572
CaO (wt. %)	13.00	12.92	13.05	12.73	12.86	16.35
Al2O3 (wt. %)	29.06	29.12	29.10	28.76	29.13	31.65
K2O (wt. %)	0.174	0.178	0.194	0.188	0.189	0.044
MgO (wt. %)	0.207	0.175	0.187	0.179	0.172	0.147
SiO2 (wt. %)	52.24	51.85	51.93	52.09	51.92	48.19
TiO2 (wt. %)	0.057	0.040	0.056	0.060	0.072	0.051
Total	99.69	99.10	99.38	98.95	99.23	99.23
Al (%)	15.38	15.41	15.40	15.22	15.42	16.75
Fe (ppm)	5994	5988	6332	5921	5135	4445
Ti (ppm)	344	238	336	360	430	307
Mg (ppm)	1251	1056	1128	1082	1039	887
XAn	62.27	62.90	63.12	61.91	61.75	79.81
XAb	36.72	36.06	35.75	36.99	37.15	19.93
XOr	1.01	1.04	1.13	1.10	1.10	0.26
Compositional group	An-poor	An-poor	An-poor	An-poor	An-poor	An-rich

Lava	1948	1948	1948	1948	1948	1948
Point	1948-04-1-Pl15_5	1948-04-1-Pl15_6	1948-04-1-Pl15_8	1948-04-1-Pl15_9	1948-04-1-Pl16_1	1948-04-1-Pl16_2
Laboratory	UoE	UoE	UoE	UoE	UoE	UoE
Na2O (wt. %)	4.44	4.19	3.99	2.22	4.34	4.59
FeO (wt. %)	0.636	0.785	0.965	0.626	0.790	0.691
CaO (wt. %)	12.37	12.67	13.02	16.28	12.30	12.35
Al2O3 (wt. %)	28.29	28.65	28.93	32.02	27.88	27.65
K2O (wt. %)	0.093	0.136	0.121	0.041	0.169	0.186
MgO (wt. %)	0.217	0.143	0.234	0.145	0.183	0.191
SiO2 (wt. %)	53.00	53.06	52.53	48.30	52.87	53.24
TiO2 (wt. %)	0.068	0.080	0.082	0.047	0.073	0.089
Total	99.11	99.71	99.98	99.76	98.71	99.08
Al (%)	14.97	15.16	15.31	16.95	14.76	14.63
Fe (ppm)	4941	6099	7503	4862	6138	5373
Ti (ppm)	406	479	490	284	435	531
Mg (ppm)	1308	859	1413	874	1101	1154
XAn	60.02	61.82	63.61	79.83	60.16	58.84
XAb	39.44	37.38	35.68	19.93	38.85	40.09
XOr	0.54	0.80	0.71	0.24	0.99	1.07
Compositional group	An-poor	An-poor	An-poor	An-rich	An-poor	An-poor

Lava	1948	1948	1948	1948	1948	1948
Point	1948-04-1-Pl16_3	1948-04-1-Pl16_4	1948-04-1-Pl16_5	1948-04-1-Pl16_6	1948-04-1-Pl16_7	1948-04-1-Gl10_3
Laboratory	UoE	UoE	UoE	UoE	UoE	UoE
Na2O (wt. %)	4.48	4.43	4.00	2.25	4.14	3.78
FeO (wt. %)	0.924	1.271	0.736	0.729	0.874	0.927
CaO (wt. %)	12.15	12.24	12.97	16.27	12.73	13.46
Al2O3 (wt. %)	27.97	27.82	28.58	32.00	28.69	29.01
K2O (wt. %)	0.193	0.164	0.140	0.063	0.145	0.120
MgO (wt. %)	0.185	0.199	0.180	0.099	0.182	0.204
SiO2 (wt. %)	53.67	53.06	52.51	48.66	52.78	51.24
TiO2 (wt. %)	0.089	0.084	0.072	0.045	0.072	0.077
Total	99.66	99.27	99.27	100.16	99.71	98.82
Al (%)	14.80	14.72	15.13	16.94	15.18	15.35
Fe (ppm)	7181	9882	5722	5664	6792	7206
Ti (ppm)	536	504	431	268	432	463
Mg (ppm)	1117	1202	1083	599	1095	1233
XAn	59.04	59.54	63.41	79.51	62.16	65.55
XAb	39.83	39.50	35.77	20.12	36.99	33.75
XOr	1.13	0.96	0.82	0.37	0.85	0.70
Compositional group	An-poor	An-poor	An-poor	An-rich	An-poor	An-poor

Lava	1948	1948	1948	1948	1948	1948
Point	1948-04-1-Gl10_4	1948-04 - Pl16-P1	1948-04 - Pl16-P2	1948-04 - Pl16-P3	1948-04 - Pl16-P4	1948-04 - Pl16-P5
Laboratory	UoE	UoB	UoB	UoB	UoB	UoB
Na2O (wt. %)	2.15	4.25	4.37	4.34	4.44	4.40
FeO (wt. %)	0.615	0.855	0.846	0.813	0.941	0.886
CaO (wt. %)	16.48	12.97	12.68	12.62	12.78	12.77
Al2O3 (wt. %)	32.31	28.75	28.78	28.74	28.60	28.68
K2O (wt. %)	0.036	0.189	0.209	0.222	0.211	0.198
MgO (wt. %)	0.165	0.177	0.185	0.149	0.223	0.176
SiO2 (wt. %)	47.20	52.73	52.69	52.75	52.88	52.84
TiO2 (wt. %)	0.056	0.078	0.066	0.058	0.073	0.076
Total	99.10	100.00	99.83	99.70	100.17	100.05
Al (%)	17.10	15.22	15.23	15.21	15.13	15.18
Fe (ppm)	4776	6646	6575	6317	7314	6889
Ti (ppm)	334	466	394	347	438	454
Mg (ppm)	993	1069	1114	901	1345	1064
XAn	80.51	61.79	60.50	60.52	60.32	60.54
XAb	19.27	37.12	38.29	38.19	38.48	38.32
XOr	0.21	1.09	1.20	1.28	1.20	1.14
Compositional group	An-rich	An-poor	An-poor	An-poor	An-poor	An-poor

Lava	1948	1948	1948	1948	1948	1948
Point	1948-04 - Pl16-P6	1948-04 - Pl16-P7	1948-04 - Pl16-P8	1948-04 - Pl16-P9	1948-04 - Pl16-P10	1948-04 - Pl16-P11
Laboratory	UoB	UoB	UoB	UoB	UoB	UoB
Na2O (wt. %)	3.92	4.50	4.24	4.13	3.55	4.37
FeO (wt. %)	0.867	0.844	0.861	0.812	0.747	0.967
CaO (wt. %)	13.29	12.66	13.14	12.94	14.32	12.64
Al2O3 (wt. %)	29.17	28.59	29.00	28.82	30.21	28.50
K2O (wt. %)	0.182	0.199	0.198	0.191	0.120	0.199
MgO (wt. %)	0.151	0.175	0.164	0.156	0.205	0.214
SiO2 (wt. %)	51.82	52.77	52.32	52.91	50.92	53.01
TiO2 (wt. %)	0.068	0.073	0.059	0.054	0.040	0.079
Total	99.46	99.83	99.99	100.04	100.16	100.04
Al (%)	15.44	15.13	15.35	15.26	15.99	15.08
Fe (ppm)	6739	6560	6693	6313	5804	7516
Ti (ppm)	405	438	356	321	242	473
Mg (ppm)	913	1054	990	941	1236	1288
XAn	64.19	59.82	62.11	62.40	68.23	60.52
XAb	34.75	39.05	36.76	36.49	31.08	38.32
XOr	1.06	1.14	1.13	1.11	0.69	1.15
Compositional group	An-poor	An-poor	An-poor	An-poor	An-poor	An-poor

Lava	1948	1948	1948	1948	1948	1948
Point	1948-04 - Pl13-P1	1948-04 - Pl13-P2	1948-04 - Pl13-P3	1948-04 - Pl13-P4	1948-04 - Pl13-P5	1948-04 - Pl13-P6
Laboratory	UoB	UoB	UoB	UoB	UoB	UoB
Na2O (wt. %)	4.41	1.78	2.41	2.44	4.25	3.92
FeO (wt. %)	0.773	0.602	0.546	0.610	0.693	0.656
CaO (wt. %)	13.18	17.54	16.58	16.49	13.00	13.75
Al2O3 (wt. %)	29.22	33.35	32.26	32.34	28.86	29.64
K2O (wt. %)	0.178	0.052	0.063	0.088	0.184	0.163
MgO (wt. %)	0.166	0.121	0.125	0.135	0.164	0.155
SiO2 (wt. %)	52.55	46.80	48.28	47.90	52.40	52.00
TiO2 (wt. %)	0.062	0.029	0.018	0.032	0.066	0.047
Total	100.54	100.28	100.32	100.04	99.68	100.34
Al (%)	15.46	17.65	17.07	17.11	15.27	15.69
Fe (ppm)	6008	4681	4244	4738	5384	5097
Ti (ppm)	372	171	110	194	394	280
Mg (ppm)	1003	728	751	816	989	936
XAn	61.28	84.06	78.63	78.23	61.85	65.03
XAb	37.72	15.64	21.01	21.27	37.09	34.03
XOr	1.00	0.30	0.36	0.51	1.06	0.93
Compositional group	An-poor	An-rich	An-rich	An-rich	An-poor	An-poor

Lava	1948	1948	1948	1948	1948	1948
Point	1948-04 - Pl13-P7	1948-04 - Pl13-P8	1948-04 - Pl14-P1	1948-04 - Pl14-P2	1948-04 - Pl14-P3	1948-04 - Pl14-P5
Laboratory	UoB	UoB	UoB	UoB	UoB	UoB
Na2O (wt. %)	4.44	3.72	2.29	1.96	1.93	4.34
FeO (wt. %)	0.741	0.792	0.583	0.604	0.576	0.738
CaO (wt. %)	12.60	13.85	16.70	17.27	17.52	12.80
Al2O3 (wt. %)	28.46	29.77	32.53	32.83	33.18	28.62
K2O (wt. %)	0.199	0.130	0.071	0.060	0.054	0.194
MgO (wt. %)	0.179	0.204	0.134	0.109	0.094	0.187
SiO2 (wt. %)	53.31	51.82	47.76	46.81	46.91	53.21
TiO2 (wt. %)	0.062	0.060	0.031	0.021	0.022	0.063
Total	99.99	100.35	100.10	99.69	100.31	100.18
Al (%)	15.06	15.76	17.22	17.38	17.56	15.15
Fe (ppm)	5757	6155	4534	4696	4478	5740
Ti (ppm)	369	357	183	125	133	378
Mg (ppm)	1082	1227	805	660	564	1129
XAn	60.07	66.53	79.54	82.49	82.92	61.00
XAb	38.79	32.71	20.05	17.17	16.77	37.88
XOr	1.14	0.76	0.41	0.35	0.31	1.12
Compositional group	An-poor	An-poor	An-rich	An-rich	An-rich	An-poor

Lava	1948	1948	1948	1948	1948	1948
Point	1948-04 - Pl14-P6	1948-04 - Pl14-P7	1948-04 - Pl9-P1	1948-04 - Pl9-P2	1948-04 - Pl9-P3	1948-04 - Pl9-P4
Laboratory	UoB	UoB	UoB	UoB	UoB	UoB
Na2O (wt. %)	4.57	3.52	1.68	1.62	1.65	4.41
FeO (wt. %)	0.683	0.812	0.659	0.680	0.767	0.844
CaO (wt. %)	12.70	14.35	17.75	17.93	17.79	12.93
Al2O3 (wt. %)	28.60	30.11	33.33	33.27	33.71	28.86
K2O (wt. %)	0.190	0.112	0.038	0.046	0.055	0.182
MgO (wt. %)	0.188	0.178	0.073	0.074	0.110	0.119
SiO2 (wt. %)	53.63	51.50	46.25	46.10	46.17	52.42
TiO2 (wt. %)	0.079	0.049	0.030	0.037	0.020	0.069
Total	100.66	100.65	99.84	99.84	100.28	99.83
Al (%)	15.14	15.94	17.64	17.61	17.84	15.28
Fe (ppm)	5311	6314	5124	5282	5959	6562
Ti (ppm)	471	291	177	224	121	411
Mg (ppm)	1134	1074	441	449	663	720
XAn	59.57	68.54	84.97	85.51	85.13	60.85
XAb	39.36	30.82	14.81	14.23	14.55	38.12
XOr	1.07	0.64	0.22	0.27	0.32	1.03
Compositional group	An-poor	An-poor	An-rich	An-rich	An-rich	An-poor

Lava	1948	1948	1948	1948	1948	1948
Point	1948-04 - Pl9-P5	1948-04 - Pl9-P6	1948-04 - Pl9-P7	1948-04 - Gl10-P5	1948-04 - Gl10-P6	1948-04 - Gl10-P7
Laboratory	UoB	UoB	UoB	UoB	UoB	UoB
Na2O (wt. %)	4.21	4.07	4.29	2.24	2.08	3.96
FeO (wt. %)	0.825	0.802	0.811	0.603	0.598	1.077
CaO (wt. %)	13.32	13.06	13.11	16.90	16.93	13.03
Al2O3 (wt. %)	29.40	29.14	28.86	32.74	32.57	29.10
K2O (wt. %)	0.164	0.164	0.162	0.056	0.049	0.159
MgO (wt. %)	0.158	0.160	0.190	0.136	0.149	0.197
SiO2 (wt. %)	52.05	52.00	52.84	47.52	47.60	52.08
TiO2 (wt. %)	0.055	0.055	0.067	0.039	0.025	0.107
Total	100.21	99.50	100.36	100.24	100.00	99.71
Al (%)	15.56	15.42	15.27	17.33	17.23	15.40
Fe (ppm)	6416	6235	6300	4687	4651	8368
Ti (ppm)	327	330	400	234	147	640
Mg (ppm)	952	968	1147	820	899	1191
XAn	62.66	63.01	61.91	80.15	81.38	63.64
XAb	36.41	36.04	37.17	19.52	18.33	35.42
XOr	0.93	0.95	0.92	0.32	0.29	0.94
Compositional group	An-poor	An-poor	An-poor	An-rich	An-rich	An-poor

Lava	1948	1971	1971	1971	1971	1971
Point	1948-04 - Gl9-P9	1971-09 - Gl1-P35	1971-09 - Gl1-P36	1971-09 - Gl1-P37	1971-09 - Gl1-P38	1971-09 - Gl1-P39
Laboratory	UoB	UoB	UoB	UoB	UoB	UoB
Na2O (wt. %)	4.51	4.28	4.00	4.02	3.82	4.28
FeO (wt. %)	0.954	0.859	0.809	0.800	0.764	0.858
CaO (wt. %)	12.67	13.32	13.46	13.64	14.03	12.63
Al2O3 (wt. %)	28.63	29.73	29.61	30.07	30.37	28.58
K2O (wt. %)	0.189	0.170	0.166	0.165	0.147	0.177
MgO (wt. %)	0.184	0.200	0.167	0.224	0.170	0.173
SiO2 (wt. %)	52.90	53.73	53.75	52.70	52.13	52.97
TiO2 (wt. %)	0.082	0.060	0.055	0.062	0.052	0.064
Total	100.16	102.36	102.01	101.71	101.53	99.74
Al (%)	15.15	15.74	15.67	15.91	16.07	15.12
Fe (ppm)	7412	6678	6287	6220	5942	6673
Ti (ppm)	492	362	330	370	314	384
Mg (ppm)	1111	1208	1005	1353	1024	1042
XAn	59.82	62.30	64.20	64.28	66.11	61.05
XAb	39.10	36.74	34.85	34.78	33.05	37.92
XOr	1.08	0.96	0.95	0.94	0.84	1.03
Compositional group	An-poor	An-poor	An-poor	An-poor	An-poor	An-poor

Lava	1971	1971	1971	1971	1971	1971
Point	1971-09 - Gl1-P40	1971-09 - Gl1-P41	1971-09 - Gl1-P42	1971-09 - Gl1-P43	1971-09 - Gl1-P44	1971-09 - Gl1-P45
Laboratory	UoB	UoB	UoB	UoB	UoB	UoB
Na2O (wt. %)	4.26	4.32	4.02	4.11	3.99	4.31
FeO (wt. %)	0.837	0.837	0.794	0.757	0.804	0.739
CaO (wt. %)	13.35	13.30	14.13	13.50	13.88	13.31
Al2O3 (wt. %)	29.67	29.74	30.45	29.95	30.17	29.58
K2O (wt. %)	0.171	0.142	0.163	0.177	0.136	0.167
MgO (wt. %)	0.135	0.189	0.180	0.154	0.176	0.178
SiO2 (wt. %)	53.65	53.47	52.71	53.36	52.81	53.08
TiO2 (wt. %)	0.059	0.070	0.048	0.052	0.048	0.067
Total	102.15	102.07	102.49	102.07	102.03	101.43
Al (%)	15.70	15.74	16.11	15.85	15.97	15.65
Fe (ppm)	6503	6509	6171	5883	6253	5746
Ti (ppm)	353	420	286	312	289	400
Mg (ppm)	815	1140	1085	930	1061	1076
XAn	62.51	62.19	65.08	63.54	64.97	62.13
XAb	36.52	37.01	34.01	35.45	34.26	36.93
XOr	0.97	0.80	0.91	1.00	0.77	0.94
Compositional group	An-poor	An-poor	An-poor	An-poor	An-poor	An-poor

Lava	1971	1971	1971	1971	1971	1971
Point	1971-09 - Gl1-P46	1971-09 - Gl1-P47	1971-09 - Gl1-P48	1971-09 - Pl 1-P1	1971-09 - Pl 1-P2	1971-09 - Pl 1-P3
Laboratory	UoB	UoB	UoB	UoB	UoB	UoB
Na2O (wt. %)	4.01	4.23	4.13	1.93	1.96	1.78
FeO (wt. %)	0.825	0.828	0.887	0.656	0.595	0.654
CaO (wt. %)	13.88	13.41	13.55	17.63	17.05	17.59
Al2O3 (wt. %)	30.13	29.71	29.84	33.57	32.68	33.78
K2O (wt. %)	0.155	0.183	0.179	0.039	0.037	0.037
MgO (wt. %)	0.149	0.186	0.162	0.117	0.106	0.094
SiO2 (wt. %)	52.92	53.64	53.00	47.12	47.05	46.92
TiO2 (wt. %)	0.054	0.059	0.051	0.019	0.022	0.015
Total	102.15	102.25	101.81	101.08	99.50	100.89
Al (%)	15.95	15.72	15.79	17.77	17.29	17.88
Fe (ppm)	6414	6439	6896	5099	4623	5084
Ti (ppm)	324	355	306	115	134	88
Mg (ppm)	898	1120	979	705	638	567
XAn	64.81	62.72	63.46	83.07	82.40	84.15
XAb	34.32	36.24	35.53	16.71	17.39	15.64
XOr	0.87	1.03	1.01	0.22	0.22	0.21
Compositional group	An-poor	An-poor	An-poor	An-rich	An-rich	An-rich

Lava	1971	1971	1971	1971	1971	1971
Point	1971-09 - Pl 1-P4	1971-09 - Pl 1-P5	1971-09 - Pl 1-P6	1971-09 - Pl 1-P7	1971-09 - Pl 1-P8	1971-09 - Pl 1-P9
Laboratory	UoB	UoB	UoB	UoB	UoB	UoB
Na2O (wt. %)	2.05	2.11	1.69	1.69	2.00	1.79
FeO (wt. %)	0.656	0.718	0.628	0.579	0.718	0.592
CaO (wt. %)	17.48	17.58	17.92	18.39	17.66	18.14
Al2O3 (wt. %)	33.53	33.18	33.91	34.30	33.67	34.22
K2O (wt. %)	0.040	0.056	0.036	0.036	0.046	0.047
MgO (wt. %)	0.117	0.125	0.116	0.105	0.114	0.077
SiO2 (wt. %)	47.96	47.49	47.14	46.99	47.87	47.36
TiO2 (wt. %)	0.030	0.014	0.017	0.006	0.017	0.027
Total	101.87	101.28	101.46	102.10	102.13	102.31
Al (%)	17.74	17.56	17.94	18.15	17.82	18.11
Fe (ppm)	5098	5580	4883	4503	5581	4600
Ti (ppm)	181	85	102	34	103	160
Mg (ppm)	705	756	698	631	686	466
XAn	82.10	81.68	85.05	85.40	82.56	84.42
XAb	17.67	18.01	14.74	14.40	17.18	15.32
XOr	0.23	0.32	0.21	0.20	0.26	0.27
Compositional group	An-rich	An-rich	An-rich	An-rich	An-rich	An-rich

Lava	1971	1971	1971	1971	1971	1971
Point	1971-09 - Pl 1-P10	1971-09 - Pl 1-P11	1971-09 - Pl 1-P12	1971-09 - Pl 1-P13	1971-09 - Pl 1-P14	1971-09 - Pl 1-P15
Laboratory	UoB	UoB	UoB	UoB	UoB	UoB
Na2O (wt. %)	1.70	4.05	3.45	4.02	4.46	3.85
FeO (wt. %)	0.601	0.769	0.721	0.738	0.739	0.697
CaO (wt. %)	17.70	13.60	14.31	14.00	13.13	14.01
Al2O3 (wt. %)	33.19	29.59	30.26	30.21	29.36	30.55
K2O (wt. %)	0.038	0.137	0.102	0.146	0.159	0.150
MgO (wt. %)	0.098	0.161	0.206	0.205	0.181	0.190
SiO2 (wt. %)	46.48	53.18	50.38	52.68	53.95	52.50
TiO2 (wt. %)	0.019	0.054	0.047	0.062	0.071	0.032
Total	99.86	101.54	99.50	102.07	102.10	101.98
Al (%)	17.57	15.66	16.01	15.99	15.54	16.17
Fe (ppm)	4674	5976	5606	5736	5746	5414
Ti (ppm)	113	322	282	369	424	192
Mg (ppm)	591	969	1245	1238	1092	1147
XAn	84.85	64.21	68.91	64.96	61.08	65.93
XAb	14.93	35.01	30.49	34.23	38.03	33.21
XOr	0.22	0.78	0.59	0.82	0.89	0.85
Compositional group	An-rich	An-poor	An-poor	An-poor	An-poor	An-poor

Lava	1971	1971	1971	1971	1971	1971
Point	1971-09 - Pl 1-P16	1971-09 - Pl 1-P17	1971-09 - Pl 1-P18	1971-09 - Pl 1-P19	1971-09 - Pl 1-P21	1971-09 - Pl 2-P1
Laboratory	UoB	UoB	UoB	UoB	UoB	UoB
Na2O (wt. %)	4.20	4.58	4.45	4.15	4.32	4.23
FeO (wt. %)	0.762	0.713	0.698	0.769	0.858	0.762
CaO (wt. %)	12.98	12.23	12.62	13.08	13.57	13.09
Al2O3 (wt. %)	28.87	28.31	28.74	28.93	30.07	28.82
K2O (wt. %)	0.152	0.181	0.161	0.162	0.137	0.136
MgO (wt. %)	0.156	0.185	0.170	0.207	0.211	0.188
SiO2 (wt. %)	52.40	53.61	53.10	53.07	52.85	52.51
TiO2 (wt. %)	0.055	0.072	0.078	0.064	0.058	0.075
Total	99.60	99.90	100.07	100.44	102.09	99.83
Al (%)	15.28	14.98	15.21	15.31	15.91	15.25
Fe (ppm)	5926	5541	5428	5981	6667	5922
Ti (ppm)	327	431	466	381	346	450
Mg (ppm)	944	1116	1025	1246	1275	1133
XAn	62.20	58.68	60.21	62.66	62.60	62.32
XAb	36.92	40.27	38.87	36.41	36.63	36.90
XOr	0.88	1.05	0.92	0.93	0.77	0.78
Compositional group	An-poor	An-poor	An-poor	An-poor	An-poor	An-poor

Lava	1971	1971	1971	1971	1971	1971
Point	1971-09 - Pl 2-P2	1971-09 - Pl 2-P3	1971-09 - Pl 2-P4	1971-09 - Pl 2-P5	1971-09 - Pl 3-P1	1971-09 - Pl 3-P2
Laboratory	UoB	UoB	UoB	UoB	UoB	UoB
Na2O (wt. %)	4.32	4.27	4.16	3.70	2.03	2.10
FeO (wt. %)	0.764	0.745	0.723	0.827	0.605	0.566
CaO (wt. %)	13.60	13.21	13.74	14.56	17.11	16.92
Al2O3 (wt. %)	29.84	29.52	30.09	30.99	32.89	32.87
K2O (wt. %)	0.169	0.144	0.144	0.141	0.051	0.055
MgO (wt. %)	0.194	0.194	0.190	0.157	0.127	0.107
SiO2 (wt. %)	53.04	53.47	53.29	51.70	46.73	47.23
TiO2 (wt. %)	0.065	0.054	0.059	0.065	0.020	0.032
Total	102.01	101.62	102.39	102.15	99.61	99.89
Al (%)	15.79	15.62	15.92	16.40	17.40	17.40
Fe (ppm)	5937	5793	5618	6425	4706	4398
Ti (ppm)	391	323	356	389	118	193
Mg (ppm)	1170	1172	1146	948	766	645
XAn	62.53	62.29	63.76	67.64	81.83	81.18
XAb	36.53	36.89	35.43	31.57	17.88	18.50
XOr	0.94	0.82	0.81	0.79	0.30	0.32
Compositional group	An-poor	An-poor	An-poor	An-poor	An-rich	An-rich

Lava	1971	1971	1971	1971	1971	1971
Point	1971-09 - Pl 3-P3	1971-09 - Pl 3-P4	1971-09 - Pl 3-P5	1971-09 - Pl 4-P1	1971-09 - Pl 4-P2	1971-09 - Pl 4-P3
Laboratory	UoB	UoB	UoB	UoB	UoB	UoB
Na2O (wt. %)	3.67	4.70	4.06	3.56	4.20	2.20
FeO (wt. %)	0.688	0.695	0.663	0.766	0.791	0.760
CaO (wt. %)	14.48	12.59	13.99	14.71	13.32	17.23
Al2O3 (wt. %)	30.88	29.10	30.26	30.81	29.33	32.85
K2O (wt. %)	0.109	0.130	0.123	0.138	0.175	0.049
MgO (wt. %)	0.164	0.213	0.195	0.164	0.142	0.158
SiO2 (wt. %)	51.76	54.48	53.11	51.51	51.88	47.52
TiO2 (wt. %)	0.044	0.071	0.043	0.043	0.054	0.033
Total	101.84	102.01	102.45	101.73	99.91	100.84
Al (%)	16.34	15.40	16.02	16.31	15.52	17.39
Fe (ppm)	5347	5399	5157	5951	6151	5906
Ti (ppm)	261	426	260	258	324	198
Mg (ppm)	986	1283	1174	989	856	954
XAn	67.82	58.95	64.79	68.73	62.68	80.77
XAb	31.56	40.32	34.52	30.49	36.33	18.95
XOr	0.62	0.74	0.69	0.78	1.00	0.28
Compositional group	An-poor	An-poor	An-poor	An-poor	An-poor	An-rich

Lava	1971 1971-09 - Pl	1971 1971-09 - Pl
Point	4-P5	4-P6
Laboratory	UoB	UoB
Na2O (wt. %)	1.86	1.62
FeO (wt. %)	0.748	0.652
CaO (wt. %)	17.69	18.11
Al2O3 (wt. %)	33.72	33.86
K2O (wt. %)	0.038	0.036
MgO (wt. %)	0.129	0.126
SiO2 (wt. %)	47.34	46.83
TiO2 (wt. %)	0.029	0.019
Total	101.59	101.30
Al (%)	17.84	17.92
Fe (ppm)	5811	5071
Ti (ppm)	171	112
Mg (ppm)	781	757
XAn	83.66	85.69
XAb	16.13	14.10
XOr	0.21	0.21
Compositional group	An-rich	An-rich

Table A.3. EPMA of olivine phenocrysts chemistry. Analysis performed at University of Exeter (UoE) and University of Bristol (UoB).

Lava		1921	1921	1921	1921	1921
Point		1921-02 - Gl 1-P1	1921-02 - Gl 1-P2	1921-02 - Gl 1-P5	1921-02 - Gl11-P2	1921-02 - Gl11-P4
Laboratory	Detection limit	UoB	UoB	UoB	UoB	UoB
MgO (wt. %)	0.02 (%)	38.38609	38.44798	38.74966	38.62926	38.74118
SiO2 (wt. %)	0.02 (%)	38.50349	38.37797	38.32711	38.10385	38.06590
Al2O3 (wt. %)	0.01 (%)	0.00962	0.04631	0.02773		0.05165
CaO (wt. %)	0.005 (%)	0.25996	0.28388	0.27168	0.27991	0.32725
TiO2 (wt. %)	0.01 (%)	0.00772	0.01882	0.01187	0.00874	0.01392
Cr2O3 (wt. %)	0.02 (%)	0.00423	0.00685	0.01482	0.01238	0.01818
MnO (wt. %)	0.02 (%)	0.36984	0.36890	0.35530	0.34404	0.35793
FeO (wt. %)	0.02 (%)	23.11586	22.83960	22.89627	22.50408	22.65388
NiO (wt. %)	0.02 (%)	0.08374	0.07430	0.10705	0.05993	0.08737
Total		100.74	100.46	100.76	99.94	100.32
Fe2+		0.4993	0.4924	0.4817	0.4770	0.4719
Mg		1.4841	1.4889	1.4954	1.5007	1.5000
Ca		0.0072	0.0079	0.0075	0.0078	0.0091
Fo		74.18	74.40	74.53	74.79	74.66
Fa		25.06	24.79	24.70	24.44	24.49
Ca-Ol		0.36	0.39	0.38	0.39	0.45

Lava	1921	1921	1921	1921	1921
Point	1921-02 - Gl 6-P3	1921-02 - Gl 6-P5	1921-02 - Gl 6-P10	1921-02 - Gl 6-P12	1921-02 - Gl 10-P2
Laboratory	UoB	UoB	UoB	UoB	UoB
MgO (wt. %)	39.43396	39.04548	38.10835	38.93132	39.01677
SiO2 (wt. %)	38.46550	38.42473	38.29916	38.38020	38.52902
Al2O3 (wt. %)	0.03625	0.03103	0.01921	0.02041	0.04121
CaO (wt. %)	0.28714	0.29613	0.32464	0.31706	0.28457
TiO2 (wt. %)	0.01423	0.00855		0.02198	0.01129
Cr2O3 (wt. %)	0.02683	0.01300	0.02143	0.02807	0.02481
MnO (wt. %)	0.36107	0.35145	0.40355	0.36243	0.33407
FeO (wt. %)	22.59775	22.61051	23.75388	22.78086	22.44987
NiO (wt. %)	0.08035	0.09841	0.04951	0.08084	0.05331
Total	101.30	100.88	100.98	100.92	100.74
Fe2+	0.4627	0.4736	0.5022	0.4761	0.4778
Mg	1.5094	1.5027	1.4730	1.4987	1.5025
Ca	0.0079	0.0082	0.0090	0.0088	0.0079
Fo	75.08	74.88	73.43	74.66	75.02
Fa	24.14	24.33	25.68	24.51	24.22
Ca-Ol	0.39	0.41	0.45	0.44	0.39

Lava	1921	1921	1921	1921	1921
Point	1921-02 - Gl 10-P5	1921-02 - Gl 10-P7	1921-02 - Gl 10-P10	1921-02 - Gl 10-P13	1921-02 - Gl 10-P15
Laboratory	UoB	UoB	UoB	UoB	UoB
MgO (wt. %)	38.79641	39.21742	39.99442	39.04393	38.99384
SiO2 (wt. %)	38.30954	38.41655	38.44254	38.48733	38.34504
Al2O3 (wt. %)	0.03644	0.04659	0.00053	0.03302	0.03572
CaO (wt. %)	0.29858	0.31308	0.37866	0.30493	0.29839
TiO2 (wt. %)	0.00459	0.01419	0.02094		
Cr2O3 (wt. %)	0.01579	0.01470	0.02217	0.03276	0.02168
MnO (wt. %)	0.38041	0.35500	0.36383	0.35420	0.36234
FeO (wt. %)	22.57349	22.39383	21.05533	22.45797	22.58859
NiO (wt. %)	0.08236	0.11352	0.08934	0.06082	0.08332
Total	100.50	100.88	100.37	100.77	100.73
Fe2+	0.4772	0.4668	0.4362	0.4746	0.4723
Mg	1.4993	1.5078	1.5364	1.5032	1.5027
Ca	0.0083	0.0087	0.0105	0.0084	0.0083
Fo	74.77	75.12	76.49	74.99	74.86
Fa	24.40	24.06	22.59	24.20	24.33
Ca-Ol	0.41	0.43	0.52	0.42	0.41

Lava	1921	1921	1921	1921	1921
Point	1921-02 - Gl 2-P2	1921-02 - Gl 2-P4	1921-02 - Mgl1-P1	1921-02 - Gl 3-P1	1921-02 - Gl 3-P3
Laboratory	UoB	UoB	UoB	UoB	UoB
MgO (wt. %)	39.10639	39.23977	38.56799	38.97821	38.65298
SiO2 (wt. %)	38.16153	38.15479	38.27538	38.34656	38.49851
Al2O3 (wt. %)	0.03368	0.01892	0.04047	0.02768	0.00994
CaO (wt. %)	0.33764	0.30062	0.29939	0.30048	0.30055
TiO2 (wt. %)	0.02875		0.01007	0.02547	0.00473
Cr2O3 (wt. %)	0.03540	0.02319	0.00595	0.01457	0.02975
MnO (wt. %)	0.38312	0.37890	0.37358	0.38438	0.37306
FeO (wt. %)	22.64788	22.39505	23.05725	22.82058	22.81347
NiO (wt. %)	0.11030	0.05760	0.05464	0.09644	0.06236
Total	100.84	100.57	100.68	100.99	100.75
Fe2+	0.4628	0.4576	0.4855	0.4738	0.4885
Mg	1.5054	1.5120	1.4902	1.4996	1.4918
Ca	0.0093	0.0083	0.0083	0.0083	0.0083
Fo	74.81	75.12	74.27	74.65	74.51
Fa	24.31	24.05	24.91	24.52	24.67
Ca-Ol	0.46	0.41	0.41	0.41	0.42

Lava	1921	1921	1921	1921	1921
Point	1921-02 - Gl 3-P5	1921-02 - Gl 3-P7	1921-02 - Gl 4-P1	1921-02 - Gl 4-P7	1921-02 - Gl 7-P5
Laboratory	UoB	UoB	UoB	UoB	UoB
MgO (wt. %)	39.30023	36.40101	38.87982	39.66705	39.03896
SiO2 (wt. %)	38.27714	37.80579	38.13972	38.33205	38.41798
Al2O3 (wt. %)	0.03723	0.0367	0.02504	0.03267	0.0168
CaO (wt. %)	0.32128	0.40549	0.26169	0.34654	0.30884
TiO2 (wt. %)	0.00757	0.02460	0.01965	0.01333	
Cr2O3 (wt. %)	0.02715	0.01463	0.02740	0.02874	0.04157
MnO (wt. %)	0.36857	0.43698	0.37598	0.31794	0.35550
FeO (wt. %)	22.56883	25.41449	22.53120	21.93363	22.47488
NiO (wt. %)	0.08554	0.04875	0.10411	0.11863	0.11206
Total	100.99	100.59	100.36	100.79	100.77
Fe2+	0.4601	0.5470	0.4705	0.4482	0.4725
Mg	1.5091	1.4255	1.5041	1.5225	1.5039
Ca	0.0089	0.0114	0.0073	0.0096	0.0086
Fo	75.00	71.10	74.88	75.70	74.97
Fa	24.16	27.85	24.34	23.48	24.21
Ca-Ol	0.44	0.57	0.36	0.48	0.43

Lava	1921	1921	1921	1921	1921
Point	1921-02 - Gl 7-P9	1921-02 - Gl 9-P5	1921-02 - Gl 9-P7	1921-02 - Gl 9-P9	1921-02 - Gl 9-P11
Laboratory	UoB	UoB	UoB	UoB	UoB
MgO (wt. %)	39.12271	38.77568	38.69623	38.48408	38.60736
SiO2 (wt. %)	38.22859	37.91414	38.32497	38.32009	38.48483
Al2O3 (wt. %)	0.04583	0.03135	0.01785	0.02324	0.01567
CaO (wt. %)	0.31130	0.31504	0.29734	0.32290	0.32039
TiO2 (wt. %)	0.00950	0.01299		0.00033	
Cr2O3 (wt. %)	0.02296	0.01035	0.02220	0.02356	0.01381
MnO (wt. %)	0.38809	0.38304	0.38294	0.35144	0.34706
FeO (wt. %)	22.74520	22.74044	22.48435	23.12780	22.47532
NiO (wt. %)	0.10159	0.08859	0.08149	0.06210	0.09169
Total	100.98	100.27	100.31	100.72	100.36
Fe2+	0.4648	0.4662	0.4804	0.4895	0.4881
Mg	1.5043	1.5020	1.4984	1.4873	1.4949
Ca	0.0086	0.0088	0.0083	0.0090	0.0089
Fo	74.77	74.60	74.79	74.16	74.76
Fa	24.38	24.54	24.38	25.00	24.41
Ca-Ol	0.43	0.44	0.41	0.45	0.45

Lava	1921	1921	1921	1921	1921
Point	1921-02 - Gl 9-P14	1921-02 - Pl 4-P19	1921-02 - Mgl 3 - P2	Gl8a - Ol (contacto cpx 2)	Gl8a - Ol (contacto cpx 4)
Laboratory	UoB	UoB	UoB	UoE	UoE
MgO (wt. %)	38.66482	38.11388	37.58411	38.27	37.57
SiO2 (wt. %)	38.39781	38.06297	38.10492	38.28	38.00
Al2O3 (wt. %)	0.01151	0.01148	0.01838		
CaO (wt. %)	0.31932	0.32850	0.32524	0.2716	0.2701
TiO2 (wt. %)	0.01450	0.02666	0.01818	0.0448	0.0450
Cr2O3 (wt. %)	0.01858	0.03019	0.01135		
MnO (wt. %)	0.39472	0.40314	0.42726	0.2096	0.2369
FeO (wt. %)	22.68457	23.51441	24.36955	23.06	24.95
NiO (wt. %)	0.09353	0.10832	0.08512	0.09620	
Total	100.60	100.60	100.94	100.23	101.07
Fe2+	0.4839	0.4945	0.5154	0.4995	0.5200
Mg	1.4942	1.4784	1.4582	1.4868	1.4560
Ca	0.0089	0.0092	0.0091	0.0076	0.0075
Fo	74.58	73.62	72.65	74.28	72.40
Fa	24.55	25.48	26.43	25.11	26.97
Ca-Ol	0.44	0.46	0.45	0.38	0.37

Lava	1921	1921	1921	1921	1921
Point	Gl8a - Ol (core)	Gl8b - Ol (contacto Cpx 10)	1921-05-1__19	1921-05-1__27	1921-05-1__28
Laboratory	UoE	UoE	UoE	UoE	UoE
MgO (wt. %)	36.84	37.80	40.54	39.53	39.80
SiO2 (wt. %)	37.92	38.61	39.36	38.46	38.92
Al2O3 (wt. %)					
CaO (wt. %)	0.2634	0.3199	0.2698	0.2630	0.2749
TiO2 (wt. %)	0.0434	0.0650	0.0475	0.0318	0.0511
Cr2O3 (wt. %)					
MnO (wt. %)	0.2344	0.2543	0.2431	0.2164	0.2285
FeO (wt. %)	25.38	23.59	20.39	21.97	21.68
NiO (wt. %)		0.0926		0.0927	
Total	100.68	100.73	100.85	100.56	100.95
Fe2+	0.5432	0.5133	0.4358	0.4604	0.4647
Mg	1.4380	1.4662	1.5446	1.5207	1.5225
Ca	0.0074	0.0089	0.0074	0.0073	0.0076
Fo	71.67	73.53	77.50	75.78	76.11
Fa	27.70	25.74	21.87	23.63	23.26
Ca-Ol	0.37	0.45	0.37	0.36	0.38

Lava	1921	1921	1948	1948	1948
Point	1921-05-1__33	1921-05-1__34	1948-04 - Ol 4-P1	1948-04 - Ol 4-P2	1948-04 - Ol 4-P3
Laboratory	UoE	UoE	UoB	UoB	UoB
MgO (wt. %)	39.15	37.33	42.96519	44.28904	42.37167
SiO2 (wt. %)	38.33	38.95	39.25617	40.10786	39.64333
Al2O3 (wt. %)			0.01635	0.02374	0.04699
CaO (wt. %)	0.2663	0.2790	0.19522	0.23312	0.16634
TiO2 (wt. %)	0.0512	0.0506	0.00108	0.00105	
Cr2O3 (wt. %)			0.01089	0.02577	0.03255
MnO (wt. %)	0.1949	0.2367	0.25609	0.16911	0.28390
FeO (wt. %)	21.73	24.22	17.27013	15.94664	18.35816
NiO (wt. %)			0.20400	0.26234	0.22629
Total	99.72	101.07	100.18	101.06	101.13
Fe2+	0.4683	0.5266	0.3599	0.3336	0.3881
Mg	1.5178	1.4468	1.6256	1.6518	1.5970
Ca	0.0074	0.0078	0.0053	0.0062	0.0045
Fo	75.81	72.84	81.16	82.79	80.02
Fa	23.60	26.51	18.30	16.72	19.45
Ca-Ol	0.37	0.39	0.27	0.31	0.23

Lava	1948	1948	1948	1948	1948
Point	1948-04 - Ol 4-P4	1948-04 - Gl10-P2	1948-04 - Gl10-P4	1948-04 - Pl13-P9	1948-04 - Pl13-P10
Laboratory	UoB	UoB	UoB	UoB	UoB
MgO (wt. %)	41.81618	43.34129	43.57357	39.70033	40.23082
SiO2 (wt. %)	39.28552	39.70374	39.42666	38.22468	38.91377
Al2O3 (wt. %)	0.02386	0.03952	0.04492	0.03893	0.01220
CaO (wt. %)	0.22744	0.25804	0.28612	0.30755	0.28467
TiO2 (wt. %)	0.00338	0.01627	0.01572	0.02516	
Cr2O3 (wt. %)	0.02230	0.02236	0.02483	0.01821	0.03046
MnO (wt. %)	0.31952	0.21197	0.28433	0.39683	0.34179
FeO (wt. %)	19.05047	17.15164	17.23539	21.19612	20.50345
NiO (wt. %)	0.14982	0.20654	0.15571	0.13648	0.10753
Total	100.90	100.95	101.05	100.04	100.42
Fe2+	0.4015	0.3610	0.3452	0.4406	0.4409
Mg	1.5833	1.6262	1.6317	1.5322	1.5422
Ca	0.0062	0.0070	0.0077	0.0085	0.0078
Fo	79.13	81.36	81.28	76.29	77.17
Fa	20.22	18.06	18.04	22.85	22.06
Ca-Ol	0.31	0.35	0.38	0.42	0.39

Lava	1948	1948	1948	1948	1948
Point	1948-04 - Gl9-P5	1948-04-1-Ol4_4	1948-04-1-Gl6_2	1948-04-1-Gl6_4	1948-04-1-Gl5_1
Laboratory	UoB	UoE	UoE	UoE	UoE
MgO (wt. %)	43.23415	42.06	41.85	41.55	41.36
SiO2 (wt. %)	39.40908	39.82	39.22	39.02	39.14
Al2O3 (wt. %)	0.04839				
CaO (wt. %)	0.25177	0.1864	0.2538	0.2811	0.2853
TiO2 (wt. %)	0.02303		0.0457	0.0350	0.0374
Cr2O3 (wt. %)	0.03129				
MnO (wt. %)	0.37111	0.2056	0.1780	0.1793	0.2254
FeO (wt. %)	17.05907	19.15	18.77	19.57	19.78
NiO (wt. %)	0.17872	0.1193	0.1380	0.0953	0.0980
Total	100.61	101.54	100.46	100.73	100.93
Fe2+	0.3534	0.4040	0.3999	0.4054	0.4149
Mg	1.6274	1.5819	1.5893	1.5774	1.5694
Ca	0.0068	0.0050	0.0069	0.0077	0.0078
Fo	81.27	79.28	79.47	78.65	78.35
Fa	17.99	20.25	19.99	20.78	21.02
Ca-Ol	0.34	0.25	0.35	0.38	0.39

Lava	1948	1948	1948	1948	1948
Point	1948-04-1-Gl1_3	1948-04-1-Gl1_4	1948-04-1-Mgl1_3	1948-04-1-Mgl1_4	1948-04-1-Mgl9_1
Laboratory	UoE	UoE	UoE	UoE	UoE
MgO (wt. %)	41.40	41.61	43.10	43.00	41.86
SiO2 (wt. %)	39.18	39.13	39.81	39.69	39.10
Al2O3 (wt. %)					
CaO (wt. %)	0.2497	0.2597	0.2563	0.2522	0.2596
TiO2 (wt. %)	0.0322	0.0519	0.0329	0.0429	0.0444
Cr2O3 (wt. %)					
MnO (wt. %)	0.1644	0.1496	0.1975	0.2135	0.2125
FeO (wt. %)	19.89	19.51	16.47	16.72	19.76
NiO (wt. %)		0.0893	0.1389	0.0793	0.0897
Total	100.92	100.80	100.01	100.00	101.33
Fe2+	0.4171	0.4081	0.3493	0.3547	0.3994
Mg	1.5696	1.5781	1.6293	1.6262	1.5796
Ca	0.0068	0.0071	0.0070	0.0069	0.0070
Fo	78.36	78.77	81.88	81.62	78.61
Fa	21.12	20.72	17.55	17.80	20.82
Ca-Ol	0.34	0.35	0.35	0.34	0.35

Lava	1948	1971	1971	1971	1971
Point	1948-04-1-Mgl9_2	1971-09 - Gl1-P2	1971-09 - Gl1-P4	1971-09 - Gl1-P8	1971-09 - Gl1-P10
Laboratory	UoE	UoB	UoB	UoB	UoB
MgO (wt. %)	41.55	39.79352	39.59978	39.28034	39.83364
SiO2 (wt. %)	38.72	39.34013	39.20970	39.42347	39.28291
Al2O3 (wt. %)		0.01183	0.02323	0.02552	0.04236
CaO (wt. %)	0.2759	0.29870	0.28858	0.29173	0.29066
TiO2 (wt. %)	0.0593	0.00445	0.01073	0.01108	0.00639
Cr2O3 (wt. %)		0.01691	0.01935	0.01878	0.02058
MnO (wt. %)	0.2261	0.33645	0.35984	0.40749	0.40873
FeO (wt. %)	19.24	22.50175	22.59863	22.74838	22.24008
NiO (wt. %)	0.0899	0.12888	0.14390	0.14398	0.10656
Total	100.16	102.43	102.25	102.35	102.23
Fe2+	0.3947	0.4772	0.4797	0.4848	0.4724
Mg	1.5844	1.5067	1.5033	1.4923	1.5098
Ca	0.0076	0.0081	0.0079	0.0080	0.0079
Fo	78.89	75.33	75.16	74.84	75.51
Fa	20.49	23.90	24.06	24.32	23.65
Ca-Ol	0.38	0.41	0.39	0.40	0.40

Lava	1971	1971	1971	1971	1971
Point	1971-09 - Gl1-P11	1971-09 - Gl1-P13	1971-09 - Gl1-P15	1971-09 - Gl1-P17	1971-09 - Gl1-P19
Laboratory	UoB	UoB	UoB	UoB	UoB
MgO (wt. %)	39.87104	39.74169	39.46226	39.62513	39.28192
SiO2 (wt. %)	38.96819	39.12428	39.39437	38.99389	39.27224
Al2O3 (wt. %)	0.03656	0.01534	0.00789	0.01531	0.01923
CaO (wt. %)	0.27540	0.27502	0.27246	0.30680	0.28946
TiO2 (wt. %)	0.01196	0.02022	0.01041	0.02043	0.00792
Cr2O3 (wt. %)	0.02014	0.02644	0.02259	0.02957	0.01196
MnO (wt. %)	0.36815	0.35711	0.36914	0.37252	0.44189
FeO (wt. %)	22.59848	22.54445	23.43885	22.91882	23.09162
NiO (wt. %)	0.15411	0.13854	0.11373	0.14486	0.13439
Total	102.30	102.24	103.09	102.43	102.55
Fe2+	0.4643	0.4731	0.4927	0.4733	0.4915
Mg	1.5114	1.5078	1.4898	1.5027	1.4905
Ca	0.0075	0.0075	0.0074	0.0084	0.0079
Fo	75.29	75.28	74.43	74.89	74.55
Fa	23.94	23.96	24.80	24.30	24.58
Ca-Ol	0.37	0.37	0.37	0.42	0.39

Lava	1971	1971	1971	1971	1971
Point	1971-09 - Gl1-P21	1971-09 - Gl1-P23	1971-09 - Gl1-P25	1971-09 - Gl1-P27	1971-09 - Gl1-P29
Laboratory	UoB	UoB	UoB	UoB	UoB
MgO (wt. %)	39.32096	38.72327	39.39319	39.58594	39.23507
SiO2 (wt. %)	39.14886	38.62259	38.95082	39.21478	38.93830
Al2O3 (wt. %)	0.04632	0.03258	0.02919	0.00049	0.04733
CaO (wt. %)	0.28751	0.30060	0.28931	0.28128	0.31903
TiO2 (wt. %)	0.01125	0.01054	0.00864	0.02383	0.02086
Cr2O3 (wt. %)	0.02240	0.01539	0.01898	0.02056	0.01906
MnO (wt. %)	0.42198	0.34627	0.37199	0.37894	0.39986
FeO (wt. %)	22.98228	23.09731	22.95250	23.04013	22.64520
NiO (wt. %)	0.13932	0.13538	0.10694	0.13608	0.09072
Total	102.38	101.28	102.12	102.68	101.72
Fe2+	0.4872	0.4917	0.4795	0.4820	0.4822
Mg	1.4937	1.4886	1.4987	1.4984	1.4980
Ca	0.0078	0.0083	0.0079	0.0077	0.0088
Fo	74.67	74.33	74.77	74.79	74.88
Fa	24.48	24.87	24.44	24.42	24.25
Ca-Ol	0.39	0.41	0.39	0.38	0.44

Lava	1971	1971	1971	1971
Point	1971-09 - Gl1-P31	1971-09 - Gl1-P33	1971-09 - Ol 1-P1	1971-09 - Ol 1-P2
Laboratory	UoB	UoB	UoB	UoB
MgO (wt. %)	39.25244	39.44942	41.32558	42.58002
SiO2 (wt. %)	38.42776	39.01213	39.61113	39.75857
Al2O3 (wt. %)	0.02934	0.01972	0.00593	0.00693
CaO (wt. %)	0.28237	0.35782	0.18353	0.27279
TiO2 (wt. %)	0.02296	0.00236	0.00266	0.00575
Cr2O3 (wt. %)	0.02378	0.02564	0.02307	0.02099
MnO (wt. %)	0.37461	0.41034	0.35029	0.33269
FeO (wt. %)	22.71802	22.49980	20.13278	19.07891
NiO (wt. %)	0.13049	0.12468	0.14806	0.11863
Total	101.26	101.90	101.78	102.18
Fe2+	0.4678	0.4755	0.4260	0.3918
Mg	1.5051	1.5026	1.5587	1.5896
Ca	0.0078	0.0098	0.0050	0.0073
Fo	74.89	75.05	78.05	79.34
Fa	24.32	24.01	21.33	19.94
Ca-Ol	0.39	0.49	0.25	0.37

Table A.4. EPMA of pyroxene phenocrysts chemistry. Analysis performed at University of Exeter (UoE) and University of Bristol (UoB).

Lava		1921	1921	1921	1921	1921	1921
Point	Detection limit	1921-02 - Gl 1-P3	1921-02 - Gl 1-P4	1921-02 - Gl 1-P8	1921-02 - Gl11-P1	1921-02 - Gl11-P3	1921-02 - Gl11-P9
Laboratory		UoB	UoB	UoB	UoB	UoB	UoB
Na2O (wt. %)	0.01 (%)	0.44605	0.31530	0.32994	0.25389	0.27358	0.26898
MgO (wt. %)	0.01 (%)	17.12930	17.37985	16.76215	17.13362	17.07616	16.87508
SiO2 (wt. %)	0.02 (%)	51.69701	52.20978	51.53517	51.87644	52.26327	51.51274
Al2O3 (wt. %)	0.02 (%)	2.63634	1.95141	2.90493	2.48814	2.51122	2.29447
CaO (wt. %)	0.01 (%)	18.96018	18.95942	19.50295	19.04864	19.19206	19.04218
TiO2 (wt. %)	0.01 (%)	0.50716	0.48387	0.51267	0.52014	0.55118	0.45840
Cr2O3 (wt. %)	0.02 (%)	0.51405	0.37213	0.73763	0.43744	0.44149	0.49325
MnO (wt. %)	0.02 (%)	0.22873	0.24017	0.21030	0.23580	0.24135	0.20490
FeO (wt. %)	0.02 (%)	7.82005	8.06482	7.50604	7.99546	8.32440	7.47242
Total		99.94	99.98	100.00	99.99	100.87	98.62
Fe2+		0.158	0.181	0.168	0.189	0.197	0.189
Mg		0.937	0.951	0.918	0.938	0.928	0.936
Ca		0.745	0.746	0.767	0.750	0.750	0.759
XWo		38.78	38.35	40.06	38.77	38.81	39.38
XEn		48.74	48.92	47.91	48.52	48.05	48.56
XFs		12.48	12.73	12.03	12.70	13.14	12.06

Lava	1921	1921	1921	1921	1921	1921
Point	1921-02 - Gl11-P11	1921-02 - Pl4-P1	1921-02 - Pl4-P4	1921-02 - Pl4-P7	1921-02 - Gl 6-P2	1921-02 - Gl 6-P4
Laboratory	UoB	UoB	UoB	UoB	UoB	UoB
Na2O (wt. %)	0.25458	0.26352	0.21441	0.28238	0.31914	0.30110
MgO (wt. %)	17.39297	16.91254	17.24387	17.10739	17.19311	16.21862
SiO2 (wt. %)	52.66681	51.20926	51.27285	52.24784	51.93562	50.18270
Al2O3 (wt. %)	2.34475	2.59989	2.40759	2.86653	2.28907	3.25827
CaO (wt. %)	19.42665	18.38176	17.72069	19.58755	19.24896	19.74246
TiO2 (wt. %)	0.48262	0.58835	0.53537	0.56548	0.49148	0.59271
Cr2O3 (wt. %)	0.53288	0.43755	0.36484	0.65120	0.41471	0.89958
MnO (wt. %)	0.25499	0.24031	0.27730	0.22148	0.21732	0.18304
FeO (wt. %)	8.06337	8.81421	9.14091	7.96827	8.07509	7.61617
Total	101.42	99.45	99.18	101.50	100.18	98.99
Fe2+	0.184	0.204	0.220	0.177	0.170	0.148
Mg	0.939	0.933	0.954	0.924	0.939	0.899
Ca	0.754	0.729	0.705	0.760	0.756	0.786
XWo	38.91	37.67	36.28	39.48	38.91	40.91
XEn	48.48	48.23	49.12	47.98	48.35	46.77
XFs	12.61	14.10	14.61	12.54	12.74	12.32

Lava	1921	1921	1921	1921	1921	1921
Point	1921-02 - Gl 6-P6	1921-02 - Gl 6-P8	1921-02 - Gl 6-P9	1921-02 - Gl 6-P11	1921-02 - Gl 10-P1	1921-02 - Gl 10-P4
Laboratory	UoB	UoB	UoB	UoB	UoB	UoB
Na2O (wt. %)	0.31178	0.29038	0.29243	0.26130	0.29627	0.31814
MgO (wt. %)	17.83151	17.21097	17.07885	17.54095	17.23002	17.25935
SiO2 (wt. %)	53.30243	52.31129	51.60962	52.09747	51.61552	51.81722
Al2O3 (wt. %)	1.79964	2.13322	2.35160	2.22931	2.21529	2.27471
CaO (wt. %)	18.15370	18.69156	19.17866	18.97549	19.02926	19.12196
TiO2 (wt. %)	0.40530	0.42634	0.48893	0.45521	0.48012	0.44819
Cr2O3 (wt. %)	0.30144	0.38314	0.33800	0.33055	0.44929	0.40723
MnO (wt. %)	0.25717	0.22036	0.23740	0.21051	0.23942	0.24606
FeO (wt. %)	8.18006	8.11288	8.08464	8.17320	7.94242	7.62987
Total	100.54	99.78	99.66	100.27	99.50	99.52
Fe2+	0.224	0.207	0.171	0.174	0.168	0.166
Mg	0.970	0.944	0.938	0.957	0.948	0.948
Ca	0.709	0.737	0.757	0.744	0.752	0.755
XWo	36.79	38.17	38.94	38.13	38.68	38.95
XEn	50.28	48.90	48.25	49.05	48.72	48.92
XFs	12.94	12.93	12.81	12.82	12.60	12.13

Lava	1921	1921	1921	1921	1921	1921
Point	1921-02 - Gl 10-P6	1921-02 - Gl 10-P11	1921-02 - Gl 10-P12	1921-02 - Gl 10-P14	1921-02 - Gl 2-P1	1921-02 - Gl 2-P3
Laboratory	UoB	UoB	UoB	UoB	UoB	UoB
Na2O (wt. %)	0.26443	0.34202	0.25076	0.24294	0.30746	0.23472
MgO (wt. %)	16.95859	17.31831	16.95100	16.93204	16.79631	16.84620
SiO2 (wt. %)	51.70770	51.93144	51.53146	52.18056	50.84241	51.60885
Al2O3 (wt. %)	2.31502	2.17630	2.67041	2.58064	3.34113	2.41562
CaO (wt. %)	19.43992	18.48121	19.19628	19.19219	18.93782	19.46622
TiO2 (wt. %)	0.48546	0.49183	0.54982	0.50603	0.64048	0.46517
Cr2O3 (wt. %)	0.51836	0.46422	0.50022	0.47818	0.40325	0.43123
MnO (wt. %)	0.20895	0.25000	0.21597	0.24429	0.19844	0.21312
FeO (wt. %)	7.68783	7.84949	7.76575	7.98125	8.11962	7.91587
Total	99.59	99.30	99.63	100.34	99.59	99.60
Fe2+	0.176	0.190	0.183	0.206	0.171	0.181
Mg	0.933	0.954	0.932	0.925	0.923	0.927
Ca	0.768	0.731	0.758	0.754	0.748	0.770
XWo	39.64	37.95	39.30	39.18	38.93	39.66
XEn	48.12	49.47	48.29	48.10	48.04	47.75
XFs	12.24	12.58	12.41	12.72	13.03	12.59

Lava	1921	1921	1921	1921	1921	1921
Point	1921-02 - Mgl1-P2	1921-02 - Gl 3-P2	1921-02 - Gl 3-P4	1921-02 - Gl 3-P6	1921-02 - Gl 3-P8	1921-02 - Gl 3-P10
Laboratory	UoB	UoB	UoB	UoB	UoB	UoB
Na2O (wt. %)	0.29598	0.30955	0.24644	0.28968	0.27151	0.24094
MgO (wt. %)	17.02432	17.10303	17.15187	17.78129	17.46884	17.01383
SiO2 (wt. %)	51.51054	51.48357	51.78753	52.45575	52.18402	51.99345
Al2O3 (wt. %)	2.31405	2.42692	2.60504	1.96367	1.77235	1.94912
CaO (wt. %)	17.32419	19.56972	19.13828	18.23877	18.13336	19.30658
TiO2 (wt. %)	0.59963	0.44679	0.56789	0.43568	0.43946	0.50201
Cr2O3 (wt. %)	0.19629	0.55044	0.56535	0.40794	0.34553	0.27865
MnO (wt. %)	0.28479	0.21757	0.20443	0.26222	0.24504	0.23175
FeO (wt. %)	10.04117	7.40844	7.90794	8.27005	8.44562	8.24720
Total	99.59	99.52	100.17	100.11	99.31	99.76
Fe2+	0.246	0.146	0.184	0.197	0.214	0.191
Mg	0.940	0.939	0.938	0.971	0.963	0.935
Ca	0.687	0.773	0.752	0.716	0.719	0.763
XWo	35.46	39.82	38.92	36.89	36.98	39.07
XEn	48.49	48.42	48.53	50.05	49.57	47.90
XFs	16.04	11.77	12.55	13.06	13.44	13.03

Lava	1921	1921	1921	1921	1921	1921
Point	1921-02 - Gl 3-P13	1921-02 - Gl 3-P15	1921-02 - Mgl2-P1	1921-02 - Gl 4-P2	1921-02 - Gl 4-P4	1921-02 - Gl 4-P6
Laboratory	UoB	UoB	UoB	UoB	UoB	UoB
Na2O (wt. %)	0.27685	0.22007	0.24217	0.26362	0.25120	0.30284
MgO (wt. %)	17.16885	17.04033	17.75356	17.77551	17.02928	17.92429
SiO2 (wt. %)	51.89793	51.75217	52.23432	52.07671	51.90498	52.30008
Al2O3 (wt. %)	2.17501	1.98113	1.81927	2.04070	2.47465	1.80363
CaO (wt. %)	18.38411	18.65261	18.07961	18.50300	18.50772	18.28863
TiO2 (wt. %)	0.49142	0.44701	0.43339	0.43898	0.54171	0.41265
Cr2O3 (wt. %)	0.26085	0.28851	0.31311	0.40400	0.38927	0.31239
MnO (wt. %)	0.23990	0.25564	0.25418	0.26014	0.24517	0.28328
FeO (wt. %)	8.86105	8.56672	8.68452	8.31692	8.54171	8.25526
Total	99.76	99.20	99.81	100.08	99.89	99.88
Fe2+	0.210	0.209	0.205	0.177	0.218	0.179
Mg	0.944	0.942	0.974	0.971	0.935	0.980
Ca	0.726	0.741	0.713	0.727	0.730	0.719
XWo	37.37	38.03	36.48	37.21	37.87	36.82
XEn	48.56	48.34	49.84	49.74	48.49	50.21
XFs	14.06	13.63	13.68	13.05	13.64	12.97

Lava	1921	1921	1921	1921	1921	1921
Point	1921-02 - Gl 7-P6	1921-02 - Gl 7-P8	1921-02 - Gl 7-P10	1921-02 - Gl 9-P6	1921-02 - Gl 9-P8	1921-02 - Gl 9-P10
Laboratory	UoB	UoB	UoB	UoB	UoB	UoB
Na2O (wt. %)	0.28537	0.26125	0.40492	0.25228	0.25201	0.30616
MgO (wt. %)	16.97085	17.35164	17.08561	17.27754	17.60476	17.29334
SiO2 (wt. %)	51.92558	52.14722	51.97797	51.85319	52.02763	51.74194
Al2O3 (wt. %)	2.42387	2.07808	2.36163	2.13804	2.27923	2.40095
CaO (wt. %)	19.50044	18.73771	19.48700	18.53904	18.29307	18.91355
TiO2 (wt. %)	0.51124	0.47789	0.46631	0.49927	0.45638	0.48768
Cr2O3 (wt. %)	0.46976	0.45671	0.48106	0.38592	0.31140	0.43649
MnO (wt. %)	0.23365	0.25113	0.21500	0.27277	0.27403	0.22171
FeO (wt. %)	7.99261	8.12468	7.57731	8.41682	8.05355	7.83692
Total	100.31	99.89	100.06	99.63	99.55	99.64
Fe2+	0.176	0.196	0.155	0.199	0.196	0.173
Mg	0.927	0.951	0.933	0.950	0.967	0.949
Ca	0.766	0.738	0.765	0.733	0.722	0.746
XWo	39.51	38.07	39.63	37.72	37.28	38.53
XEn	47.85	49.05	48.34	48.91	49.91	49.01
XFs	12.64	12.88	12.03	13.37	12.81	12.46

Lava	1921	1921	1921	1921	1921	1921
Point	1921-02 - Gl 9-P12	1921-02 - Gl 9-P13	1921-02 - Pl 4-P20	1921-02 - Mgl 3 - P1	1921-05-1__1	1921-05-1__2
Laboratory	UoB	UoB	UoB	UoB	UoE	UoE
Na2O (wt. %)	0.24755	0.26632	0.29099	0.27469	0.3339	0.3210
MgO (wt. %)	17.13260	16.90504	17.17360	18.12347	16.65	16.90
SiO2 (wt. %)	51.97998	51.65677	52.26897	51.59423	51.89	52.28
Al2O3 (wt. %)	2.33549	2.54834	1.89315	2.40456	2.63	2.40
CaO (wt. %)	18.65932	18.77621	19.29772	16.70961	18.47	18.29
TiO2 (wt. %)	0.44570	0.57787	0.47217	0.50846	0.6093	0.5534
Cr2O3 (wt. %)	0.33909	0.33482	0.39394	0.44890	0.3723	0.2759
MnO (wt. %)	0.24155	0.23925	0.22023	0.29073	0.1080	
FeO (wt. %)	8.32677	8.53293	7.87537	9.37763	8.40	8.38
Total	99.71	99.84	99.89	99.73	99.46	99.40
Fe2+	0.207	0.204	0.185	0.211	0.235	0.246
Mg	0.941	0.929	0.941	0.994	0.918	0.932
Ca	0.737	0.741	0.760	0.659	0.732	0.725
XWo	38.08	38.35	39.11	33.93	38.32	37.83
XEn	48.65	48.04	48.43	51.21	48.07	48.64
XFs	13.26	13.60	12.46	14.86	13.60	13.53

Lava	1921	1921	1921	1921	1921	1921
Point	1921-05-1__4	1921-05-1__9	1921-05-1__10	1921-05-1__26	1921-05-1__30	1921-05-1__31
Laboratory	UoE	UoE	UoE	UoE	UoE	UoE
Na2O (wt. %)	0.3198	0.2734	0.2934	0.2751	0.2631	0.2887
MgO (wt. %)	16.73	17.22	17.64	16.97	17.59	16.24
SiO2 (wt. %)	52.48	53.07	52.90	51.54	53.12	52.14
Al2O3 (wt. %)	2.45	2.13	1.8013	2.44	1.6484	2.92
CaO (wt. %)	19.72	17.89	17.77	19.12	17.39	19.80
TiO2 (wt. %)	0.5442	0.4779	0.3925	0.4446	0.4683	0.5450
Cr2O3 (wt. %)	0.3229	0.1553	0.2772	0.3121	0.1264	0.3674
MnO (wt. %)	0.1088	0.1798	0.1935	0.1492	0.1851	0.1083
FeO (wt. %)	7.91	8.31	8.29	7.46	8.85	7.39
Total	100.59	99.71	99.56	98.71	99.64	99.80
Fe2+	0.201	0.256	0.242	0.182	0.273	0.218
Mg	0.912	0.946	0.969	0.940	0.967	0.892
Ca	0.772	0.706	0.702	0.761	0.687	0.782
XWo	40.10	37.01	36.43	39.38	35.66	41.11
XEn	47.34	49.57	50.31	48.63	50.18	46.91
XFs	12.56	13.42	13.26	11.99	14.16	11.98

Lava	1948	1948	1948	1948	1948	1948
Point	1948-04 - Gl10-P1	1948-04 - Gl10-P3	1948-04 - Gl4-P1	1948-04 - Gl4-P2	1948-04 - Gl4-P3	1948-04 - Gl4-P4
Laboratory	UoB	UoB	UoB	UoB	UoB	UoB
Na2O (wt. %)	0.30270	0.29564	0.31245	0.32008	0.29357	0.28428
MgO (wt. %)	16.88608	16.80160	17.29605	17.33411	17.39459	16.90873
SiO2 (wt. %)	51.58185	51.37685	52.11157	52.05646	51.95918	51.62578
Al2O3 (wt. %)	2.87237	3.46912	2.70069	2.54619	2.67759	3.18663
CaO (wt. %)	21.53377	20.80431	19.82612	19.51614	19.67200	20.34926
TiO2 (wt. %)	0.41771	0.43641	0.42830	0.40118	0.41917	0.39312
Cr2O3 (wt. %)	0.45972	0.78605	0.38493	0.36883	0.40822	0.67616
MnO (wt. %)	0.15508	0.14225	0.20168	0.24279	0.18106	0.14508
FeO (wt. %)	6.13491	6.36377	7.14955	7.28224	7.37228	6.41169
Total	100.34	100.48	100.41	100.07	100.38	99.98
Fe2+	0.086	0.113	0.147	0.152	0.145	0.135
Mg	0.918	0.913	0.940	0.946	0.946	0.923
Ca	0.841	0.812	0.775	0.765	0.769	0.798
XWo	43.23	42.33	40.08	39.57	39.64	41.63
XEn	47.16	47.56	48.64	48.90	48.77	48.13
XFs	9.61	10.11	11.28	11.53	11.59	10.24

Lava	1948	1948	1948	1948	1948	1948
Point	1948-04 - Gl4-P5	1948-04 - Gl4-P6	1948-04 - Gl9-P1	1948-04 - Gl9-P2	1948-04 - Gl9-P3	1948-04 - Gl9-P6
Laboratory	UoB	UoB	UoB	UoB	UoB	UoB
Na2O (wt. %)	0.34111	0.30797	0.02211	0.23368	0.27621	0.30042
MgO (wt. %)	17.02766	16.79326	28.60406	17.48108	17.18907	16.88725
SiO2 (wt. %)	51.50624	51.11301	54.54034	51.67250	51.83264	51.13947
Al2O3 (wt. %)	3.39049	3.32793	1.62516	3.07742	3.18217	3.40683
CaO (wt. %)	19.48214	20.24701	2.34513	19.74850	20.55982	20.59728
TiO2 (wt. %)	0.46931	0.48366	0.18430	0.38176	0.41645	0.43532
Cr2O3 (wt. %)	0.62496	0.55170	0.19964	0.54532	0.66993	0.67473
MnO (wt. %)	0.19897	0.22772	0.26047	0.17607	0.20836	0.21427
FeO (wt. %)	7.23849	6.84855	12.01274	6.81765	6.27421	6.21000
Total	100.28	99.90	99.79	100.13	100.61	99.87
Fe2+	0.150	0.123	0.329	0.135	0.118	0.105
Mg	0.927	0.918	1.520	0.952	0.931	0.922
Ca	0.763	0.795	0.090	0.773	0.801	0.808
XWo	39.90	41.36	4.55	39.98	41.64	42.09
XEn	48.53	47.73	77.25	49.24	48.44	48.01
XFs	11.57	10.92	18.20	10.77	9.92	9.90

Lava	1948	1948	1948	1948	1948	1948
Point	1948-04 - Gl9-P7	1948-04 - Gl9-P8	1948-04-1-Gl10_2	1948-04-1-Gl6_1	1948-04-1-Gl6_3	1948-04-1-Gl6_5
Laboratory	UoB	UoB	UoE	UoE	UoE	UoE
Na2O (wt. %)	0.03779	0.31042	0.3021	0.3105	0.3153	0.2900
MgO (wt. %)	27.15414	17.34009	17.10	16.96	16.73	17.04
SiO2 (wt. %)	54.34636	51.75853	51.28	52.46	52.24	51.77
Al2O3 (wt. %)	1.36460	2.65342	2.45	2.40	2.67	2.42
CaO (wt. %)	2.34301	18.90170	19.50	19.08	19.79	19.08
TiO2 (wt. %)	0.26761	0.52513	0.3405	0.3281	0.5583	0.5022
Cr2O3 (wt. %)	0.11959	0.52385	0.2516	0.3642	0.3426	0.2298
MnO (wt. %)	0.40627	0.28686	0.1537	0.0995	0.0934	0.1710
FeO (wt. %)	13.92882	8.08650	7.06	7.13	7.37	7.53
Total	99.97	100.39	98.44	99.13	100.11	99.03
Fe2+	0.398	0.168	0.143	0.210	0.191	0.186
Mg	1.455	0.945	0.947	0.935	0.915	0.941
Ca	0.090	0.740	0.776	0.756	0.778	0.757
XWo	4.59	38.31	39.96	39.55	40.54	39.21
XEn	74.09	48.90	48.75	48.91	47.68	48.72
XFs	21.32	12.79	11.29	11.54	11.78	12.08

Lava	1948	1948	1948	1948	1948	1948
Point	1948-04-1-Gl6_6	1948-04-1-Gl6_7	1948-04-1-Gl5_2	1948-04-1-Gl5_5	1948-04-1-Gl5_6	1948-04-1-Gl5_8
Laboratory	UoE	UoE	UoE	UoE	UoE	UoE
Na2O (wt. %)	0.0439	0.0661	0.3013	0.2667	0.2480	0.2798
MgO (wt. %)	27.29	27.12	17.61	18.51	18.24	17.43
SiO2 (wt. %)	54.69	54.69	51.76	53.23	52.68	52.05
Al2O3 (wt. %)	1.3490	1.3188	2.20	1.5606	1.7041	2.42
CaO (wt. %)	2.32	2.33	18.52	17.79	18.37	18.68
TiO2 (wt. %)	0.3386	0.3273	0.4824	0.3848	0.4006	0.5296
Cr2O3 (wt. %)			0.1619	0.1789	0.1074	0.2039
MnO (wt. %)	0.1965	0.2333	0.1089	0.1344	0.0950	0.1428
FeO (wt. %)	13.73	14.20	7.81	7.80	7.52	7.59
Total	99.96	100.29	98.95	99.86	99.37	99.33
Fe2+	0.411	0.414	0.176	0.209	0.186	0.193
Mg	1.460	1.449	0.971	1.010	1.000	0.958
Ca	0.089	0.089	0.734	0.697	0.724	0.738
XWo	4.55	4.56	37.70	35.84	37.02	38.23
XEn	74.44	73.77	49.88	51.89	51.15	49.64
XFs	21.01	21.67	12.41	12.27	11.83	12.13

Lava	1948	1948	1948	1948	1948	1948
Point	1948-04-1-Gl5_9	1948-04-1-Gl5_10	1948-04-1-Gl5_11	1948-04-1-Gl5_12	1948-04-1-Gl1_1	1948-04-1-Gl1_2
Laboratory	UoE	UoE	UoE	UoE	UoE	UoE
Na2O (wt. %)	0.0511	0.3258	0.2897	0.0638	0.3084	0.2853
MgO (wt. %)	28.32	16.32	16.97	27.12	16.43	16.66
SiO2 (wt. %)	54.70	52.10	52.49	54.90	51.67	51.70
Al2O3 (wt. %)	1.1042	2.29	2.58	1.1115	3.10	2.89
CaO (wt. %)	2.39	18.88	18.88	2.36	19.08	18.67
TiO2 (wt. %)	0.2906	0.5521	0.4854	0.2669	0.5934	0.5838
Cr2O3 (wt. %)		0.3529	0.2760	0.1151	0.2682	0.1867
MnO (wt. %)	0.1848	0.1442	0.1152	0.2208	0.1372	0.1404
FeO (wt. %)	12.48	8.34	7.52	13.50	7.71	7.81
Total	99.52	99.31	99.61	99.66	99.30	98.93
Fe2+	0.350	0.244	0.225	0.407	0.217	0.226
Mg	1.512	0.903	0.932	1.456	0.906	0.922
Ca	0.092	0.751	0.745	0.091	0.757	0.743
XWo	4.64	39.25	39.04	4.66	39.78	38.94
XEn	76.46	47.21	48.82	74.53	47.67	48.35
XFs	18.90	13.53	12.14	20.81	12.55	12.71

Lava	1948	1948	1948	1948	1948	1948
Point	1948-04-1-Gl1_5	1948-04-1-Gl1_7	1948-04-1-Gl1_8	1948-04-1-Mgl1_1	1948-04-1-Mgl1_2	1948-04-1-Mgl9_3
Laboratory	UoE	UoE	UoE	UoE	UoE	UoE
Na2O (wt. %)	0.2909	0.0538	0.2336	0.2977	0.2895	0.3175
MgO (wt. %)	17.06	27.14	18.40	16.96	16.77	16.84
SiO2 (wt. %)	51.76	53.52	53.83	51.22	51.91	52.27
Al2O3 (wt. %)	2.23	1.3646	1.3694	3.94	2.25	2.39
CaO (wt. %)	18.26	2.24	18.97	19.27	18.37	19.06
TiO2 (wt. %)	0.5179	0.3335	0.3484	0.5258	0.5555	0.5047
Cr2O3 (wt. %)	0.1389			0.4543	0.1890	0.1702
MnO (wt. %)	0.1271	0.2287	0.1572		0.1649	0.0955
FeO (wt. %)	9.10	14.29	6.62	6.15	8.05	7.92
Total	99.48	99.17	99.93	98.82	98.55	99.57
Fe2+	0.219	0.380	0.193	0.167	0.238	0.214
Mg	0.940	1.465	1.001	0.934	0.932	0.926
Ca	0.723	0.087	0.742	0.763	0.734	0.753
XWo	37.19	4.38	38.14	40.43	38.28	39.16
XEn	48.34	73.82	51.47	49.50	48.62	48.14
XFs	14.47	21.80	10.39	10.07	13.09	12.70

Lava	1948	1948	1971	1971	1971	1971
Point	1948-04-1-Mgl9_4	1948-04-1-Mgl9_5	1971-09 - Gl1-P1	1971-09 - Gl1-P3	1971-09 - Gl1-P5	1971-09 - Gl1-P6
Laboratory	UoE	UoE	UoB	UoB	UoB	UoB
Na2O (wt. %)	0.3212	0.3045	0.33961	0.27704	0.00000	0.30404
MgO (wt. %)	16.96	17.14	16.70885	16.72061	28.13774	17.13812
SiO2 (wt. %)	51.83	52.70	51.84937	52.23982	55.31375	52.44102
Al2O3 (wt. %)	2.34	2.28	2.72702	2.79745	1.59324	2.71426
CaO (wt. %)	18.34	18.32	20.01346	19.99868	2.29993	19.83048
TiO2 (wt. %)	0.5536	0.5762	0.58653	0.57907	0.21745	0.52940
Cr2O3 (wt. %)	0.1716		0.49921	0.56549	0.20143	0.68530
MnO (wt. %)	0.1274	0.1393	0.26567	0.22750	0.28177	0.26424
FeO (wt. %)	8.63	8.95	8.73927	8.58043	13.70345	8.09207
Total	99.27	100.41	101.73	101.99	101.75	102.00
Fe2+	0.221	0.244	0.159	0.183	0.381	0.167
Mg	0.936	0.936	0.902	0.901	1.477	0.921
Ca	0.728	0.719	0.777	0.774	0.087	0.766
XWo	37.68	37.27	39.96	40.03	4.41	39.67
XEn	48.48	48.52	46.42	46.57	75.08	47.70
XFs	13.84	14.21	13.62	13.41	20.51	12.63

Lava	1971	1971	1971	1971	1971	1971
Point	1971-09 - Gl1-P7	1971-09 - Gl1-P9	1971-09 - Gl1-P12	1971-09 - Gl1-P14	1971-09 - Gl1-P16	1971-09 - Gl1-P18
Laboratory	UoB	UoB	UoB	UoB	UoB	UoB
Na2O (wt. %)	0.32366	0.33455	0.36963	0.28356	0.25648	0.28532
MgO (wt. %)	17.07857	16.60583	16.73487	16.98971	16.91362	16.66390
SiO2 (wt. %)	52.58906	52.54607	52.04659	52.24784	52.61949	51.85038
Al2O3 (wt. %)	2.60788	2.67292	2.59143	2.55256	2.63963	2.72502
CaO (wt. %)	20.32253	19.89347	19.99309	18.94521	20.02635	20.14166
TiO2 (wt. %)	0.51326	0.57547	0.57886	0.54537	0.50422	0.57152
Cr2O3 (wt. %)	0.61707	0.49850	0.47880	0.48754	0.63464	0.60330
MnO (wt. %)	0.23699	0.25061	0.21276	0.30200	0.28558	0.16540
FeO (wt. %)	8.00863	8.67500	8.74451	9.22622	7.97880	8.25826
Total	102.30	102.05	101.75	101.58	101.86	101.26
Fe2+	0.154	0.195	0.163	0.206	0.184	0.168
Mg	0.915	0.894	0.903	0.919	0.911	0.903
Ca	0.783	0.770	0.775	0.737	0.775	0.785
XWo	40.37	39.97	39.90	38.05	40.22	40.47
XEn	47.21	46.42	46.47	47.48	47.27	46.58
XFs	12.42	13.61	13.62	14.46	12.51	12.95

Lava	1971	1971	1971	1971	1971	1971
Point	1971-09 - Gl1-P20	1971-09 - Gl1-P22	1971-09 - Gl1-P24	1971-09 - Gl1-P26	1971-09 - Gl1-P28	1971-09 - Gl1-P30
Laboratory	UoB	UoB	UoB	UoB	UoB	UoB
Na2O (wt. %)	0.30734	0.32955	0.30566	0.34195	0.33666	0.32843
MgO (wt. %)	17.53369	16.87169	17.08371	17.48618	17.32299	16.72219
SiO2 (wt. %)	52.01287	52.07346	52.68554	52.16503	52.41368	52.22234
Al2O3 (wt. %)	2.68808	2.63270	2.52326	2.43320	2.55768	2.66351
CaO (wt. %)	18.37372	20.07971	19.71430	19.02744	19.28976	20.26376
TiO2 (wt. %)	0.57256	0.51866	0.52909	0.51338	0.51932	0.53141
Cr2O3 (wt. %)	0.50694	0.58785	0.59989	0.52189	0.53601	0.61209
MnO (wt. %)	0.26561	0.23885	0.28558	0.28052	0.22454	0.23098
FeO (wt. %)	8.97849	7.96585	8.23596	8.51134	8.42376	8.16575
Total	101.24	101.30	101.96	101.28	101.62	101.74
Fe2+	0.189	0.157	0.183	0.164	0.174	0.163
Mg	0.949	0.913	0.919	0.945	0.934	0.902
Ca	0.715	0.781	0.762	0.739	0.747	0.786
XWo	36.91	40.34	39.50	38.05	38.60	40.60
XEn	49.01	47.16	47.62	48.66	48.24	46.62
XFs	14.08	12.49	12.88	13.29	13.16	12.77

Lava	1971	1971
Point	1971-09 - Gl1-P32	1971-09 - Gl1-P34
Laboratory	UoB	UoB
Na2O (wt. %)	0.29141	0.27989
MgO (wt. %)	17.30123	17.54203
SiO2 (wt. %)	52.34935	52.72896
Al2O3 (wt. %)	2.48056	2.11193
CaO (wt. %)	19.45052	18.94879
TiO2 (wt. %)	0.50593	0.49542
Cr2O3 (wt. %)	0.64496	0.48686
MnO (wt. %)	0.17157	0.29004
FeO (wt. %)	8.25652	8.56063
Total	101.45	101.44
Fe2+	0.175	0.193
Mg	0.934	0.948
Ca	0.755	0.736
XWo	38.93	37.87
XEn	48.18	48.78
XFs	12.90	13.35

Capítulo 4 : Conclusiones

En esta tesis se concluye que las lavas estudiadas del Volcán Villarrica, eruptadas en el siglo XX, registran procesos pre-eruptivos similares, que incluyen calentamiento (*thermal mixing*) y adición de agua. Para reproducir las plagioclasas ricas en An, alrededor de núcleos reabsorbidos pobres en An, es necesario un calentamiento de cerca de 100 °C (desde ~1090 a ~ 1190 °C) a ~0.5 kbar. Sin embargo, la incorporación de pequeñas cantidades de volátiles y magma máfico caliente en el reservorio también podrían explicar la reabsorción y modificación de las composiciones de plagioclasa (*compositional mixing*). En este escenario, una mayor interacción del magma caliente con el reservorio (*cryptic mixing*) podría explicar las altos contenidos modales de rica en An/pobre en An en el magma híbrido más máfico, caliente y rico en volátiles (lava de 1948) que últimamente resultarían en erupciones de mayor intensidad.

Bibliografía

Asimow, P. D., & Ghiorso, M. S. (1998). Algorithmic modifications extending MELTS to calculate subsolidus phase relations. *American Mineralogist*, *83*(9–10), 1127–1132. https://doi.org/10.2138/am-1998-9-1022

Bachmann, O., & Bergantz, G. W. (2006). Gas percolation in upper-crustal silicic crystal mushes as a mechanism for upward heat advection and rejuvenation of near-solidus magma bodies. *Journal of Volcanology and Geothermal Research*, *149*(1–2), 85–102. https://doi.org/10.1016/j.jvolgeores.2005.06.002

Bertin, D., Amigo, A., & Bertin, L. (2015). Erupción del volcán Villarrica 2015: Productos emitidos y volumen involucrado. In *14º Congreso Geológico Chileno* (Vol. 3, pp. 249–251).

Bouvet de Maisonneuve, C., Dungan, M. A., Bachmann, O., & Burgisser, A. (2013). Petrological insights into shifts in eruptive styles at Volcán Llaima (Chile). *Journal of Petrology*, *54*(2), 393–420. https://doi.org/10.1093/petrology/egs073

Boynton, W. V. (1984). Chapter 3 - Cosmochemistry of the Rare Earth Elements: Meteorite Studies. In P. B. T.-D. in G. Henderson (Ed.), *Rare Earth Element Geochemistry* (Vol. 2, pp. 63–114). Elsevier. https://doi.org/https://doi.org/10.1016/B978-0-444-42148-7.50008-3

Cashman, K., & Blundy, J. (2013). Petrological cannibalism: The chemical and textural consequences of incremental magma body growth. *Contributions to Mineralogy and Petrology*, *166*(3), 703–729. https://doi.org/10.1007/s00410-013-0895-0

Cembrano, J., Hervé, F., & Lavenu, A. (1996). The Liquiñe Ofqui fault zone: a long-lived intra-arc fault system in southern Chile. *Tectonophysics*, *259*(1–3), 55–66.

https://doi.org/10.1016/0040-1951(95)00066-6

Clavero, J., & Moreno, H. (1994). Ignimbritas Licán y Pucón: Evidencias de erupciones explosivas andesítico-basálticas postglaciales del Volcán Villarrica, Andes del Sur, 39°25′S. *Actas VII Congreso Geológico Chileno*, 250–254.

D'Lemos, R. S. (1996). Mixing between granitic and dioritic crystal mushes, Guernsey, Channel Island, UK. *Lithos*, *38*, 233–257. https://doi.org/10.1016/0024-4937(96)00007-2

de Silva, S., Salas, G., & Schubring, S. (2008). Triggering explosive eruptions-The case for silicic magma recharge at Huaynaputina, southern Peru. *Geology*, *36*(5), 387–390. https://doi.org/10.1130/G24380A.1

Droop T.,R., G. (1987). A General Equation for Estimating Fe3+ Concentrations in Ferromagnesian Silicates and Oxides from Microprobe Analyses, Using Stoichiometric Criteria. *Mineralogical Magazine*, *51*(361), 431–435. https://doi.org/10.1180/minmag.1987.051.361.10

Ghiorso, M. S., & Sack, R. O. (1995). Chemical mass transfer in magmatic processes IV. A revised and internally consistent thermodynamic model for the interpolation and extrapolation of liquid-solid equilibria in magmatic systems at elevated temperatures and pressures. *Contributions to Mineralogy and Petrology*, *119*(2–3), 197–212. https://doi.org/10.1007/BF00307281

Grove, T. L., Donnelly-Nolan, J. M., & Housh, T. (1997). Magmatic processes that generated the rhyolite of Glass Mountain, Medicine Lake volcano, N. California. *Contributions to Mineralogy and Petrology*, *127*, 205–223. https://doi.org/10.1007/s004100050276

Gutiérrez, F., & Parada, M. A. (2010). Numerical modeling of time-dependent fluid dynamics and differentiation of a shallow basaltic magma chamber. *Journal of Petrology*, *51*(3), 731–762. https://doi.org/10.1093/petrology/egp101

Hickey -Vargas, R., Roa, H. M., Escobar, L. L., & Frey, F. A. (1989). Geochemical variations in Andean basaltic and silicic lavas from the Villarrica-Lanin volcanic chain (39.5° S): an evaluation of source heterogeneity, fractional crystallization and crustal assimilation. *Contributions to Mineralogy and Petrology*, *103*(3), 361–386. https://doi.org/10.1007/BF00402922

Housh, T. B., & Luhr, J. F. (1991). Plagioclase-melt equilibria in hydrous systems. *American Mineralogist*, *76*(3–4), 477–492.

Humphreys, M. C. S., Blundy, J. D., & Sparks, R. S. J. (2006). Magma evolution and open-system processes at Shiveluch Volcano: Insights from phenocryst zoning. *Journal of Petrology*, *47*(12), 2303–2334. https://doi.org/10.1093/petrology/egl045

Köhler, T. P., & Brey, G. P. (1990). Calcium exchange between olivine and clinopyroxene calibrated as a geothermobarometer for natural peridotites from 2 to 60 kb with applications. *Geochimica et Cosmochimica Acta*, *54*(9), 2375–2388. https://doi.org/10.1016/0016-7037(90)90226-B

Lange, R. A., Frey, H. M., & Hector, J. (2009). A thermodynamic model for the plagioclase-liquid hygrometer/thermometer. *American Mineralogist*, *94*(4), 494–506. https://doi.org/10.2138/am.2009.3011

Le Bas, M. J., Le Maitre, R. W., Streckeisen, A., & Zanettin, B. (1986). A chemical classification of volcanic rocks based on the total alkali silica diagram. *Journal of Petrology*, *27*(3), 745–

750. https://doi.org/10.1093/petrology/27.3.745

Lohmar, S. (2008). *Petrología de las Ignimbritas Licán y Pucón (Volcán Villarrica) y Cutacautín (Volcán Llaima) en los Andes del Sur de Chile*. *PhD Thesis*. Université Blaise Pascal (France) - Universidad de Chile (Santiago, Chile).

Lohmar, S., Parada, M., Gutiérrez, F., Robin, C., & Gerbe, M. C. (2012). Mineralogical and numerical approaches to establish the pre-eruptive conditions of the mafic Licán Ignimbrite, Villarrica Volcano (Chilean Southern Andes). *Journal of Volcanology and Geothermal Research*, *235–236*, 55–69. https://doi.org/10.1016/j.jvolgeores.2012.05.006

López-Escobar, L., Cembrano, J., & Moreno, H. (1995). Geochemistry and tectonics of the Chilean Southern Andes basaltic Quaternary volcanism (37-46^{o}S). *Revista Geológica de Chile*, *22*(2), 219–234.

Loucks, R. R. (1996). A precise olivine-augite Mg-Fe-exehange geothermometer. *Contributions to Mineralogy and Petrology*, *125*(2–3), 140–150. https://doi.org/10.1007/s004100050211

Moreno, H., & Clavero, J. (2006). Geología del volcán Villarrica, Regiones de la Araucanía y de los Lagos. Servicio Nacional de Geología y Minería. *Carta Geológica de Chile, Serie Geología Básica*, *98*.

Moreno, H., & Clavero, J. (2006). Geología del volcán Villarrica, Regiones de la Araucanía y de los Lagos. Servicio Nacional de Geología y Minería. *Carta Geológica de Chile, Serie Geología Básica*.

Morgado, E., Parada, M. A., Contreras, C., Castruccio, A., Gutiérrez, F., & McGee, L. E. (2015). Contrasting records from mantle to surface of Holocene lavas of two nearby arc volcanic

complexes: Caburgua-Huelemolle Small Eruptive Centers and Villarrica Volcano, Southern Chile. *Journal of Volcanology and Geothermal Research*, *306*, 1–16. https://doi.org/10.1016/j.jvolgeores.2015.09.023

Nakamura, M., & Shimatika, S. (1998). Dissolution origin and syn-entrapment compositional changes of melt inclusions in plagioclase. *Earth and Planetary Science Letters*, *161*(1–4), 119–133. Retrieved from http://www.sciencedirect.com/science/article/B6V61-3V72DR0-2R/2/256c1872cb9d3914948debc7a73e672a

Nelson, S. T., & Montana, A. (1992). Sieve-textured plagioclase in volcanic rocks produced by rapid decompression. *American Mineralogist*, *77*(11–12), 1242–1249.

Newhall, C. G. (1979). Temporal variation in the lavas of Mayon volcano, Philippines. *Journal of Volcanology and Geothermal Research*, *6*(1–2), 61–83. https://doi.org/10.1016/0377-0273(79)90047-7

Petit-Breuilh, M. E. (1994). Contribución al conocimiento de la cronología eruptiva histórica del Volcán Villarrica, 1558-1985. *Revista Frontera*, *13*, 71–99.

Renjith, M. L. (2014). Micro-textures in plagioclase from 1994-1995 eruption, Barren Island Volcano: Evidence of dynamic magma plumbing system in the Andaman subduction zone. *Geoscience Frontiers*, *5*(1), 113–126. https://doi.org/10.1016/j.gsf.2013.03.006

Roduit, N. (2007). JMicroVision : un logiciel d'analyse d'images pétrographiques polyvalent. *Uiniversité de Genève*, 116.

Ruprecht, P., & Wörner, G. (2007). Variable regimes in magma systems documented in plagioclase zoning patterns: El Misti stratovolcano and Andahua monogenetic cones.

Journal of Volcanology and Geothermal Research, *165*(3–4), 142–162. https://doi.org/10.1016/j.jvolgeores.2007.06.002

Sides, I., Edmonds, M., Maclennan, J., Houghton, B. F., Swanson, D. A., & Steele-MacInnis, M. J. (2014). Magma mixing and high fountaining during the 1959 K īlauea Iki eruption, Hawai'i. *Earth and Planetary Science Letters*, *400*, 102–112. https://doi.org/10.1016/j.epsl.2014.05.024

Stern, C. R., Moreno, H., López-Escobar, L., Clavero, J. E., Lara, L. E., Naranjo, J. a., … Skewes, M. A. (2007). Chilean volcanoes. In T. Moreno & W. Gibbons (Eds.), *The Geology of Chile* (pp. 147–178). Geological Society of London. Retrieved from https://doi.org/10.1144/GOCH.5

Streck, M. J. (2008). Mineral Textures and Zoning as Evidence for Open System Processes. *Reviews in Mineralogy and Geochemistry*, *69*(1), 595–622. https://doi.org/10.2138/rmg.2008.69.15

Taddeucci, J., Edmonds, M., Houghton, B., James, M. R., & Vergniolle, S. (2015). *Hawaiian and Strombolian Eruptions*. *The Encyclopedia of Volcanoes* (Second Edi). Elsevier Inc. https://doi.org/10.1016/B978-0-12-385938-9.00027-4

Tsuchiyama, A. (1985). Dissolution kinetics of plagioclase in the melt of the system diopside-albite-anorthite, and origin of dusty plagioclase in andesites. *Contributions to Mineralogy and Petrology*, *89*(1), 1–16. https://doi.org/10.1007/BF01177585

Turner, M. B., Cronin, S. J., Smith, I. E., Stewart, R. B., & Neall, V. E. (2008). Eruption episodes and magma recharge events in andesitic systems: Mt Taranaki, New Zealand. *Journal of Volcanology and Geothermal Research*, *177*(4), 1063–1076.

https://doi.org/10.1016/j.jvolgeores.2008.08.001

Ustunisik, G., Kilinc, A., & Nielsen, R. L. (2014). New insights into the processes controlling compositional zoning in plagioclase. *Lithos*, *200–201*(1), 80–93. https://doi.org/10.1016/j.lithos.2014.03.021

Van Daele, M., Moernaut, J., Silversmit, G., Schmidt, S., Fontijn, K., Heirman, K., … De Batist, M. (2014). The 600 yr eruptive history of Villarrica Volcano (Chile) revealed by annually laminated lake sediments. *Bulletin of the Geological Society of America*, *126*(3–4), 481–498. https://doi.org/10.1130/B30798.1

Viccaro, M., Barca, D., Bohrson, W. A., D'Oriano, C., Giuffrida, M., Nicotra, E., & Pitcher, B. W. (2016). Crystal residence times from trace element zoning in plagioclase reveal changes in magma transfer dynamics at Mt. Etna during the last 400 years. *Lithos*, *248–251*, 309–323. https://doi.org/10.1016/j.lithos.2016.02.004

Viccaro, M., Giacomoni, P. P., Ferlito, C., & Cristofolini, R. (2010). Dynamics of magma supply at Mt. Etna volcano (Southern Italy) as revealed by textural and compositional features of plagioclase phenocrysts. *Lithos*, *116*(1–2), 77–91. https://doi.org/10.1016/j.lithos.2009.12.012

Waters, L. E., & Lange, R. A. (2015). An updated calibration of the plagioclase-liquid hygrometer-thermometer applicable to basalts through rhyolites. *American Mineralogist*, *100*(10), 2172–2184. https://doi.org/10.2138/am-2015-5232

Witter, J. B., Kress, V. C., Delmelle, P., & Stix, J. (2004). Volatile degassing, petrology, and magma dynamics of the Villarrica Lava Lake, Southern Chile. *Journal of Volcanology and Geothermal Research*, *134*(4), 303–337. https://doi.org/10.1016/j.jvolgeores.2004.03.002

Anexo

Tabla A1. Microanálisis de sonda electrónica de la química de los microlitos de plagioclasas. Análisis realizados en la *University of Bristol (UoB)*.

Lava		1921	1921	1921	1921	1921
Point		1921-02 - GM-Pl1	1921-02 - GM-Pl2	1921-02 - GM-Pl3	1921-02 - GM-Pl4	1921-02 - GM-Pl5
Laboratory	Detection limit	UoB	UoB	UoB	UoB	UoB
Na2O (wt. %)	0.01 (%)	4.76	4.79	5.17	5.51	5.13
FeO (wt. %)	0.02 (%)	1.14	1.15	1.73	1.45	1.32
CaO (wt. %)	0.01 (%)	11.80	11.86	10.70	10.30	11.37
Al2O3 (wt. %)	0.01 (%)	28.07	28.06	27.20	26.43	27.99
K2O (wt. %)	0.005 (%)	0.2256	0.2406	0.3168	0.3224	0.2692
MgO (wt. %)	0.01 (%)	0.1885	0.1861	0.3135	0.1606	0.1640
SiO2 (wt. %)	0.02 (%)	53.72	53.60	55.35	55.33	55.11
TiO2 (wt. %)	0.01 (%)	0.0864	0.0987	0.1383	0.1298	0.0848
Total		100.03	99.99	100.94	99.64	101.44
Al (%)		1.31	1.39	1.86	1.87	1.54
Fe (ppm)		8832	8941	13486	11262	10278
Ti (ppm)		518	591	829	778	508
Mg (ppm)		1137	1122	1890	968	989
XAn		56.69	56.62	52.03	49.54	53.88
XAb		42.00	42.00	46.11	48.59	44.58
XOr		1.31	1.39	1.86	1.87	1.54

Lava	1921	1921	1921	1921	1921
Point	1921-02 - GM-Pl6	1921-02 - GM-Pl7	1921-02 - GM-Pl8	1921-02 - GM-Pl9	1921-02 - GM-Pl10
Laboratory	UoB	UoB	UoB	UoB	UoB
Na2O (wt. %)	5.31	5.06	5.41	5.22	4.39
FeO (wt. %)	1.22	1.23	1.45	1.37	0.84
CaO (wt. %)	10.60	11.67	10.03	11.30	12.51
Al2O3 (wt. %)	26.80	28.03	26.20	27.44	28.91
K2O (wt. %)	0.2682	0.2682	0.3170	0.2602	0.2156
MgO (wt. %)	0.2258	0.1642	0.1953	0.2214	0.2047
SiO2 (wt. %)	55.05	54.38	55.27	55.50	52.36
TiO2 (wt. %)	0.0875	0.0875	0.1260	0.1176	0.0694
Total	99.60	100.89	99.01	101.43	99.51
Al (%)	1.57	1.52	1.88	1.47	1.24
Fe (ppm)	9498	9587	11301	10654	6507
Ti (ppm)	524	524	755	705	416
Mg (ppm)	1362	990	1177	1335	1235
XAn	51.31	54.82	49.34	53.65	60.41
XAb	47.12	43.66	48.78	44.88	38.35
XOr	1.57	1.52	1.88	1.47	1.24

Lava	1948	1948	1948	1948	1948
Point	1948-04 - GM-Pl1	1948-04 - GM-Pl2	1948-04 - GM-Pl3	1948-04 - GM-Pl4	1948-04 - GM-Pl5
Laboratory	UoB	UoB	UoB	UoB	UoB
Na2O (wt. %)	4.45	3.48	3.79	4.43	3.37
FeO (wt. %)	1.19	0.88	0.95	1.04	0.86
CaO (wt. %)	12.49	14.14	14.18	12.39	14.78
Al2O3 (wt. %)	28.52	30.03	30.18	28.41	30.80
K2O (wt. %)	0.2346	0.1075	0.1534	0.1991	0.1142
MgO (wt. %)	0.1459	0.2190	0.1909	0.2046	0.1727
SiO2 (wt. %)	52.95	51.25	51.41	53.32	50.08
TiO2 (wt. %)	0.1198	0.0629	0.0530	0.0820	0.0611
Total	100.11	100.20	100.91	100.12	100.28
Al (%)	1.34	0.63	0.86	1.15	0.65
Fe (ppm)	9273	6859	7413	8052	6702
Ti (ppm)	718	377	318	491	366
Mg (ppm)	880	1320	1151	1234	1041
XAn	59.98	68.49	66.79	60.00	70.03
XAb	38.67	30.88	32.35	38.85	29.31
XOr	1.34	0.63	0.86	1.15	0.65

Lava	1948	1948	1948	1948	1948
Point	1948-04 - GM-Pl6	1948-04 - GM-Pl7	1948-04 - GM-Pl8	1948-04 - GM-Pl9	1948-04 - GM-Pl10
Laboratory	UoB	UoB	UoB	UoB	UoB
Na2O (wt. %)	4.24	3.19	3.98	4.08	4.92
FeO (wt. %)	0.89	0.85	0.91	1.06	1.87
CaO (wt. %)	12.77	15.10	14.01	13.48	11.83
Al2O3 (wt. %)	28.77	31.10	29.64	29.47	27.24
K2O (wt. %)	0.1965	0.0944	0.1429	0.1619	0.2758
MgO (wt. %)	0.2241	0.1829	0.2675	0.2825	0.2345
SiO2 (wt. %)	53.36	49.72	51.64	52.45	54.11
TiO2 (wt. %)	0.0774	0.0630	0.0582	0.0831	0.1875
Total	100.56	100.36	100.65	101.09	100.71
Al (%)	1.13	0.54	0.80	0.92	1.56
Fe (ppm)	6955	6588	7077	8246	14511
Ti (ppm)	464	378	349	498	1124
Mg (ppm)	1351	1103	1613	1704	1414
XAn	61.75	71.99	65.14	64.03	56.15
XAb	37.12	27.48	34.06	35.06	42.29
XOr	1.13	0.54	0.80	0.92	1.56

Lava	1971	1971	1971	1971	1971
Point	1971-09 - GM-Pl1	1971-09 - GM-Pl2	1971-09 - GM-Pl3	1971-09 - GM-Pl4	1971-09 - GM-Pl5
Laboratory	UoB	UoB	UoB	UoB	UoB
Na2O (wt. %)	4.74	4.76	5.54	4.76	4.85
FeO (wt. %)	1.36	1.28	1.12	1.08	1.37
CaO (wt. %)	12.18	12.38	10.65	12.74	12.45
Al2O3 (wt. %)	28.13	28.50	27.08	29.01	28.63
K2O (wt. %)	0.2366	0.2000	0.2946	0.1720	0.2145
MgO (wt. %)	0.1814	0.2245	0.1496	0.2467	0.1987
SiO2 (wt. %)	54.76	54.81	56.31	54.20	54.44
TiO2 (wt. %)	0.1071	0.1211	0.1152	0.0933	0.0996
Total	101.75	102.27	101.29	102.33	102.28
Al (%)	1.34	1.13	1.68	0.96	1.20
Fe (ppm)	10577	9924	8729	8431	10638
Ti (ppm)	642	726	691	559	597
Mg (ppm)	1094	1354	902	1488	1198
XAn	57.91	57.98	50.34	58.73	57.57
XAb	40.75	40.89	47.98	40.31	41.23
XOr	1.34	1.13	1.68	0.96	1.20

Lava	1971	1971	1971	1971	1971
Point	1971-09 - GM-Pl6	1971-09 - GM-Pl7	1971-09 - GM-Pl8	1971-09 - GM-Pl9	1971-09 - GM-Pl10
Laboratory	UoB	UoB	UoB	UoB	UoB
Na2O (wt. %)	5.03	4.97	4.92	4.39	5.15
FeO (wt. %)	1.13	1.45	1.18	1.18	1.92
CaO (wt. %)	12.35	12.01	11.98	12.94	11.01
Al2O3 (wt. %)	28.50	27.83	28.58	29.17	27.00
K2O (wt. %)	0.2084	0.2196	0.2266	0.1772	0.3876
MgO (wt. %)	0.1726	0.3229	0.1754	0.2404	0.2691
SiO2 (wt. %)	54.39	55.01	54.81	53.96	55.41
TiO2 (wt. %)	0.0795	0.1186	0.0912	0.0970	0.2285
Total	101.89	101.94	101.98	102.17	101.42
Al (%)	1.15	1.24	1.29	1.01	2.24
Fe (ppm)	8786	11297	9199	9195	14906
Ti (ppm)	476	711	547	581	1370
Mg (ppm)	1041	1947	1057	1450	1622
XAn	56.52	56.10	56.32	61.00	52.57
XAb	42.33	42.66	42.40	37.99	45.19
XOr	1.15	1.24	1.29	1.01	2.24

Tabla A2. Microanálisis de sonda electrónica de la química de los microlitos de piroxeno. Análisis realizados en la *University of Bristol (UoB)*.

Lava		1921	1921	1921	1921	1921	1948
Point		1921-02 - GM-Cpx1	1921-02 - GM-Cpx2	1921-02 - GM-Cpx3	1921-02 - GM-Cpx4	1921-02 - GM-Cpx5	1948-04 - GM-Cpx1
Laboratory	Detection limit	UoB	UoB	UoB	UoB	UoB	UoB
Na2O (wt. %)	0.01 (%)	0.267	0.354	0.292	0.357	0.131	0.224
MgO (wt. %)	0.01 (%)	17.54	15.29	16.42	16.10	16.27	18.66
SiO2 (wt. %)	0.02 (%)	51.64	49.54	50.38	49.87	50.65	51.59
Al2O3 (wt. %)	0.02 (%)	2.58	3.18	2.53	3.06	3.11	2.28
CaO (wt. %)	0.01 (%)	16.94	18.69	17.96	17.66	17.48	15.36
TiO2 (wt. %)	0.01 (%)	0.791	1.034	0.755	0.997	0.817	0.600
Cr2O3 (wt. %)	0.02 (%)	0.255	0.154	0.145	0.099	0.320	0.181
MnO (wt. %)	0.02 (%)	0.290	0.268	0.294	0.308	0.291	0.316
FeO (wt. %)	0.02 (%)	10.58	10.29	10.32	11.10	10.22	11.24
Total		100.93	98.84	99.14	99.57	99.32	100.49
Fe2+		0.24	0.22	0.22	0.23	0.28	0.24
Mg		0.96	0.86	0.91	0.89	0.90	1.02
Ca		0.66	0.75	0.72	0.70	0.70	0.60
XWo		34.16	38.94	36.75	36.25	36.35	30.66
XEn		49.19	44.32	46.76	45.98	47.07	51.83
XFs		16.65	16.74	16.48	17.78	16.59	17.51

Lava	1948	1948	1948	1948	1948	1948
Point	1948-04 - GM-Cpx2	1948-04 - GM-Cpx3	1948-04 - GM-Cpx4	1948-04 - GM-Cpx5	1948-04 - GM-Cpx6	1948-04 - GM-Cpx7
Laboratory	UoB	UoB	UoB	UoB	UoB	UoB
Na2O (wt. %)	0.283	0.340	0.270	0.317	0.278	0.431
MgO (wt. %)	17.26	18.17	17.74	17.53	17.08	17.32
SiO2 (wt. %)	50.07	51.10	51.38	51.19	51.72	49.34
Al2O3 (wt. %)	3.74	3.55	2.73	2.83	3.06	4.34
CaO (wt. %)	16.82	13.84	16.21	15.77	14.79	15.20
TiO2 (wt. %)	0.974	0.697	0.735	0.712	0.812	1.186
Cr2O3 (wt. %)	0.305	0.659	0.216	0.280	0.102	0.109
MnO (wt. %)	0.307	0.337	0.296	0.295	0.368	0.327
FeO (wt. %)	9.88	10.47	10.60	11.12	11.30	11.95
Total	99.65	99.25	100.20	100.09	99.70	100.26
Fe2+	0.21	0.30	0.25	0.27	0.35	0.23
Mg	0.95	1.00	0.97	0.96	0.95	0.95
Ca	0.67	0.55	0.64	0.62	0.59	0.60
XWo	34.65	29.26	32.98	32.29	31.22	31.26
XEn	49.47	53.46	50.20	49.94	50.16	49.55
XFs	15.88	17.27	16.83	17.77	18.62	19.19

Lava	1948	1948	1948	1971	1971	1971
Point	1948-04 - GM-Cpx8	1948-04 - GM-Cpx9	1948-04 - GM-Cpx10	1971-09 - GM-Cpx1	1971-09 - GM-Cpx2	1971-09 - GM-Cpx3
Laboratory	UoB	UoB	UoB	UoB	UoB	UoB
Na2O (wt. %)	0.249	0.449	0.283	0.221	0.107	0.307
MgO (wt. %)	16.31	17.02	17.07	19.21	22.56	17.32
SiO2 (wt. %)	49.86	50.61	50.56	52.65	52.88	50.19
Al2O3 (wt. %)	3.55	2.89	3.60	2.34	1.96	3.54
CaO (wt. %)	16.56	16.71	16.92	10.83	8.17	16.30
TiO2 (wt. %)	1.052	0.867	0.854	0.759	0.550	0.817
Cr2O3 (wt. %)	0.166	0.105	0.307	0.094	0.076	0.435
MnO (wt. %)	0.300	0.399	0.287	0.411	0.399	0.308
FeO (wt. %)	11.32	10.28	9.66	15.24	14.42	10.02
Total	99.40	99.36	99.60	101.78	101.18	99.24
Fe2+	0.28	0.22	0.23	0.43	0.37	0.23
Mg	0.91	0.94	0.94	1.04	1.22	0.96
Ca	0.66	0.66	0.67	0.42	0.32	0.65
XWo	34.44	34.52	35.10	21.90	16.08	33.81
XEn	47.19	48.91	49.26	54.04	61.76	49.97
XFs	18.37	16.57	15.64	24.06	22.16	16.22

Lava	1971	1971	1971	1971	1971
Point	1971-09 - GM-Cpx5	1971-09 - GM-Cpx6	1971-09 - GM-Cpx7	1971-09 - GM-Cpx8	1971-09 - GM-Cpx10
Laboratory	UoB	UoB	UoB	UoB	UoB
Na2O (wt. %)	0.241		0.266	0.254	0.439
MgO (wt. %)	17.87	23.92	17.19	17.08	15.50
SiO2 (wt. %)	52.42	53.25	50.73	51.37	50.76
Al2O3 (wt. %)	2.46	2.57	3.63	3.09	3.66
CaO (wt. %)	16.97	7.09	15.42	16.97	18.93
TiO2 (wt. %)	0.708	0.556	1.099	0.858	1.098
Cr2O3 (wt. %)	0.203	0.157	0.093	0.223	0.172
MnO (wt. %)	0.318	0.405	0.341	0.313	0.309
FeO (wt. %)	10.66	13.49	12.67	11.07	10.98
Total	101.91	101.43	101.45	101.25	101.91
Fe2+	0.25	0.36	0.30	0.26	0.23
Mg	0.96	1.28	0.94	0.93	0.84
Ca	0.66	0.27	0.60	0.66	0.74
XWo	33.83	13.92	31.33	34.37	38.58
XEn	49.58	65.39	48.59	48.13	43.95
XFs	16.58	20.69	20.09	17.50	17.47

Tabla A3. Microanálisis de sonda electrónica de la química de los microlitos de olivino. Análisis realizados en la *University of Bristol (UoB)*.

Lava		1921	1921	1948	1948	1948	1948
Point		1921-02 - GM-Ol1	1921-02 - GM-Ol3	1948-04 - GM-Ol1	1948-04 - GM-Ol2	1948-04 - GM-Ol3	1948-04 - GM-Ol4
Laboratory	Detection limit	UoB	UoB	UoB	UoB	UoB	UoB
MgO (wt. %)	0.02 (%)	36.85	38.27	38.59	38.95	38.55	38.84
SiO2 (wt. %)	0.02 (%)	37.46	37.93	38.47	38.40	38.26	38.45
Al2O3 (wt. %)	0.01 (%)	0.050	0.012	0.019	0.069	0.001	0.048
CaO (wt. %)	0.005 (%)	0.317	0.321	0.304	0.287	0.284	0.293
TiO2 (wt. %)	0.01 (%)	0.043	0.033	0.024	0.031	0.029	0.037
Cr2O3 (wt. %)	0.02 (%)	0.010	0.019	0.015	0.022	0.014	0.024
MnO (wt. %)	0.02 (%)	0.438	0.364	0.383	0.459	0.415	0.430
FeO (wt. %)	0.02 (%)	24.64	23.41	22.37	21.77	22.51	22.69
NiO (wt. %)	0.02 (%)	0.052	0.092	0.120	0.108	0.084	0.131
Total		99.88	100.49	100.31	100.11	100.16	100.97
Fe2+		0.52	0.49	0.49	0.47	0.48	0.48
Mg		1.45	1.48	1.50	1.51	1.50	1.50
Ca		0.0090	0.0090	0.0085	0.0080	0.0079	0.0081
Fo		72.05	73.83	74.82	75.44	74.68	74.66
Fa		27.02	25.33	24.33	23.66	24.47	24.46
Ca-Ol		0.45	0.45	0.42	0.40	0.40	0.40

Lava	1948	1948	1948	1948	1948	1948
Point	1948-04 - GM-Ol5	1948-04 - GM-Ol6	1948-04 - GM-Ol7	1948-04 - GM-Ol8	1948-04 - GM-Ol9	1948-04 - GM-Ol10
Laboratory	UoB	UoB	UoB	UoB	UoB	UoB
MgO (wt. %)	38.75	41.18	40.85	40.47	39.48	39.36
SiO2 (wt. %)	38.39	39.05	38.83	38.81	38.51	38.36
Al2O3 (wt. %)	0.037	0.033	0.033	0.021	0.024	0.039
CaO (wt. %)	0.265	0.245	0.274	0.275	0.276	0.296
TiO2 (wt. %)	0.031	0.014	0.017	0.028	0.019	0.038
Cr2O3 (wt. %)	0.029	0.026	0.022	0.016	0.021	0.026
MnO (wt. %)	0.378	0.290	0.334	0.313	0.336	0.357
FeO (wt. %)	22.34	19.81	19.86	20.92	21.50	21.62
NiO (wt. %)	0.146	0.154	0.147	0.132	0.127	0.140
Total	100.42	100.82	100.45	100.99	100.31	100.24
Fe2+	0.48	0.42	0.42	0.44	0.46	0.46
Mg	1.50	1.57	1.56	1.54	1.52	1.52
Ca	0.0074	0.0067	0.0075	0.0075	0.0077	0.0082
Fo	74.97	78.24	77.99	76.96	76.02	75.84
Fa	24.25	21.11	21.27	22.32	23.23	23.36
Ca-Ol	0.37	0.33	0.38	0.38	0.38	0.41

Lava	1971	1971	1971	1971	1971	1971
Point	1971-09 - GM-Ol1	1971-09 - GM-Ol2	1971-09 - GM-Ol3	1971-09 - GM-Ol4	1971-09 - GM-Ol5	1971-09 - GM-Ol6
Laboratory	UoB	UoB	UoB	UoB	UoB	UoB
MgO (wt. %)	36.63	34.36	35.56	39.41	42.29	37.76
SiO2 (wt. %)	38.38	36.84	37.47	38.90	39.67	38.49
Al2O3 (wt. %)	0.044	0.023	0.049	0.034	0.026	0.057
CaO (wt. %)	0.339	0.338	0.379	0.319	0.240	0.348
TiO2 (wt. %)	0.036	0.046	0.042	0.039	0.013	0.043
Cr2O3 (wt. %)	0.014	0.013	0.021	0.020	0.015	0.018
MnO (wt. %)	0.380	0.467	0.432	0.401	0.315	0.378
FeO (wt. %)	25.77	27.40	27.18	22.54	19.40	24.36
NiO (wt. %)	0.063	0.101	0.062	0.116	0.180	0.085
Total	101.78	99.61	101.19	101.80	102.17	101.69
Fe2+	0.56	0.59	0.57	0.48	0.40	0.52
Mg	1.42	1.37	1.39	1.50	1.58	1.46
Ca	0.0094	0.0097	0.0107	0.0087	0.0065	0.0096
Fo	71.06	68.39	69.29	75.05	79.01	72.77
Fa	28.04	30.59	29.70	24.08	20.33	26.34
Ca-Ol	0.47	0.48	0.53	0.44	0.32	0.48

Lava	1971	1971	1971	1971
Point	1971-09 - GM-Ol7	1971-09 - GM-Ol8	1971-09 - GM-Ol9	1971-09 - GM-Ol10
Laboratory	UoB	UoB	UoB	UoB
MgO (wt. %)	37.67	36.88	38.67	39.59
SiO2 (wt. %)	38.51	37.97	38.64	38.85
Al2O3 (wt. %)	0.039	0.036	0.062	0.055
CaO (wt. %)	0.353	0.360	0.320	0.330
TiO2 (wt. %)	0.058	0.051	0.054	0.045
Cr2O3 (wt. %)	0.013	0.007	0.025	0.029
MnO (wt. %)	0.411	0.410	0.372	0.419
FeO (wt. %)	25.39	25.53	22.54	22.06
NiO (wt. %)	0.098	0.073	0.093	0.112
Total	102.56	101.31	100.79	101.51
Fe2+	0.53	0.54	0.49	0.47
Mg	1.44	1.43	1.49	1.51
Ca	0.0097	0.0100	0.0089	0.0091
Fo	71.89	71.34	74.71	75.49
Fa	27.18	27.71	24.43	23.60
Ca-Ol	0.48	0.50	0.44	0.45